THE EFFECT OF ELECTRICAL STIMULATION ON MUSCLE DISUSE ATROPHY

WAN QING

Ph.D

The Hong Kong Polytechnic University

2012

The Hong Kong Polytechnic University

Department of Rehabilitation Sciences

The Effect of Electrical Stimulation on Muscle Disuse Atrophy

Wan Qing

A thesis submitted in partial fulfillment of the requirements

for the degree of Doctor of Philosophy

October 2011

CERTIFICATE OF ORIGINALITY

I hereby declare that this thesis is my own work and that, to the best of my knowledge and belief, it reproduces no material previously published or written, nor material that has been accepted for the award of any other degree or diploma, except where due acknowledgement has been made in the text.

_____ (Signed)

Wan Qing (Name of student)

Abstract of thesis entitled

"**The effect of electrical stimulation on muscle disuse atrophy**"

submitted by **Wan Qing**

for the degree of Doctor of Philosophy

at the Hong Kong Polytechnic University in June 2012

Skeletal muscle atrophy occurs with decreased mechanical loading resulting in decreased muscle mass and strength. Satellite cells are stem cells for muscle regeneration and are important for normal adaptive functions. Impaired satellite cell proliferation and/or increased apoptosis are possible mechanisms underlying disuse atrophy. Electrical stimulation has been used as a countermeasure to counteract disuse atrophy. The hypothesis is that through optimization of different stimulation protocols, electrical stimulation can attenuate muscle atrophy by influencing satellite cell activity.

One hindlimb of male Balb/c mice received electrical stimulation while the contralateral limb served as control during 14-day hindlimb suspension. Different durations (3 h/day or 2×3 h/day) and frequencies (2, 10 or 20 Hz) of stimulation were used. Muscle mass, cross-sectional area, fiber-type composition and maximal tetanic force of soleus were measured. Immunohistochemical staining was used to evaluate satellite cell content, activation, proliferation and differentiation. Cell apoptosis was detected by TUNEL assay. The results showed that stimulation at 2 Hz for 2×3 h/day achieved the best effect in attenuating muscle mass and force. Furthermore, this stimulation parameter led to a 1.2 fold increase in satellite cell proliferation and was effective in rescuing cells from apoptosis.

To understand the possible mechanism of the favorable effect from electrical stimulation, mechano-growth factor (MGF), a splice variant of insulin-like growth factor-I was investigated. Hindlimb suspension induced MGF downregulation. In response to electrical stimulation, MGF was upregulated at days 2 and 3 prior to increased satellite cell content and proliferation at day 7. The results suggested that MGF was mechanically sensitive and might be, at least in part, related to the beneficial effects of electrical stimulation on satellite cell proliferation.

The function of MGF was further characterized using C2C12 cells. The endogenous MGF was highly expressed during the proliferation phase and gradually decreased as differentiation proceeded. Furthermore treatment with synthetic MGF peptides promoted proliferation in a dose-dependent manner. Using electroporation in an *in vivo* model, MGF plasmid DNA could be successfully delivered into muscle.

The study findings form basis for further investigation into the effects of electrical stimulation for disuse atrophy and the functional role of MGF.

ACKNOWLEDGEMENTS

I would like to take this opportunity to thank the following persons during my PhD study:

Dr. Ella W Yeung, my chief supervisor, for her patient guidance and education. I understand the scientific way of thinking and the essential quality of a researcher from her.

Dr. Simon S Yeung, my co-supervisor, for his clear explanation and enlightening guidance, for his caring and support for all these years.

Dr. Guo Xia, my co-supervisor, for her kindness and suggestions whenever I turn to her during my study, she helped me through some difficult time.

Dr. Alex Cheung, for his valuable advice and support during my experiments and thesis writing. Thank him for his patience and guidance to resolve some tough problems.

My former teammates: Dr. Zhang Baoting, Mr. Guo Baosheng, Mr. Wang Daan, Mr. Dai Zhongquan and Mr. Chai Zacary, as well as all the friends working in the Muscle Physiology Laboratory, for their sharing of experience and experimental techniques, they never make me feel lonely and helpless.

Dr. Raymond Chung, for his advice on statistical analysis in my thesis.

Mr. Siu Sik Cheung, Mr. Philip Ng and Mr. Wilson Lam, for their technical expertise and patience.

My friends in the Department of Rehabilitation Sciences and elsewhere; for their confidence in me and for giving me hope and courage whenever I encountered obstacles during my study.

Finally, I want to thank my family: my parents always respect my choice and give me support without limitation; thanks to my husband Hong wei, for his consideration and love.

I will not forget the animals that served themselves for my experiments

This study was partially supported by grant from the Innovation and Technology Commission, Government of Hong Kong Special Administrative Region, China (ITS/029/07).

TABLE OF CONTENTS

(Cont'd) *Page*

(*Cont'd*) *Page*

LIST OF FIGURES

ABBREVIATIONS

AIF	apoptosis-inducing factor
ATPase	adenosinetriphosphatase
ATCC	american type culture collection
Bcl-2	B-cell lymphoma 2
BrdU	5-bromo-2'-deoxyuridine
CSA	cross-sectional area
DAPI	4, 6-diamidino-2-phenylindole
DM	differentiation medium
DMEM	Dulbecco's Modified Eagle's Medium
EGFP	enhanced green fluorescent protein
GH/IGF-I	growth hormone/insulin-like growth factor I
GM	growth medium
H & E	hematoxylin and eosin
HGF	hepatocyte growth factor
HS	hindlimb suspension
IGF-I	insulin like growth factor-I
IPC	intermediate progenitor cell
LIF	leukemia inhibitory factor
MAFbx	muscle atrophy F-box
MCS	multiple cloning site
MGF	mechno growth factor
MHC	myosin heavy chain
MRF	myogenic regulatory factor
MuRF1	muscle ring finger 1
Nedd4	neuronal precursor cell-expressed developmentally downregulated-4
NFAT	nuclear factor of activated T cells
P_0	maximum isometric tetanic force
PBS	phosphate buffered saline
PCNA	proliferator cell nuclear antigen
PCR	polymerase chain reaction

PFA	paraformaldehyde
PI3K	phospharidylinositol-3-OH kinase
SEM	standard error of mean
TA	tibialis anterior
TRPC3	transient receptor potential channel
TUNEL	TdT-mediated dUTP nick end labeling
WB	weight bearing
VEGF	vascular endotherial growth factor
XIAP	X-chromosome-linked inhibitor of apoptosis

CHAPTER 1

General Introduction

1.1 GENERAL INTRODUCTION

Skeletal muscle atrophy is a common but debilitating condition, resulting from inactivity, aging or diseases. Disused muscles show characteristics of decline in muscle size and strength. Satellite cells are muscle stem cells that contribute to adaptive functions of skeletal muscle. They are normally in quiescent state but can be activated by injury, exercise or stretch (Anderson, 2000). The capacity of satellite cells to increase muscle mass requires activation, proliferation and fusion of satellite cells to form new muscle fibers. On the other hand, apoptosis is involved in aging (Alway & Siu, 2008) and mechanically unloading (Ferreira *et al*., 2008) induced muscle disuse atrophy. Therefore, the survival and proliferative potential of satellite cells are playing important roles in skeletal muscle adaptation.

Many countermeasures have been reported to counteract muscle atrophy and electrical stimulation is frequently used in clinical conditions such as spinal cord injury (Sheffler & Chae, 2007), immobilization and muscle disuse after surgery (Bax *et al.*, 2005). The effect of electrical stimulation depends on the atrophic conditions and the stimulation parameters, particularly the stimulation duration and frequency. Previous study has demonstrated that low frequency electrical stimulation partially attenuated the decrease in muscle size and the impaired satellite cell activities in hindlimb suspension induced atrophy (Zhang *et al*., 2010). However the beneficial effects were only modest. As such there is a need to optimize the stimulation parameters to achieve the best desirable responses. The underlying mechanism as to how electrical stimulation influences satellite cell activity is not clear.

To gain insight into the possible mechanisms which may lead to the beneficial effect of electrical stimulation, many possible candidates responsible for muscle regeneration and related to satellite cell proliferation have been considered, such as leukemia inhibitory factor (LIF) (Spangenburg & Booth, 2002), hepatocyte growth factor (HGF) (Li *et al.*, 2009) and mechano growth factor (MGF) (Goldspink, 2006). Among these factors, MGF is locally expressed in skeletal muscle and it is sensitive to mechanical signals. Experimental evidence has shown upregulation of MGF expression in response to mechanical stimulus such as exercise (Hameed *et al.*, 2008), stretch and electrical stimuli (McKoy *et al.*, 1999). It is, therefore, possible that MGF participates in the regulation of satellite cell activity in response to electrical stimulation. Since there is no specific antibody and identified receptors of MGF, the functional roles of MGF in regulating satellite cell activity and muscle mass are not well understood. *In vitro* experiments have demonstrated that when C2C12 cells were transfected with MGF cDNA, the cellular proliferation increased after 24 hours (Yang & Goldspink, 2002). C2C12 is a mouse myoblast cell line originally derived from satellite cells (Yaffe & Saxel, 1977), thus it is possible that MGF expression is related to proliferative activity of satellite cells *in vivo*. In order to further characterize the functional role of MGF, delivery of MGF plasmid DNA into skeletal muscle using electroporation technique may possibly constitutively express MGF *in vivo*. This technique may be feasible to investigate the role of MGF in relation to satellite cell activity *in vivo*.

In this review chapter, the adaptations of skeletal muscle and the consequences following disuse muscle atrophy are first addressed. This is followed by a review on the signaling pathways involved in muscle disuse atrophy. The cellular and molecular

regulation of muscle regeneration is discussed with emphasis on the satellite cell activities. Finally, the possible function of electrical stimulation in attenuating skeletal muscle atrophy and its effects on satellite cell activities are discussed. This chapter concludes with the hypothesis and objectives of the thesis. The experimental investigations are divided into three chapters (Chapters 2 to 4) each with specific methods, results and discussion. The last two chapters are general discussion (Chapter 5) and the conclusion (Chapter 6).

1.2 PLASTICITY OF SKELETAL MUSCLE

Skeletal muscles demonstrate an impressive capability to adapt to various stimuli in functional demands. The adaptation of muscle is characterized by the adjustments in muscle size, force production and alteration in phenotype (Harridge, 2007). Skeletal muscle is remarkably sensitive to the mechanical loads. Decreased mechanical signals resulting from bed rest or exposure to a microgravity environment induce muscle atrophy (Ferrando *et al.*, 1995; Akima *et al.*, 2000). The results from a bed rest study showed that there was a 17 % reduction in muscle cross-sectional area (CSA) in vastus lateralis muscle after 42 days of bed rest, and the decrease of fiber CSA was similar in slow- and fast-twitch fibers (Adams *et al.*, 2003). Spaceflight of 6 months leads to a decrease in the maximal voluntary contraction by 20-48 %; furthermore, the decline of force production is due to decrease in muscle size and selective loss of contractile fibers (Fitts *et al*., 2000). Hindlimb suspension of rodents leads to selective atrophy of slow-twitch muscles (Ingalls *et al.*, 1999; Stelzer & Widrick, 2003). It has been demonstrated that 7 days of hindlimb

unloading reduced soleus CSA by 33 % and 16 % in type I and type IIb fibers respectively (Stelzer & Widrick, 2003). The underlying mechanisms of myocellular adaptations to decreased mechanical loading are complex. It has been demonstrated that activation of the ubiquitin-proteasome pathway, the NF-kappa B pathway and apoptosis are involved in muscle atrophy (Fluck & Hoppeler, 2003). The expression of many genes related to fiber transformation, protein turnover and cell regulation were also changed in response to mechanical unloading (Wittwer *et al.*, 2002).

Increased muscle mass and fiber CSA are characteristics of skeletal muscle hypertrophy. Resistance exercise training causes overload-induced skeletal muscle hypertrophy (Kosek *et al.*, 2006; Martel *et al.*, 2006). A human study has demonstrated that fiber CSA of vastus lateralis muscle increased by 30 % after 12 week-resistance training (Widrick *et al.*, 2002). Resistance training causes hypertrophy of muscle fiber types but preferential hypertrophy of fibre types is dependent on the type of training. For instance, repetitive and low-load exercise training cause muscle adaptation towards a fatigue-resistance slow-twitch phenotype (Fluck, 2006). It has been demonstrated that specific exercise training program affects the rate of synthesis and degradation of gene transcripts during the functional adjustments of skeletal muscles (Fluck & Hoppeler, 2003). Since skeletal muscle undergoes adaptive responses to a given stimulus, the external stimulus could be used to attenuate the atrophic changes by providing mechanical signals through exercises and/or electrical stimulation.

1.3 SKELETAL MUSCLE ATROPHY

1.3.1 Etiology of skeletal muscle atrophy

Skeletal muscle atrophy refers to the loss of muscle mass. It is characterized by a decrease in protein content, fiber size, force production, and fatigue resistance (Jackman & Kandarian, 2004). Muscle atrophy occurs in a wide range of diseases and conditions such as disuse, immobilization, spaceflight, aging, muscular dystrophy, AIDS-, cardiac-, pulmonary- and cancer-related cachexia (Bajotto & Shimomura, 2006). The main focus of this thesis is on disuse muscle atrophy caused by mechanical unloading.

The onset of muscle atrophy can be as early as 4 hours on bed rest (Kasper *et al.*, 2002). The decrease in absolute and relative myosin protein content of skeletal muscles is responsible for the early stages atrophic changes (Haddad *et al.*, 2003). In the first few weeks of bed rest or limb immobilization, the antigravity muscles show more significant atrophy than non-antigravity muscles (Fitts *et al.*, 2000). During prolonged disuse conditions, not only the function of muscle is impaired, but also there are deleterious alterations in the morphology of muscle such as a decrease in muscle mass, a reduction of muscle fiber CSA, and a reduction in the total number of muscle fibers (Boonyarom & Inui, 2006).

Apart from reduced muscle mass and CSA, there is a transition in the myofibril type from slow type I to fast type II fibers in skeletal muscle atrophy (Caiozzo *et al.*, 1996; 1997). The fiber transformation is responsible for alterations in functional properties such as decreased tetanic tension and shortening velocity of contraction (Riley *et al.*, 2005). The following sections focus on the morphological and functional changes of skeletal muscle atrophy.

1.3.2 Reduced muscle mass

A previous animal study demonstrated a 20 % reduction in mouse soleus muscle mass after 48 hours of hindlimb suspension (Ferreira *et al.*, 2006). The duration of disuse has been shown to be positively correlated with the extent of muscle mass reduction, but the rate of decrease is not linear. The soleus muscle of adult rats was observed to decrease in mass rapidly during the first 5 days of hindlimb suspension, and then the decline trend slowly reached a plateau up to 30 days (Thomason & Booth, 1990).

In humans, skeletal muscle size is usually measured by muscle volume. A 3 % decrease in segmental thigh muscle volume has been reported after 7 days of bed rest (Ferrando *et al.*, 1995). Using magnetic resonance imaging, the volume of knee extensor, knee flexor and plantar flexor muscles have been found to reduce by 15.4 %, 14.1 % and 15.9 % respectively after 14 days of space flight (Akima *et al*., 2000). However, increase in the interstitial fluid volume in muscle has been observed in muscle atrophy and it may be a confounding factor for evaluation of atrophic changes. As such, direct quantification by measurement of muscle fiber cross-sectional area is the most accurate method to detect muscle atrophy.

1.3.3 Reduced muscle CSA

Fiber CSA decreases dramatically in response to muscle atrophy. A reduction of soleus CSA by 9 % after 48 hours of himdlimb suspension in mice has been reported (Ferreira *et al*., 2006). In a human bed rest study, the reduction of thigh adductor muscles CSA was 6.7 % after 20 days of bed rest (Kawashima *et al.*, 2004). The extent of fiber atrophy is different under disuse conditions. It was demonstrated that the decrease in fiber

CSA is more pronounced in type IIb, followed by type IIa and then type I fibers after 11 days of spaceflight in vastus lateralis muscle (Edgerton *et al.*, 1995). Hindlimb suspension for 7 days resulted in a decline in soleus fiber CSA by 33 % and 16 % in type I and type IIb fibers respectively (Stelzer & Widrick, 2003). These findings demonstrated selective atrophy of the antigravity slow-twitch fibers in response to disuse conditions.

Since the force output of a skeletal muscle is proportional to muscle CSA, the decrease in muscle fiber CSA due to the atrophic condition can affect the maximal force and power output (Boonyarom & Inui, 2006).

1.3.4 Muscle tetanic force

Muscle atrophy leads to a decline in tetanic force production. The loss of muscle strength is due both to muscle atrophy and to selective loss of contractile proteins, resulting in decrease in force per CSA (Fluck & Hoppeler, 2003). Fourteen days of immobilization has been showed to cause a 22 % decrease in isometric muscle tetanic force (Hespel *et al.*, 2001). Similarly, it has been reported that the muscle tetanic force of the triceps surae group decreased by 45 % for male and 36 % for female subjects after 120 days of bed rest (Koryak, 1999). Six months of spaceflight induced decline of the tetanic force of calf plantar flexor by 34 % (Fitts *et al.*, 2000).

In animal studies, it has been reported that 21 days of hindlimb suspension induced significant reduction in twitch (63 %) and tetanic force (75.8 %) in the soleus muscle (Canon *et al.*, 1998). The peak tetanic tension is known to be highly correlated to the CSA (Adams *et al.*, 2003), therefore the peak tetanic tension normalized to CSA is a better reflection for evaluating the contractile function of muscle fibers. Hindlimb

suspension results in decrease of tetanic force of muscle or myofiber when normalized to CSA. It was demonstrated that the peak force of mouse soleus muscle decreased by 58 % and the tetanic force normalized to fiber CSA reduced by 24 % after 14 days of hindlimb suspension (Ingalls *et al.*, 1999).

1.3.5 Muscle fiber type transition

Muscle fibers can be classified into type I slow-twitch fibers, which are recruited for repetitive postural or chronic activity, and type II fast-twitch fibers, which are either oxidative and glycolytic type IIa, or glycolytic type IIb (Peter *et al.*, 1972). Fiber type transformation in skeletal muscle can occur with normal and under environmental changes. After 4 weeks of immobilization, type I fibers in skeletal muscle assumed the characteristics of type II fibers (Booth, 1982). In spinal cord injury patients, their muscles are dominated by fibers expressing myosin heavy chain (MHC) - II isoforms with almost no fibers containing the MHC - I isoform (Harridge, 2007). In animals studies, there was a significant decline in the MHC I isoform in rat soleus muscle with an increase in MHC IIa or IIx isoform after 14 days of hindlimb suspension (Stevens *et al.*, 2000) or spaceflight (Allen *et al.*, 1996). The transformation towards type II fiber may affect the endurance of skeletal muscle.

Besides slow-to-fast transformations, there are also fast-to-slow transformations in skeletal muscles. In aging people, the predominance of type I fiber in skeletal muscles is possibly due to a conversion of type II fibers to type I (Poggi *et al.*, 1987). The transitions of fiber types influence the power output and sports performance.

1.3.6 Functional changes

The decrease of muscle mass and CSA leads to a decline in force production of skeletal muscles. The impaired force and power production can have severe impact to daily functional activities or in sports performance. For instance, reduced vertical jump power and height of young healthy men were reported after 90 days of bed rest (Rittweger *et al.*, 2007). The slow-to-fast fiber transition causes skeletal muscle to be more susceptible to fatigue. Four weeks of knee immobilization in healthy volunteers caused a significant decrease of quadriceps endurance (Veldhuizen *et al.*, 1993). In an animal study, the atrophied soleus muscle showed decreased resistance to fatigue after 12 days of hindlimb suspension in mice (Arbogast *et al.*, 2007).

1.4 SIGNALING PATHWAYS INVOLVED IN DISUSE ATROPHY OF SKELETAL MUSCLE

The maintenance of muscle mass is controlled by a balance between protein synthesis and degradation regulated by various anabolic and catabolic signaling cascades; the balance shifts towards protein degradation under disuse conditions. The following sections discuss the main signaling pathways involved in protein degradation and protein synthesis.

1.4.1 Ubiquitin-proteasome pathway in protein degradation

The ubiquitin-proteasome pathway is one of the proteolytic systems involved in muscle protein degradation. It has been demonstrated that hindlimb suspension induces

atrophy and loss of protein of the rat soleus muscle through activation of the ubiquitin-proteasome pathway (Bodine *et al.*, 2001a; Gomes *et al.*, 2001). The addition of ubiquitin to a protein substrate is demonstrated to be a modulated process during protein degradation. Three enzymes are involved in the activation of ubiquitin, namely E1 ubiquitin-activating enzyme, E2 ubiquitin-conjugating enzyme and E3 ubiquitin ligating enzyme (Hershko & Ciechanover, 1998). The E1 ubiquitin-activating enzyme firstly activates ubiquitin, and this activated ubiquitin is transferred to E2. Then E3 transfers an activated form of ubiqitin from E2 to a lysine residue on the substrate, and E3 plays an important role in determining proteins which are degradation targets by proteasome (Zhang *et al.*, 2007).

The protein degradation process in disused skeletal muscle was demonstrated in part to be due to the activation of ubiquitin-proteasome pathway. There are two muscle-specific ubiquitin ligases which increase more significantly than other genes in disused conditions: muscle ring finger 1 (MuRF1) and muscle atrophy F-box (MAFbx). MuRF1 and MAFbx have been shown to be significantly upregulated in immobilization, denervation and unloading models (Bodine *et al.*, 2001a). MuRF1 mRNA was upregulated after 24 h after muscle denervation, while MAFbx mRNA level increased rapidly before muscle weight loss was detectable (Zhang *et al.*, 2007). As such, MuRF1 and MAFbx could be used as early markers to detect disuse muscle atrophy. Two other E3 ligases are upregulated in disuse soleus muscle in response to hindlimb suspension: the neuronal precursor cell-expressed developmentally downregulated-4 (Nedd4) and X-chromosome-linked inhibitor of apoptosis (XIAP) (Dupont-Versteegden *et al.*, 2006a). The transcription factors of the nuclear factor (NF)-kB family is also activated during the

proteolysis in muscle disuse atrophy (Kandarian & Jackman, 2006). The activation of NF-kB through ubiquitin-dependent proteolysis degradation was demonstrated in disused muscle and blocking of NF-kB reduced atrophy in response to denervation (Cai *et al.*, 2004).

The ubiquitin-proteosome pathway plays a complex role in the regulation of apoptosis. Apoptosis is an energy-dependent internally encoded biological destructive process which involves regulated cellular signaling resulting in cell death (Siu *et al.*, 2005). In disuse skeletal muscle, apoptosis of myonuclei likely contributes to the loss of muscle mass (Boonyarom & Inui, 2006). There are two main apoptotic pathways: the death receptor (extrinsic) pathway and the mitochondrial (intrinsic) pathway. Moreover, there is an additional pathway involves T-cell mediated cytotoxicity and perforin-granzyme-dependent cell killing process. Granzyme B or granzyme A can induce apoptosis via the perforin/granzyme pathway (Elmore, 2007). The extrinsic, intrinsic, and granzyme B pathways converge on the activation of caspase-3. The granzyme A pathway activates a parallel, caspase-independent cell death pathway (Elmore, 2007). When apoptotic program triggers in response to an extrinsic or intrinsic signal, a few proapoptotic proteins, such as Bcl-2 associate-X protein, apoptosis-inducing factor (AIF), are activated, synthesized or translocated (Cregan *et al.*, 2004). Meanwhile, some antiapoptotic proteins, such as B-cell lymphoma 2 (Bcl-2) is inactivated or dysfunctional (Belka & Budach, 2002).

1.4.2 IGF-I/Akt/FoxO signaling pathway in protein synthesis

Protein synthesis plays an important role in the maintenance of muscle mass. The mechanisms of regulation of protein synthesis and muscle mass include, but are not limited to, the local growth factors and the signaling events in response to mechanical stimulus (Miyazaki & Esser, 2009). The IGF-I/insulin pathway is a well-defined pathway in regulating mTOR, which belongs to the phosphatidylinositol kinase-related kinase family and has a wide function including regulation of protein synthesis, cell proliferation and apoptosis (Miyazaki & Esser, 2009). Insulin like growth factor-I (IGF-I) is a peptide hormone which has many different functions. In skeletal muscle it plays a role in development, muscle mass maintenance, adaptation and repair (Hameed *et al.*, 2008). IGF-I is able to rapidly suppress the expression of atrophy-related ubiquitin ligases, atrogin-1 and MuRF1 (Sacheck *et al.*, 2004). Thus, the degradation of myofibrillar proteins is suppressed and muscle growth is promoted.

IGF-I induces muscle hypertrophy through the phospharidylinositol-3-OH kinase (PI3K)-Akt-mTOR pathway, and the Akt/mTOR pathway has been shown upregulated during muscle hypertrophy but downregulated during muscle atrophy (Bodine *et al.*, 2001b). Furthermore, the IGF-I/PI3K/Akt pathway suppresses the expression of atrogin-1/MAFbx and MuRF1, which are muscle atrophy-induced ubiquitin ligases, by inhibiting FoxO transcription factors (Sandri *et al.*, 2004; Stitt *et al.*, 2004). The FoxO family in skeletal muscle is comprised of three isoforms, including FoxO1, FoxO3 and FoxO4. The upregulation of atrogin-1/MAFbx and MuRF1 is related to the translocation and activity of FoxO members, and FoxO3 was demonstrated to promote atrogin-1/MAFbx expression and muscle atrophy when transfected in skeletal muscles (Sandri *et al.*, 2004).

There was significant reduction of muscle mass and fiber size in FoxO1 transgenic mice (Kamei *et al.*, 2004); this indicates that FoxO expression is able to promote muscle atrophy. On the other hand, the knockdown of FoxO gene was demonstrated to block the upregulation of atrogin-1/MAFbx expression during skeletal muscle atrophy (Sandri *et al.*, 2004).

1.4.3 IGF-I splicing - MGF

As mentioned in the previous section, IGF-I is one of the growth factors for postnatal growth and is important for regulation of muscle mass. Alternative splicing of IGF-I pre-mRNA generates two isoforms in murine: IGF-IEa and IGF-IEb; In human, there are three isoforms including IGF-IEa, IGF-IEb, and IGF-IEc. Murine IEb isoform and human IEc isoform are also known as mechano-growth factor (MGF) (Matheny *et al*., 2010).

MGF is expressed in resting skeletal muscle in an autocine/paracrine pattern and it is sensitive to mechanical signals (Goldspink, 2005). In the skeletal muscle of healthy human, MGF expression has been demonstrated to be upregulated through resistance exercise (Hameed *et al.*, 2003; Hameed *et al.*, 2004), isometric and eccentric exercises (Greig *et al.*, 2006; Hameed *et al.*, 2008). The response of MGF expression to mechanical stimuli occurs as early as 2.5 h after exercises (Greig *et al.*, 2006). In rodent skeletal muscles, MGF mRNA expression was observed to increase by electrical stimuli (McKoy *et al.*, 1999) and mechanically induced local damage (Hill & Goldspink, 2003). In a recent study (van Dijk-Ottens *et al.*, 2010), MGF has been shown to act as an individual

growth factor and respond to mechanical signals (heart beating activity) in mediating physiological cardiac hypertrophic response induced by thyroid horomone.

The MGF expression in healthy skeletal muscle alters with age. In a surgically overloaded model, there was a marked increase of MGF expression in young rats, a moderate increase in middle aged rats, while it was attenuated in old rats (Owino *et al.*, 2001). A human study demonstrated that an acute bout of 10 repetitions of resistance exercise had no effect on MGF expression level in older men (Hameed *et al.*, 2003).

1.4.4 Role of MGF in inducing satellite cell activity

IGF-I has been demonstrated to promote both proliferation and differentiation of satellite cells and increase protein synthesis in several studies (Coleman *et al.*, 1995; Engert *et al.*, 1996; Florini *et al.*, 1996). MGF, one of the splice variants of IGF-I, was also demonstrated to increaes C2C12 cell proliferation (Yang & Goldspink, 2002). MGF has a unique E domain resulting from a 48 bp insert during the splicing of exons 5 and 6, and it has been reported that MGF E domain could increase the muscle satellite cell pool *in vitro* in skeletal muscles (Ates *et al.*, 2007). When C2C12 cells in culture were transfected with the MGF cDNA, the cellular proliferation increased after 24 hours (Yang & Goldspink, 2002).

Due to the lack of specific antibody against MGF, the precise mechanism of MGF in mediating satellite cell activation and proliferation is unclear. Addition of synthetic MGF peptide to C2C12 myoblasts has been shown to increase the proliferation of myoblasts, but the causal relationship between MGF and satellite cell proliferation has yet to be determined (Matheny *et al*., 2010).

It was demonstrated *in vivo* that MGF upregulated rapidly at day 1 in response to local muscle damage and downregulated at day 5 (Hill & Goldspink, 2003). In another *in vivo* study, MGF expression preceded that of markers to satellite cell activation (Goldspink, 2005a). These results indicate that the function of MGF may be transient and the time frame for MGF expression related to satellite cell activities need to be further characterized.

1.5 CELLULAR AND MOLECULAR REGULATION OF MUSCLE REGENERATION

Adult skeletal muscle undergoes profound adaptations in response to disuse atrophy, and the regeneration and development of muscle fibers are closely related to satellite cells. Therefore, the association between muscle atrophy and satellite cell regulation needs to be reviewed. The following section discusses the quantitative and functional changes of satellite cell in skeletal muscle atrophy.

1.5.1 Satellite cells

Satellite cells are the stem cells in skeletal muscle that contribute to muscle regeneration. They are flattened and spindle shaped cells located between the plasma membrane and the basal lamina of the muscle fibers. Satellite cells are normally in quiescent state but can be activated by injury, exercise, stretch or hypertrophy (Anderson, 2000). Upon activation, satellite cells start expressing myogenic regulatory factors and become highly proliferating. The activated satellite cells proliferate and differentiate into

myocytes and fuse with each other and with the existing muscle fibers to form myofibers. In addition, activated satellite cells can undergo self-renewal process to replenish or maintain the satellite cells population (Morgan & Partridge, 2003). It has also been reported that satellite cells are more plentiful in slow-twitch muscles than in fast-twitch muscles (Dusterhoft *et al.*, 1990).

1.5.2 Molecular regulation of satellite cell activity

Satellite cells are responsible for the development of myonuclei during normal muscle growth via proliferation and differentiation. This section discusses three aspects of satellite cell activity: (i) the molecular regulation of quiescent state of satellite cells; (ii) the interaction among muscle regulatory factors during satellite cell activation, proliferation and differentiation; and (iii) the self-renewal of satellite cells.

Most satellite cells in resting skeletal muscle express M-cadherin in its quiescent state (Beauchamp *et al.*, 2000). M-cadherin is a muscle-specific cell adhesion molecule and M-cadherin protein is detectable to the membrane between the satellite cell and the adjacent myofiber. Quiescent satellite cells express several proteins in their nuclei, such as CD34, Pax7, syndecan-3, syndecan-4 and c-met (Beauchamp *et al.*, 2000; Cornelison *et al.*, 2001). None of these proteins is uniquely expressed in quiescent satellite cells. Myostatin is expressed in quiescent satellite cells and myostatin-null mice have demonstrated to increase satellite cell proliferation activity (McCroskery *et al.*, 2003). It indicates that myostatin maintains quiescent state of satellite cells and negatively regulates the activation and/or proliferation activities.

The quiescent satellite cells express Pax7 while the expression of two myogenic regulatory factor (MRF) members: MyoD and Myf5, is in a low or nondetectable level (Seale *et al.*, 2000). When satellite cells are activated, the MyoD expression in satellite cells is rapidly initiated within 12 hours (Yablonka-Reuveni & Rivera, 1994), and satellite cells coexpress Pax7 and Myf5 at this state. The expression of Myf5 and MyoD has been demonstrated to be modulated by Pax7 (Zammit *et al.*, 2006a; McKinnell *et al.*, 2008). In MyoD-/- animals, an increase in the number of mononuclear cells in the damaged muscle was observed and the fusion of proliferated cells and differentiation were impaired (Megeney *et al.*, 1996). This suggests that the expression of MyoD possibly plays a role in modulating satellite cell differentiation and muscle regeneration.

Once the satellite cells are activated, they undergo proliferation process. This is characterized by a decline in expression level of CD34 and an upregulation of Pax3 expression. This process is regulated by the Notch signaling pathway (Conboy & Rando, 2002). When satellite cells begin to divide, they express additional genes such as the proliferator cell nuclear antigen (PCNA). PCNA protein expression is very low in intact muscles, and it is markedly increased in regenerating muscles (Crassous *et al.*, 2009). The expression of Pax7 persists from satellite cell quiescent state to myoblast resulting from satellite cell proliferation, while the Pax7 level is rapidly down-regulated in satellite cells committed to terminal differentiation (Olguin & Olwin, 2004; Zammit *et al.*, 2004). The expression of myogenin protein can down-regulate Pax7. Myogenin and Pax 7 coexpressed between 8 and 12 hours of differentiation until Pax7 was not detectable after 12 hours of differentiation of satellite cells in cell culture (Olguin *et al.*, 2007). On the other hand, overexpression of Pax7 downregulates MyoD in satellite cells and prevents

terminal differentiation and cell cycle progression (Olguin & Olwin, 2004). This interaction among Pax7 and the myogenic regulator factors suggests that there is a reciprocal inhibition between Pax7 and muscle regulatory factors, and the relationship modulates satellite cell fate for proliferation and differentiation.

The number of satellite cells in mature skeletal muscle remains relatively constant for muscle repair and regeneration requirement (Schultz & McCormick, 1994). The replenishment of satellite cell pool relies on the self-renewal of satellite cells. Two satellite cell replenishment models have been proposed; the asymmetric cell division model and the stochastic cell fate model (Dhawan & Rando, 2005). In the asymmetric division model, a quiescent satellite cell activates in response to external stimulus and an asymmetric cell division occurs, one daughter cell returns to quiescent satellite cell and the other daughter begins proliferation to become intermediate progenitor cells (IPC). At this stage the asymmetric cell division can also occur with one daughter returning to quiescent state and the other continues proliferation to expand myoblast pool. In the stochastic cell fate model, the activated satellite cell begins to proliferate and the progeny of cells progress along the myogenic lineage to become IPCs and myoblasts. At some time points, such as the IPC stage or the myoblast stage, one progeny exits from the cell cycle and returns to quiescent satellite cells. Experimental evidence suggests that the expression of Pax7 and MyoD of satellite cells possibly contributes to determination of satellite cell fate during the cell cycle (Holterman & Rudnicki, 2005). It has been demonstrated that synchronously activated satellite cells on isolated single muscle fibers express both Pax7 and MyoD. Among the activated satellite cells, some downregulate Pax7 and progress to proliferation and terminal differentiation; other proliferating

satellite cells maintain the expression of Pax7 and downregulate MyoD level, these satellite cells returned to quiescent state to be ready for activation again (Zammit *et al.*, 2004). The mechanisms involved in regulating of satellite cell fate are not well understood. It has been suggested that Notch signaling modulate satellite cells activation and determination of cell fates (Conboy & Rando, 2002).

Satellite cells express specific proteins at different stages in cell cycle, therefore the corresponding markers can be used to detect satellite cells at different status.

1.5.3 Markers to detect satellite cell

In the past, the most widely used method to positively identify satellite cells is by electron microscopy since it is difficult to distinguish satellite cells from myonuclei by light microscopy. With the discovery of molecular markers for satellite cells at different states of the cell cycle, it is now possible to identify the satellite cells by immunological methods under light microscope.

Quiescent satellite cells express a variety of proteins, and the most widely studied of those are M-cadherin, Pax7, CD34, syndecan-3, syndecan-4 and c-met (Irintchev *et al.*, 1994; Beauchamp *et al.*, 2000; Seale *et al.*, 2000; Cornelison *et al.*, 2001). M-cadherin is an adhesion molecule and is expressed in a subpopulation of the quiescent cell pool; however, it also expressed when the satellite cells become activated in response to a stimulus (Cornelison & Wold, 1997; Kaufmann *et al.*, 1999). The satellite cells on single muscle fiber of mouse were evaluated by light and electron microscopy, and it was found that at least 94 % of the quiescent satellite cells are M-cadherin positive. Thus, M-cadherin can be regarded as a reliable marker of quiescent satellite cells in mouse skeletal

muscle (Cornelison & Wold, 1997). Numerous studies have used M-cadherin immunostaining technique to evaluate quiescent satellite cells quantitatively (Putman *et al.*, 2001; Wang *et al.*, 2006).

Pax7, the paired box transcription factor, expresses selectively in quiescent and proliferating satellite cells in regenerating muscle (Seale *et al.*, 2000). Thus, Pax7 is accepted as a useful marker for identifying satellite cell pool (Zammit *et al.*, 2004; Shefer *et al.*, 2006). Because it is difficult to distinguish satellite cells from other positive cells especially by one single marker on muscle sections, some non-specific markers such as CD34 are less reliable unless on isolated myofibers. Syndecan-3, syndecan-4 and c-met are considered to be expressed in quiescent and activated satellite cells, and once activated, all satellite cells maintain expression of syndecan-3 and syndecan-4 for at least 96 h, implicating their role in skeletal muscle regeneration (Cornelison *et al.*, 2001).

Quiescent satellite cells do not express myogenic regulatory factors of the MyoD or MEF2 families or other known markers of terminal differentiation (Megeney *et al.*, 1996; Cornelison & Wold, 1997). MyoD expression occurs early during the activation of the satellite cells (within 6 hours following muscle injury) (Koishi *et al.*, 1995; Megeney *et al.*, 1996). Although MyoD expression was observed in the activated and proliferating satellite cells in adult skeletal muscle, this marker was primarily used to evaluate the activation state of satellite cells (Dedkov *et al.*, 2003; Krajnak *et al.*, 2006).

Proliferating satellite cells can be identified by several nonselective markers immunohistochemically, these markers include PCNA (Crassous *et al.*, 2009), 5-bromo-2'-deoxyuridine (BrdU) (Blaauw *et al.*, 2009) and ^{3}H thymidine (Chazaud *et al.*, 2003). BrdU is a thymidine analogue which is incorporated into all mitotically active cells. It is

frequently used for identification and quantification of proliferating satellite cells in skeletal muscle (Brotchie *et al.*, 1995; Putman *et al.*, 2000; Wang *et al.*, 2006). During terminal differentiation of cell cycle, myogenin is strongly upregulated in satellite cells and they can be identified by the immunohistochemical reaction (Putman *et al.*, 2000). Desmin acts as a marker in differentiated myocytes and myotubes in culture.

In order to determine whether the labeled cells are satellite cells or myonuclei in muscle cross-sectional profile, multiple immunofluorescence staining is widely performed. Dystrophin and laminin are commonly used to mark the sarcolemma and basal lamina of the muscle fiber to help identifying the location of the satellite cells, while 4, 6-diamidino-2-phenylindole (DAPI) is used to present all the nuclei and is normally used as counterstain.

1.6 COUNTERMEASURES FOR MUSCLE DISUSE ATROPHY

1.6.1 Strategies for muscle disuse atrophy

Skeletal muscles are highly plastic and adapt to external stimuli. Exercise is an important countermeasure in attenuating muscle atrophy in both animals and humans. Numerous studies have assessed the effectiveness of exercise interventions, including stretching (Falempin & Mounier, 1998), short-duration periodic weight support (Zhang *et al.*, 2003) and resistance exercises (Adams *et al.*, 2007). In recent years, flywheel resistance exercise has been frequently used to counteract muscle atrophy induced by bed rest, limb immobilization and spaceflight. It was demonstrated that knee extension exercise in a flywheel for 5 weeks significantly increased quadriceps volume by 7.7 %

and maintained the basal strength in a limb immobilization study (Tesch *et al.*, 2004). In a bed rest study, flywheel exercises increased the thigh CSA by 8.3 % compared to control after 90 days of bed rest in healthy young subjects (Rittweger *et al.*, 2005).

Electrical stimulation has also been used as an effective intervention to attenuate muscle atrophy. Its beneficial effects are discussed in the following section. Currently, there is no single intervention strategy that can fully recover muscle atrophy, as such a combined intervention would provide a more beneficial effect in attenuating muscle atrophy.

1.6.2 Historical perspective of electrical stimulation

Electrical stimulation uses an electrical current to cause a single muscle or a group of muscles to contract. This therapeutic intervention is commonly used in clinical conditions for disuse atrophy where the nerve supply to the muscle is intact. Clinically, electrical stimulation has been applied to achieve many beneficial effects including strengthening and re-education of muscles, reduction of oedema, relief of pain and wound repair (Durmus *et al.*, 2007). A prolonged (6 weeks) electrical stimulation program has been demonstrated to be effective in improving strength in healthy sedentary adults (Banerjee *et al.*, 2005). When electrical stimulation was used in healthy subjects, an increase in type I muscle fibre CSA and whole muscle CSA was observed (Requena Sanchez *et al.*, 2005). In athletes, electrical stimulation of specific muscle groups also resulted in a marked increase in the strength and power during a 12-week period (Babault *et al.*, 2007).

The most often stimulated muscle group is the quadriceps femoris in physiotherapy practices (Fitzgerald *et al*., 2003). Bax *et al.* (2005) performed a systematic review of randomized controlled trials that evaluated the effectiveness of electrostimulation in strengthening quadriceps muscle group. The authors suggested that electrostimulation was effective in strengthening normal and impaired quadriceps femoris muscle and even more effective than volitional exercises during a period of immobilization, especially under a cast.

Although muscle re-education is most often performed with electromyographic biofeedback techniques, electrical stimulation has been extensively used to initiate and facilitate voluntary contraction of muscle. Stimulation of the pelvic floor muscle in the control of incontinence was also used in clinical practices (Rivalta *et al.*, 2009). Electrical stimulation has been reported to be frequently used in other conditions such as neurological rehabilitation (Sheffler & Chae, 2007), although this aspect will not be discussed in this section. Emphasis of the next section is on the effectiveness of electrical stimulation for skeletal muscle atrophy.

1.6.3 Use of electrical stimulation in attenuating muscle atrophy

The use of electrical stimulation in attenuating muscle atrophy has been investigated in both animal and human studies. Electrostimulation has been shown to be effective in attenuating the decreases in muscle strength, muscle mass and oxidative capacity of thigh muscles following knee immobilization (Lake, 1992). Moreover, electrostimulation was shown to be superior in preventing the atrophic changes due to knee immobilization when compared to isometric exercises of both hamstrings and

quadriceps femoris muscle groups (Delitto *et al.*, 1988). The application of electrical stimulation from day 2 post anterior cruciate ligament reconstruction for 4 weeks demonstrated that the decline of knee extension strength was significantly less in the stimulated group than in the control group, and the stimulated group showed greater recovery of knee extension strength at 3 months post-operation (Hasegawa *et al.*, 2011).

In animal models, electrical stimulation has also been suggested to be effective in preventing skeletal muscle atrophy (Canon *et al.*, 1998; Dupont Salter *et al.*, 2003). Dupont-Salter *et al*. (2003) found that low frequency (2 and 10 Hz) electrical stimulation could attenuate disuse atrophy of rat skeletal muscles to different extent. The most significant effect was in the slow-twitch soleus muscle, which had only a 10 % decrease in muscle mass when stimulated at 2 Hz compared to a decrease by 36 % in unstimulated muscle. Canon *et al*. (1998) investigated the effects of low frequency stimulation (10 Hz, 8 hours/day) on contractile properties of hindlimb suspended rat soleus muscle. The authors reported that the implanted electrical stimulation partially attenuated the reduction of twitch and tetanic tension of soleus induced by 3 weeks of hindlimb suspension, but did not modify the normalized tetanic tension to muscle mass. Cotter *et al.* (1991) investigated the effects of chronic stimulation (10 Hz, 8 hours/day) on immobilized rabbit soleus muscle, the results showed that 2 weeks of stimulation completely normalized muscle weight, restored fiber CSA and increased greater twitch and tetanic tension than natural recovery.

The effectiveness of electrical stimulation using different parameters was rarely compared. Therefore, it is essential to find a novel electrical stimulation paradigm in preventing skeletal muscle atrophy.

1.6.4 Effect of electrical stimulation on satellite cell function

The satellite cells in skeletal muscle activate and replenish the satellite cell pool in response to muscle damage (Zammit *et al.*, 2006a). It has also been shown that electrical stimulation activates satellite cells to re-enter the cell cycle, to proliferate and fuse with their associated fibers (Putman *et al.*, 2000). Furthermore, electrical stimulation has been demonstrated to significantly elevate the absolute content of satellite cells in rat skeletal muscle (Putman *et al.*, 1999; 2001). Putman *et al*. (1999) applied continuous electrical stimulation (10 Hz, 10 hours/day) to the peroneal nerve of hypothyroid rats and found that the number of satellite cells in extensor digitorum longus (EDL) muscle increased 2.6, 3 and 3.7-fold after 5, 10 and 20 days of stimulation respectively. Putman *et al*. (2001) used the same stimulation parameters and proceeded to the duration for 50 days. The results showed that the number of satellite cells in rat tibialis anterior (TA) muscle increased more than 2-fold.

Pronounced satellite cell proliferation has been shown in electrically stimulated EDL muscle in rabbit (Schuler & Pette, 1996). Although electrical stimulation increased the absolute numbers of quiescent, proliferating, and differentiating satellite cells; it did not alter the proportions of satellite cell within the three compartments (Putman *et al.*, 2001). Electrical stimulation probably contributed to increase in the potentiality of muscle growth and regeneration by increasing the population of satellite cell pool.

Electrical stimulation of fast-twitch muscle has been shown to induce fast-to-slow fiber type transitions in rats (Putman *et al.*, 2001; Martins *et al.*, 2006). These fiber type transitions are associated with increases in satellite cell activation, proliferation and fusion capacity (Putman *et al.*, 2000; 2001). Putman *et al*. (2001) found that satellite cell

progeny selectively fused to the fastest IIb fibers of TA muscle in the early phase of electrostimulation. After 20 days of stimulation, transformation in the IIb fibers showed increased proliferation and differentiation of satellite cells, leading to increased myonuclear density which was typically found in slow-twitch fibers. In order to determine whether satellite cells are playing a direct role in fast-to-slow fiber-type transitions, Martins *et al*. (2006) ablated the satellite cells of rat TA muscle by exposure to γ-irradiation during 21 days of electrical stimulation (10 Hz, 12 hours/day); the results showed that electrostimulation-induced fast-to-slow fiber-type transitions were moderately attenuated in TA muscles in which the satellite cells were ablated. This suggests that satellite cell may play a role in inducing fiber-type transitions in response to electrical stimulation.

There are only very few studies that investigated the effect of electrical stimulation on satellite cell activation and proliferation, and how this effect could attenuate disuse muscle atrophy. As such, it will be necessary to carry out a series of studies to fill in the missing gap for optimal electrical stimulation parameters in influencing satellite cell activity and for attenuating disuse muscle atrophy.

1.7 MODELS OF MUSCLE ATROPHY

1.7.1 Introduction

Researches have established several experimental models to study skeletal muscle atrophy. The commonly used ground-based models to simulate disuse atrophy conditions in humans are bed rest (with or without head-down tilt) (Berg *et al.*, 1997), limb

immobilization (Booth, 1982) and unilateral lower limb suspension (Berg *et al.*, 1991). For animals, especially rats and mice, hindlimb suspension (Morey-Holton & Globus, 2002), joint immobilization (Booth, 1982), tenotomy (Herbison *et al.*, 1979), denervation (Siu, 2009) and spinal cord transaction (Dupont-Versteegden *et al.*, 1999) are laboratorial models to induce skeletal muscle atrophy. Among these animal models, hindlimb suspension by tail harnessing is the most common procedure.

1.7.2 Hindlimb suspension model

The unloading model induced by hindlimb suspension (HS) was developed to simulate weightlessness. Morey (1979) first described an unloading model of rat to simulate bone turnover in spaceflight. A back harness and a cantilevered rotating beam were used in this model, the head-down animal could move in a 360º arc accessing to food and water. The author concluded that the changes of periosteal bone formation rate and days required to form total bone volume in rat induced by this model were similar to real spaceflight. Musacchia *et al.* (1980) used a similar unloading model to study rat muscle atrophy by hypokinesia after 7 days of unloading. They have shown a significant atrophy in gastrocnemius muscle, which was similar to the changes observed during spaceflight. The tail traction model appears to be less stressful to animals based on changes of corticosterone level, adrenal, thymus and body weight compared to whole body harnesses (Halloran *et al.*, 1988). The tail-traction models were widely used to investigate muscle atrophy in microgravity in animals (Canon *et al.*, 1998; Mozdziak *et al.*, 2001; Wang *et al.*, 2006).

The hindlimb unloading model has further been extended to mice for investigation of the musculoskeletal responses to unloading (Dapp *et al.*, 2004). Due to smaller body size and differences in animal behavior compared with rats, a number of modifications have been made to the device when traction is applied to the mouse tail. Such modifications include using smaller cages and setting up devices to prevent mice from climbing the unloading apparatus (Morey-Holton & Globus, 2002).

1.8 AIMS OF THE INVESTIGATION

The overall purpose of the investigation is to examine the effect of electrical stimulation on disuse skeletal muscle atrophy. The hypothesis is that electrical stimulation can attenuate muscle atrophy by influencing satellite cell activity. The beneficial effects of electrical stimulation are mediated via the regulation of MGF. The specific aims are:

(i) To investigate the efficacy of different electrical stimulation protocols to determine the optimal stimulation parameters in attenuating disuse muscle atrophy induced by hindlimb suspension model for 14 days. The effectiveness of the protocol is determined by muscle mass, fiber cross-sectional area, maximum tetanic force and fiber-type composition. The expression of markers indicative of satellite cell activity and apoptosis (myonuclei and satellite cells) were also evaluated for determination of effectiveness.

(ii) To examine MGF as a possible cellular mechanism causing favorable induced changes from electrical stimulation. The time frame for MGF expression in

relation to satellite cell proliferation during hindlimb suspension, with or without electrical stimulation was determined.

(iii) To characterize the function of MGF *in vitro* where C2C12 myoblasts were treated with synthetic MGF E peptides.

(iv) To determine the feasibility of delivering MGF *in vivo* using electroporation technique in which MGF plasmid DNA was injected into the muscle.

CHAPTER 2

Effect of Electrical Stimulation in Unloading-Induced Muscle Atrophy: The Efficacy of Different Stimulation Protocols on Satellite Cell Activity and Apoptosis

2.1 INTRODUCTION

Electrical stimulation has frequently been used to attenuate skeletal muscle atrophy induced by disuse conditions in both human (Banerjee *et al.*, 2005; Babault *et al.*, 2007; Adams *et al.*, 2011) and animal studies (Putman *et al.*, 2001; Banerjee *et al.*, 2005; Fujita *et al.*, 2011). The stimulation parameters varied in these studies producing very different outcomes. In animal models inducing disuse atrophy, different parameters in terms of the stimulation duration and frequency have been applied to investigate the effect of electrical stimulation (Canon *et al*., 1998; Dupont Salter *et al.*, 2003; Boonyarom *et al.*, 2009). It was demonstrated that low frequency (2 and 10 Hz) electrical stimulation for 2 h/d or 10 h/d could prevent disuse atrophy of rat soleus muscle to some extent (Dupont Salter *et al.*, 2003), and the results showed that stimulation at 2 Hz was more effective than 10 Hz whether it was applied for 2 or 10 h. Canon *et al*. (1998) investigated the effects of implanted electrical stimulation (10 Hz, 8 h/d) on the contractile properties of in rat soleus muscles with 3- week hindlimb suspension. The authors reported that this protocol partially attenuated the reduction of twitch and tetanic tension of soleus muscle. In another experiment where rats were subjected to 2-week unloading, electrical stimulation applied to the soleus muscle at 20 Hz and 30 Hz for 2×15 min/d on alternate days has shown that 20 Hz was more effective in attenuating decline of muscle mass and fiber cross sectional area (Boonyarom *et al.*, 2009).

Although electrical simulation has been shown to be effective in attenuating disuse muscle atrophy the underlying mechanism is far from clear. Hindlimb suspension leads to a decrease in satellite cell number as well as its activation and proliferation activities (Mozdziak *et al.*, 2001; Wang *et al*., 2006; Matsuba *et al*., 2009). Studies have

demonstrated that electrical stimulation could preserve satellite cell number and improve satellite cell activation and proliferation activities in skeletal muscles (Putman *et al.*, 2000; Zhang *et al.*, 2010). Zhang *et al*. (2010) showed that electrical stimulation at 20 Hz for 2 × 3 h/d could attenuate the reduction of quiescent, proliferating and differentiated satellite cells during 28 days of unloading (Zhang *et al.*, 2010). An implanted electrical stimulation at 10 Hz for 10 h/d was reported to increase satellite cell proliferation at day 5 and day 10 using a hypothyroid model (Putman *et al.*, 2000). Since unloading leads to a decrease in satellite cell number and proliferation activity and electrical stimulation seems to be beneficial in improving satellite cell activities, there is a need to find the optimal stimulation parameters that could enhance satellite cell activities.

Satellite cell proliferation and cell apoptosis control the balance of cell survival under disuse conditions. Previous studies have found that apoptosis plays an important role in the muscle atrophy process in response to aging (Chung & Ng, 2006), spinal cord transection (Dupont-Versteegden *et al.*, 1999), and hindlimb suspension (Allen *et al.*, 1997; Ferreira *et al.*, 2008). Two recent studies have demonstrated the effect of electrical stimulation on apoptosis using a denervation model (Arakawa *et al.*, 2010; Lim & Han, 2010). Electrical stimulation for two weeks significantly decreased apoptotic nuclei in skeletal muscle and the apoptosis related factors: Bax and Bcl-2 were downregulated (Lim & Han, 2010). Another study where electrical stimulation was applied to denervated soleus muscles at 2 Hz for 1 h/d for 4 weeks showed that electrical stimulation prevented muscle atrophy and increased the expression of anti-apoptosis related protein (valosin-containing protein) (Arakawa *et al.*, 2010). The stimulation parameters for the optimal

effects of electrical stimulation on inhibition of cell apoptosis (myonuclei and satellite cells) need to be determined.

2.1.1 Aim of the study

We hypothesize that the impaired satellite cell activity and cell apoptosis contribute to skeletal muscle disuse atrophy and electrical stimulation could partially attenuated muscle atrophy. However the effects would be different with varied stimulation protocols. Therefore, this study aims to evaluate the effects of different parameters of electrical stimulation protocol (in terms of duration and frequency) on satellite cell activities and apoptosis (myonuclei and satellite cells) during the muscle atrophic process. The morphological changes, fiber type composition and the contractile properties of the soleus muscles were also assessed.

2.2 MATERIALS AND METHODS

2.2.1 Animals and ethical approval

Male Balb/c mice (8-10 wk) were obtained from The Chinese University of Hong Kong. All the mice were housed in a temperature and light-dark cycle controlled room for one week before experiments. All the animal handling procedures and experimental protocols were approved by the Animal Subjects Ethics Committee of The Hong Kong Polytechnic University before conducting the experiments (ASESC No.07/23, Appendix I). A license to conduct animal experiments was also endorsed by the Department of Health of the Hong Kong Government (Appendix II).

2.2.2 Hindlimb suspension model

Hindlimb suspension was performed using a protocol for tail suspension of mice (Dapp *et al.*, 2004). Prior to the suspension procedure, the animal was weighed and anesthetized with an intraperitoneal injection of ketamine (100 mg/kg body weight) and xylazine (5 mg/kg body weight) to attach the suspension device and electrical stimulation electrodes. A movable swivel hook was raised to a metal bar on the top of the cage; a strip (~12 cm×0.5 cm) of adhesive tape (Primapore, Smith & Nephew Medical Ltd, UK) distally enclosed the mouse tail on both sides and was fixed to the swivel hook by metal rings. The body of the mouse makes about a 30º angle from the cage floor, and the height was checked daily and adjusted if necessary to assure that toes of the unloaded hindlimb did not touch the floor (Fig. 2.1). The animals were free to move with their forelimbs to access food and water within the cage. The animals' overall appearance, their drinking and eating habits, and the blood flow of tail were monitored four times per day. The distal

tip of the tail (i.e., the tail maintained pink) was examined to ensure that the suspension procedure did not occlude blood flow to the tail. Body weight was measured every day with a suspension apparatus so that the hindlimbs remained suspended when the animals were weighed.

Figure 2.1 The hindlimb suspension model.

2.2.3 Experimental design

The male Balb/c mice were randomly divided into weight bearing group (WB, n=4) and hindlimb unloaded group. During unloading, one hindlimb was subjected to electrical stimulation (HS+ES) while the contralateral hindlimb suspended (HS) limb served as control. For the HS+ES groups (N = 8 for each group) different stimulation protocols in terms of duration (3 h/d, 2 × 3 h/d) and frequencies (2 Hz, 10 Hz and 20 Hz) were performed. The unloading period was 14 days. The flow chart (Fig. 2.2) shows the experimental design.

To assess possible systemic effects of electrical stimulation on the contralateral hindlimb unloaded soleus muscle (i.e. HS group), control experiments were performed in which the effects on contralateral HS soleus was compared with that on the soleus of the 14-day unloaded mice without electrical stimulation.

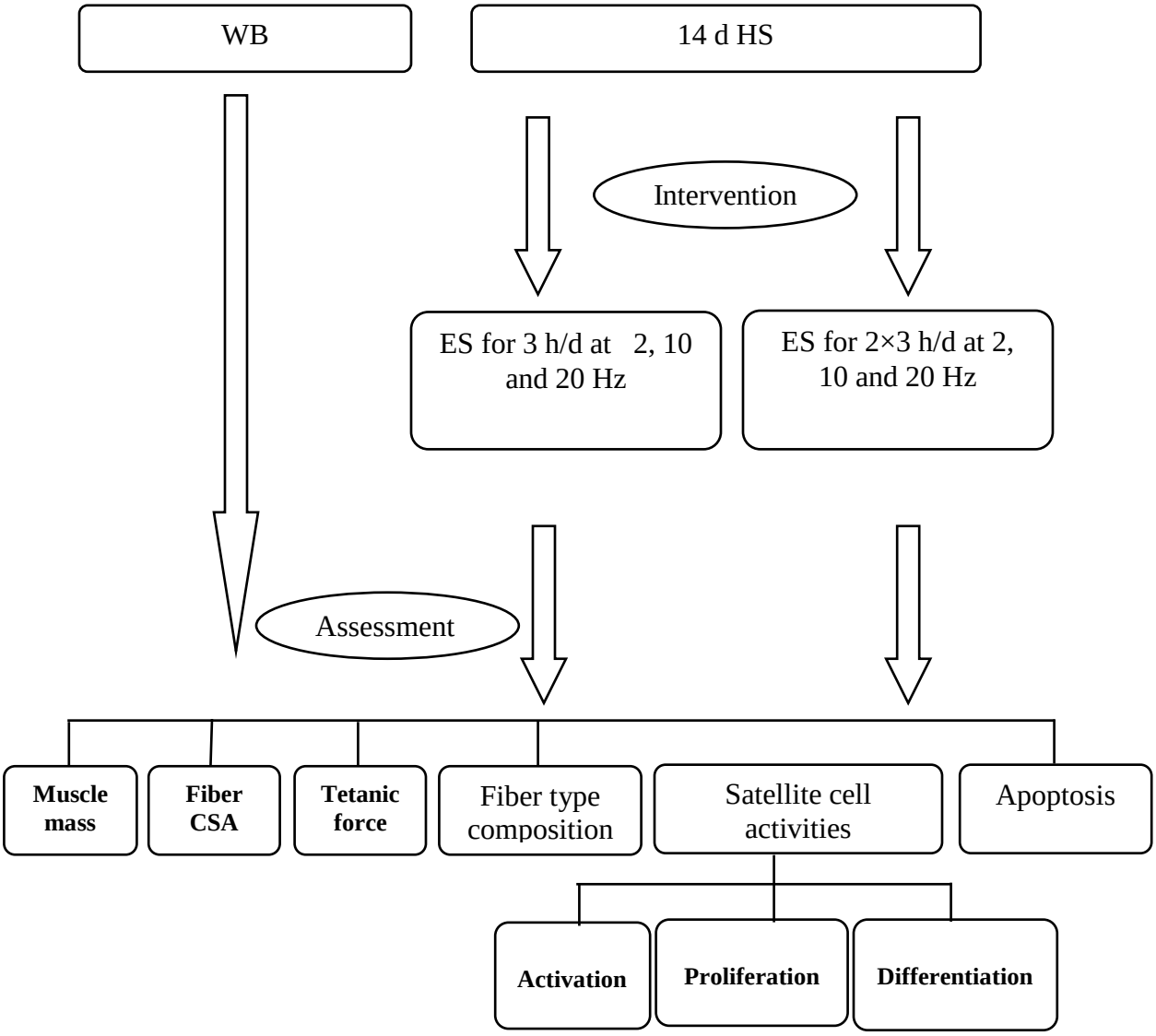

Figure 2.2 The experimental design.

2.2.4 Electrical stimulation

One hindlimb was randomly selected to receive transcutaneous electrical stimulation for each unloaded mouse. To ensure that electrical currents were efficiently delivered to the muscles, the limb was shaved under anesthesia before attaching the surface electrodes. In order to apply electrical stimulation to the target soleus muscle, which lies beneath the gastrocnemius muscle, one electrode was placed over the gastrocnemius muscle. The other electrode was applied to the quadriceps muscle which serves as a cathode (Fig 2.3). The insulation of two electrode tips was removed and the fan-shaped fine carbon fibrous materials (Fig. 2.4) were attached to the skin with conducting resin, and covered with ventilated adhesive wound dressing (~6 cm×0.5 cm) (Smith & Nephew Medical Limited, England). The surface electrodes were renewed every 3 days to ensure intact attachment with new covered dressing and any skin damage was checked. The repeated shave before replacement of electrodes also prevented resistance caused by hair growth.

A portable electrical stimulator (Vital EMS+^{TM}, Taiwan) (Fig. 2.5) was used to deliver a biphasic, asymmetrical square wave stimulation. The pulse width (250 μs), and duty cycle (5:10 s) were held constant. The stimulus was ramped up for 1 s, held constant for 5 s, and ramped down for 1 s. The stimulation protocols were manipulated to different frequencies (2, 10 and 20 Hz) and different durations (3 h per day or 2 × 3 h per day with 2 h interval) for different HS+ES groups. The intensity was set to induce visible muscle contraction.

Figure 2.3 The fan-shaped electrode tip.

Figure 2.4 Positions of two electrodes.

Figure 2.5 The electrical stimulator (Vital EMS+^{TM}, Taiwan).

2.2.5 Body weight

Animals were weighed daily to monitor the well-being of animals during the suspension period and to document the decrease of body mass induced by muscle disuse atrophy. The body weight was measured using a suspension apparatus so that the hindlimbs of the animal remained suspended.

2.2.6 Wet muscle mass

After 14 days the animals were sacrificed by cervical dislocation and the soleus muscles were dissected immediately. The muscles were weighed using a platform digital balance.

2.2.7 Fiber cross-sectional area (CSA)

The interstitial matrix, vascular tissue and the hydration status of the muscle could lead to variances of wet muscle mass. Myofiber cross-sectional area is a more direct parameter in evaluating muscle atrophy. Isolated solues muscle was frozen in liquid nitrogen chilled isopentane, embedded with OCT compound (Metronet Technology Limited, Hong Kong) and stored at -70 ºC until cryosectioning. Frozen sections of 5 μm thick were cut in a cryostat (Leica, USA) and mounted on Superfrost® Plus microscopic slides (VWR Scientific, Ireland). Muscles were cryosectioned at their midbelly and stained with hematoxylin and eosin (H & E) to reveal nuclei and myofibrils.

The sections were examined by an eclipse 80i microscope (Nikon, Japan) and the images were captured with a Spots RT digital camera (Zeiss, Germany). At least two cryosections of the same muscle were included. The entire muscle cross-section was

determined from digital images (4× or 10×) of H & E stained muscle sections. The outline of the individual fibers was traced using an image morphometry program (ImageJ 1.32j, NIH, Bethesda, USA) and the total number of fibers was counted. The area was expressed in μm^2.

2.2.8 Fiber type composition

Two methods were used to evaluate the fiber type composition of the soleus: (i) the adenosinetriphosphatase (ATPase) staining; (ii) the myosin heavy chain (MHC) gene expression.

Cryostat sections were stained for myofibrillar ATPase to identify type I and type II fibers. At least two cryosections of the same sample were included for each staining. The slides were first incubated in pH 4.2 pre-incubating solution (composition: 5 ml Barbital Acetate solution, 10 ml 0.1N HCl and 4 ml mQH_2O) for 5 min. The slides were rinsed with mQH_2O several times to remove all the trace of pre-incubating solution. This was followed by incubation in pH 9.4 ATP solution (composition: 60 mg adenosine triphosphate powder, 6 ml 0.1 M sodium barbital, 21 ml mQH_2O, 3 ml 0.18M $CaCl_2 \cdot 2H_2O$) for 25 min. The slides were rinsed 3 times with 1 % $CaCl_2$ for approximately 10 min and then 2 % $CoCl_2$ was added onto the sections and incubated for 10 min. The slides were rinsed with 1:20 (0.1 M) sodium barbital for 5 changes and rinsed with mQH_2O for 5 times. In a fume hood, the sections were incubated in 2% $(NH_4)_2S$ for 20-30 sec and rinsed with mQH_2O immediately for 5 times. Finally, the slides were dehydrated in 70 %, 80 %, 95 % and 100 % ethanol and then xylene for 2 times. DPX was used to mount the sections. The type I fibers were stained dark color and

the type II fibers were light (Verdijk *et al.*, 2007). The numbers of type I fiber and total muscle fibers were determined using an image morphometry program (ImageJ 1.32j, NIH, Bethesda, USA), and type I fiber composition was expressed in percentage of number of type I fiber over total muscle fibers per section.

Since ATPase staining at this pH only identifies type I and II fibers, real time PCR was used to evaluate the MHC I, IIa and IIb mRNA expression in soleus (Martins *et al.*, 2006). The RNA of soleus was extracted using the SV total RNA Isolation System according to the technical manual provided by Promega Corporation (USA) and the RNA purification protocol is shown in Appendix III. The concentrations and purity of RNA extracts were evaluated by measuring the absorbance at 230, 260 and 280 nm, respectively, using a U-0080D spectrophotometer (Hitachi High-Technologies Corporation, Japan). A total of 500 ng RNA from each sample was converted into cDNA in 21 μl using the SuperScript III first-strand synthesis system (Invitrogen, Life Technologies, Burlington, ON, Canada) according to the manufacturer's protocol, which is shown in Appendix IV.

Taqman-MGB probes (Applied Biosystems, Foster City, CA, USA) of MHC I, IIa and IIb were used for PCR amplification. For each sample, 1.5 μl of cDNA was amplified in a 25 μl TaqMan Master Mix (Applied Biosystems, the component for each sample was 1.5 μl cDNA, 12.5 μl Master Mix, 1.25 μl probe and 9.75 μl H_20), using a 7500 real time PCR system (Applied Biosystems). GAPDH was used as the endogenous control. Relative changes in MHC isoform gene expression were determined using the $2^{-\Delta\Delta Ct}$ method of analysis (Livak and Schmittgen, 2001).

The $2^{-\Delta\Delta Ct}$ method for relative gene expression analysis is widely used. This method assumes that both target and reference genes are amplified with efficiencies near 100 % and within 5 % of each other. The relative difference in expression level of target gene in different samples can be determined using the steps below:

(1) normalize the C_T of the target gene to that of the reference (ref) gene, for both the test sample and the calibrator sample:

$$\Delta C_{T(test)} = C_{T(target,\ test)} - C_{T(ref,\ test)}$$

$$\Delta C_{T(calibrator)} = C_{T(target,\ calibrator)} - C_{T(ref,\ calibrator)}$$

(2) normalize the ΔC_T of the test sample to the ΔC_T of the calibrator:

$$\Delta\Delta C_T = \Delta C_{T(test)} - \Delta C_{T(calibrator)}$$

(3) calculate the expression ratio:

$2^{-\Delta\Delta Ct}$ = normalized expression ratio

The result obtained is the fold increase or decrease of the target gene in the test sample relative to the calibrator sample and is normalized to the expression of a reference gene. Normalizing the expression of the target gene to that of the reference gene compensates for any difference in the amount of sample tissue.

2.2.9 Maximum isometric tetanic force (P_0)

Force measurement was conducted immediately after muscle dissection. The soleus muscles were placed in Krebs solution (composition in mM: NaCl 118, KCl 4.5, $CaCl_2$ 1.4, $NaHCO_3$ 25, $MgSO_4$ 1.2, NaH2PO_4 1.4, glucose 11, pH 7.4) maintained at room temperature (22-24 ºC) and oxygenated (95 % O_2-5 % CO_2). The proximal and distal tendons of the soleus muscle were carefully isolated and gripped with T-shaped

aluminum foil clips. Each muscle was then transferred to the experimental chamber and mounted horizontally. One end of the tendon was attached to a hook connected to the lever arm of a position feedback motor (300B-LC, Aurora Scientific Inc., Canada), and the other end was attached to a force transducer (Model BG-10, Kulite Semiconductor Products Inc., USA). The force transducer was clamped to a mechanical micromanipulator to adjust the muscle length. The schematic diagram of the experimental chamber is illustrated in (Fig. 2.6). The muscle was stimulated with 0.5-ms pulses at 1 Hz and the voltage gradually increased to determine the threshold voltage of muscle twitch. Tetanic stimulation was delivered at 100 Hz for 400 ms train duration with the stimulation intensity of 1.2× threshold. The optimal muscle length was subsequently adjusted to the length that produced the maximal isometric tetanic force (P_0). The P_0 was normalized to muscle CSA, which were determined by H&E staining. The normalized P_0 was expressed in mN/mm^2.

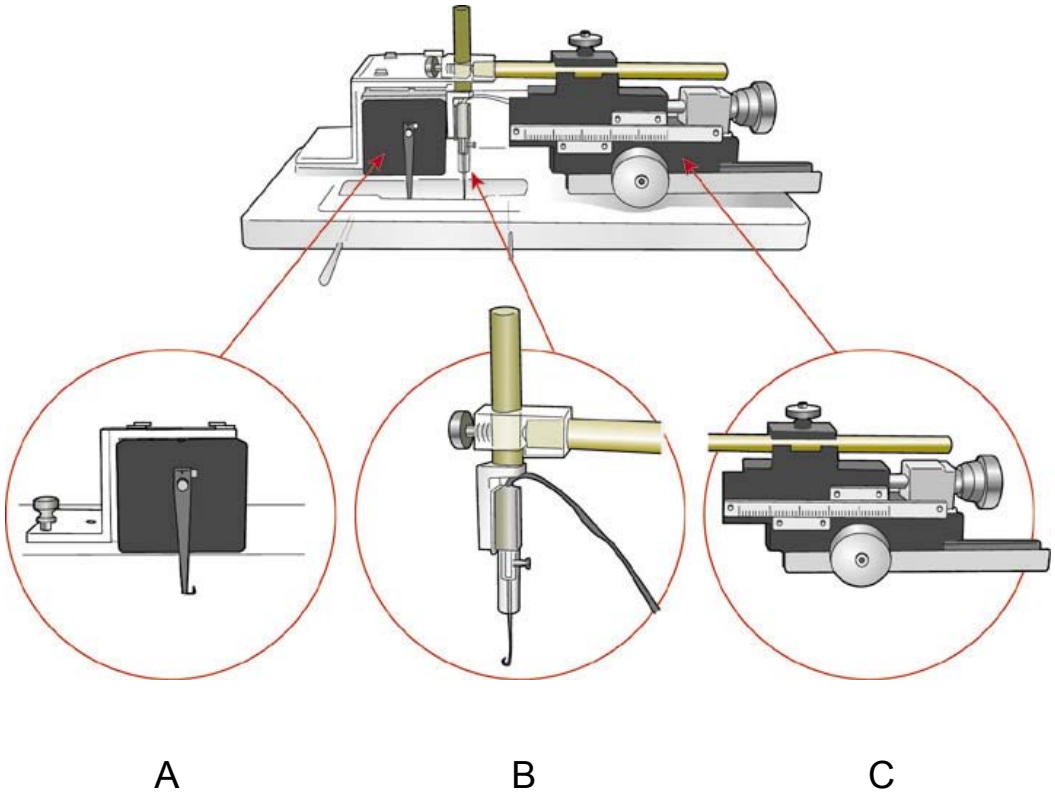

Figure 2.6 Schematic diagram of the experimental chamber. *A*: Position feedback motor where the muscle is attached via the fine hook. *B*: Force transducer with a glass extension and a fine hook. *C*: Mechanical micromanipulator with resolutions to 10 μm.

2.2.10 Satellite cell activity

Immunohistochemical staining was performed to detect the markers of total (Pax7), activated (MyoD) and differentiating (myogenin) satellite cells (Dedkov *et al.*, 2003; Shefer *et al.*, 2006; Zammit *et al.*, 2006b). Immunostaining against dystrophin, a skeletal muscle-specific cytoskeletal protein associated with the sarcolemma, was also performed in some experiments to help identifying the position of satellite cells. To determine satellite cell proliferation *in vivo* at a given timepoint, bromodeoxyuridine (BrdU) incorporation as well as Pax7 and BrdU colabeling were performed. For BrdU incorporation, mice were injected intraperitoneally with BrdU (50 mg per kg body weight) 24 h before the sacrifice.

Cryosections were fixed in ice-cold acetone for 10 minutes and rinsed with 0.1 M phosphate buffered saline (PBS, pH 7.4). The sections were permeabilized with 0.2 % Triton X-100 in PBS for 20 min, and subsequently blocked with PBS containing 5 % normal donkey serum for 30 min at room temperature to prevent non-specific binding. For BrdU detection, the cryosections were denatured with 2 N HCl in PBS for 25 min prior to blocking. The primary antibodies (goat monoclonal anti-dystrophin, 1: 100 dilution, Santa Cruz, CA, USA; mouse monoclonal anti-MyoD 1: 100 dilution, BD PharMingen, San Diego, CA, USA; or mouse monoclonal anti-myogenin, 1: 100 dilution, Sigma-Aldrich, USA; mouse monoclonal anti-Pax7, 1: 200 dilution, Developmental Studies Hybridoma Bank, Iowa, USA; with rat monoclonal anti-BrdU, 1: 800 dilution, Sigma, SL, USA) were appropriately diluted with 2 % BSA in PBS. The sections were incubated in the mixture of two primary antibodies (Pax7+BrdU, MyoD+dystrophin, or myogenin+dystrophin) at appropriate dilution at 4^{o}C overnight. Next day the sections

were rinsed in PBS 3 times before further incubating with the corresponding fluorescent-conjugated secondary antibodies (Alexa Fluor 555-labelled donkey anti-goat IgG, 1: 400 dilution; Alexa Fluor 488-labelled donkey anti-mouse IgG, 1: 400 dilution, Molecular Probes, Eugene, OR, USA; Alexa Fluor 555-labelled donkey anti-mouse IgG, Alexa Fluor 488-labelled donkey anti-rat IgG, 1: 400 dilution, Molecular Probes, Eugene, OR, USA) for 2 h at room temperature. The washed sections were then mounted with 40, 60-diamidino-2-phenylindole (DAPI) -containing medium (Vector, USA) for nuclei identification. Nuclei labeled for MyoD and myogenin outside dystrophin and nuclei colabeled for Pax7 and BrdU were quantified in two sections for each muscle. Those slides for Pax7 and BrdU double immunostaining, H&E staining was performed after immunostaining to evaluate the total muscle fibers using an image morphometry program (ImageJ 1.32j, NIH, Bethesda, USA). The total number of positive nuclei was counted and expressed per 1000 muscle fibers.

2.2.11 Cell apoptosis

TdT-mediated dUTP nick end labeling (TUNEL) assay was used to detect apoptotic nuclei on two sections of each muscle. The sections were fixed in 4 % paraformaldehyde (PFA) at room temperature for 20 min, washed with PBS 3 times and incubated with 0.1 % Triton X-100 in 0.1 % sodium citrate for 2 min on ice. The slides were rinsed twice with PBS. TUNEL reaction was incubated at 37 ºC for 1 h. After the sections were rinsed twice with PBS, the sections were blocked with PBS containing 5% normal donkey serum for 30 min at room temperature to prevent non-specific binding. Sections were then incubated with a goat monoclonal anti-dystrophin (Santa Cruz, CA,

USA, at 1:100 dilution) at 4 ºC overnight to help identifying the positions of TUNEL positive nuclei. Afterwards, the sections were rinsed 3 times and further incubated with the corresponding secondary antibody (Alexa Fluor 555-labelled donkey anti-goat IgG, 1: 400 dilution) for 2 h at room temperature. The washed sections were mounted with DAPI -containing medium (Vector, USA) for nuclei identification. The total number of TUNEL positive nuclei was counted and expressed per 1000 muscle fibers.

2.2.12 Statistics

The values were expressed as means ± SEM. Differences between group means were assessed by analyses of variance (one-way ANOVA) followed by post-hoc comparison t-tests with Bonferroni correction. Differences between stimulated and non-stimulated conditions were assessed by paired-sample t-tests. For multiple comparisons, statistic significant difference was set at $P < 0.05$, and the adjusted P-value with appropriate Bonferroni was used.

2.3 RESULTS

2.3.1 Animal well-being

To evaluate the well-being of animals during hindlimb suspension, food and water intake were monitored daily. Hindlimb suspension has no significant influence on drinking and eating behaviors of the animals (Fig. 2.7).

A

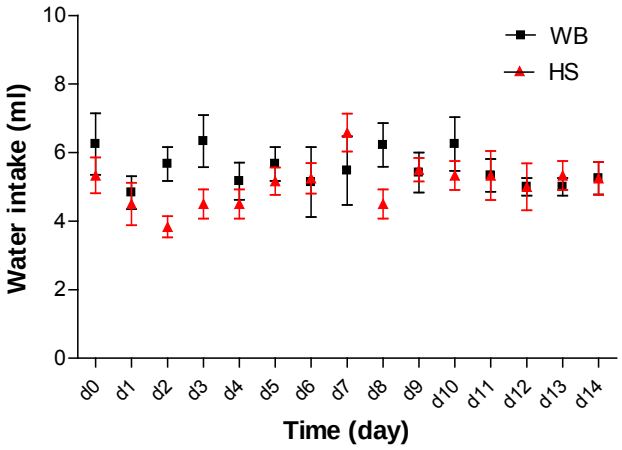

B

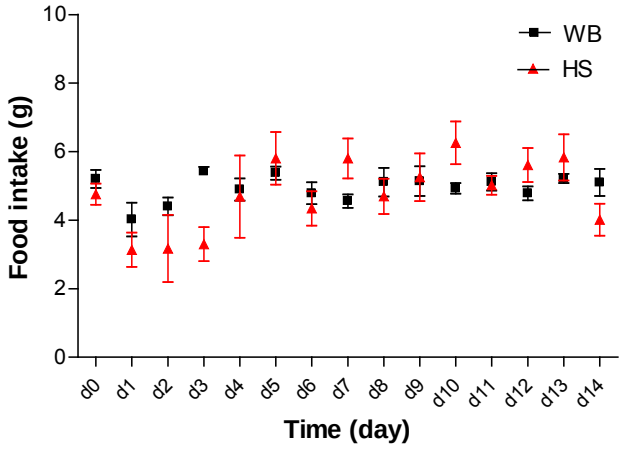

Figure 2.7 Comparison of the water intake (A) and food intake (B) between WB and HS groups during 14 d hindlimb suspension. Data are means ± SEM.

2.3.2 Systemic effect

To assess possible systemic effects of electrical stimulation on the contralateral soleus muscle of HS+ES group, control experiments were performed. The effects of 14 d hindlimb suspension on the contralateral HS soleus muscle of HS+ES group were compared with soleus muscles of the 14-day unloaded mice without electrical stimulation. The muscle mass (7.75 ± 0.25 mg *vs* 7.5 ± 0.50 mg) and the maximal tetanic force (469.02 ± 5.13 mN *vs* 450.10 ± 23.30 mN) were compared and no significant difference was observed.

2.3.3 Effect of different stimulation frequencies for 3 h/d on soleus disuse atrophy

Body weight

The body weight between WB and HS+ES groups did not differ at the start of the experiment. Hindlimb suspension induced a significant reduction of body weight by 7.8 % in HS+ES group (from 23.51 ± 0.18 g to 21.68 ± 0.19 g, $P < 0.001$). There was a 2.6 % growth-associated increase in body weight in WB group after 14 days.

Muscle mass and fiber CSA

After 14 days of hindlimb suspension, the soleus muscle mass of the HS group decreased by 41.5 ± 0.5 % compared to WB group ($P < 0.01$). Electrical stimulation at 10 or 20 Hz slightly improved muscle mass compared with HS group, but no significant effect was observed. Electrical stimulation at 2 Hz produced a significant improvement of muscle mass by 16.7 % in HS+ES group compared with that of HS group (HS: 7.5 ± 0.54

mg; HS+ES: 8.75 ± 1.0 mg; $P < 0.05$), but the muscle mass in HS+ES group was less than the WB group (WB: 14.13 ± 0.37; $P < 0.05$) (Fig. 2.8).

Electrical stimulation at 10 or 20 Hz had no significant effect in attenuating the reduction of muscle mass normalized to body weight in HS+ES group compared with that of HS group. However, a significant difference was observed in the muscle mass normalized to body weight between HS+ES at 2 Hz (0.40 ± 0.02 mg/g) with HS (0.35 ± 0.01 mg/g) group ($P < 0.05$). Electrical stimulation at 2 Hz improved the muscle mass normalized to body weight by 14.3 %, however the beneficial effect obtained by this stimulation protocol still resulted in significantly lower normalized mass than in the WB group (0.58 ± 0.03 mg/g) ($P < 0.05$) (Fig. 2.9).

Hindlimb suspension significantly reduced the fiber CSA in the HS group by 25 % when compared with the WB group ($P < 0.05$).

Electrical stimulation at 10 and 20 Hz had no significant effect on attenuating the decrease of fiber CSA. Electrical stimulation at 2 Hz for 3 h/d improved fiber CSA of the HS+ES group (1104.72 ± 48.89 μm^2) compared with that of the HS group (955.80 ± 54.74 μm^2), but there was no significant difference observed. With the intervention of electrical stimulation at 10 and 20 Hz, the fiber CSA of the HS+ES groups were still significantly decreased compared with that of the WB group. However electrical stimulation at 2 Hz significantly prevented the decline in fiber CSA to the level of the WB group (HS+ES: 1104.72 ± 48.89 μm^2; WB: 1309.31 ± 65.88 μm^2) (Fig. 2.10).

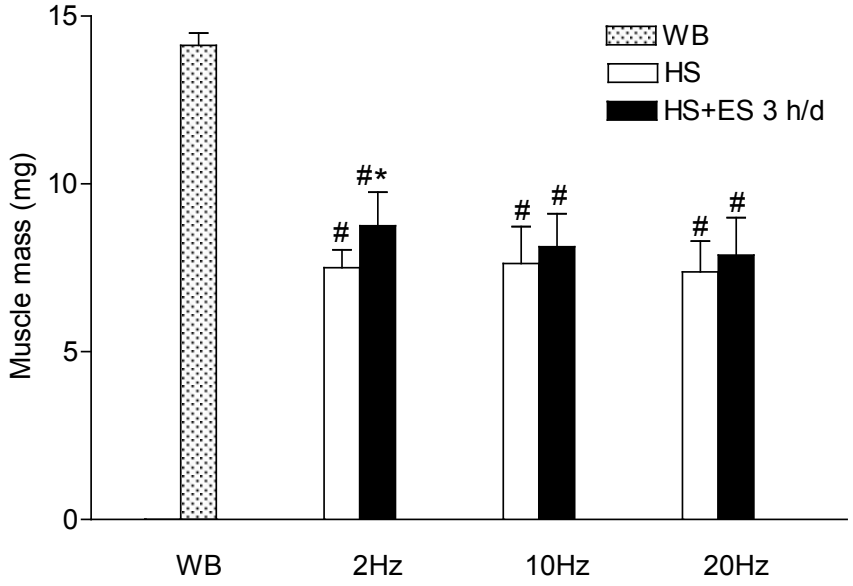

Figure 2.8 Muscle mass in stimulated (HS+ES), HS and WB groups. Data are means ± SEM; * Statistical significance ($P < 0.05$) between HS+ES and HS groups using the same frequency. # Statistical significance ($P < 0.05$) compared with WB group.

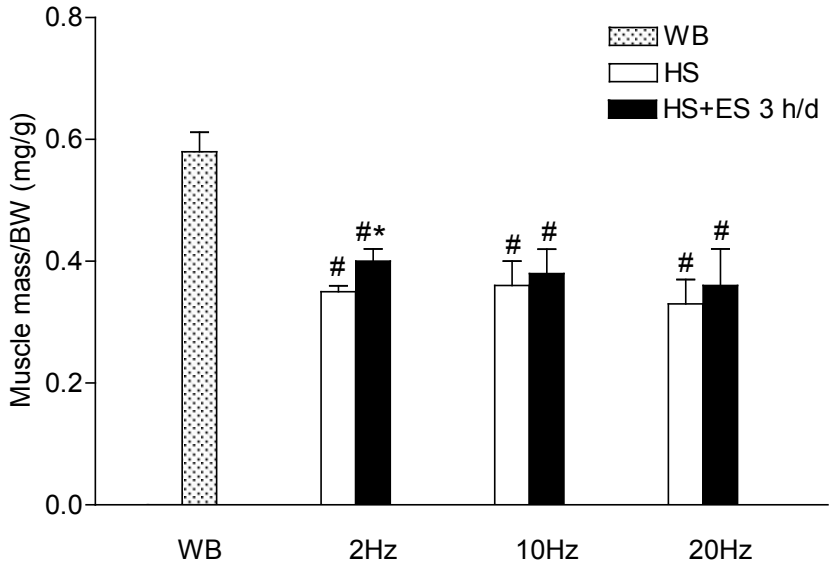

Figure 2.9 Muscle mass normalized to body weight in stimulated (HS+ES), HS and WB groups. Data are means ± SEM; * Statistical significance ($P < 0.05$) between HS+ES and HS groups using the same frequency. # Statistical significance ($P < 0.05$) compared with WB group.

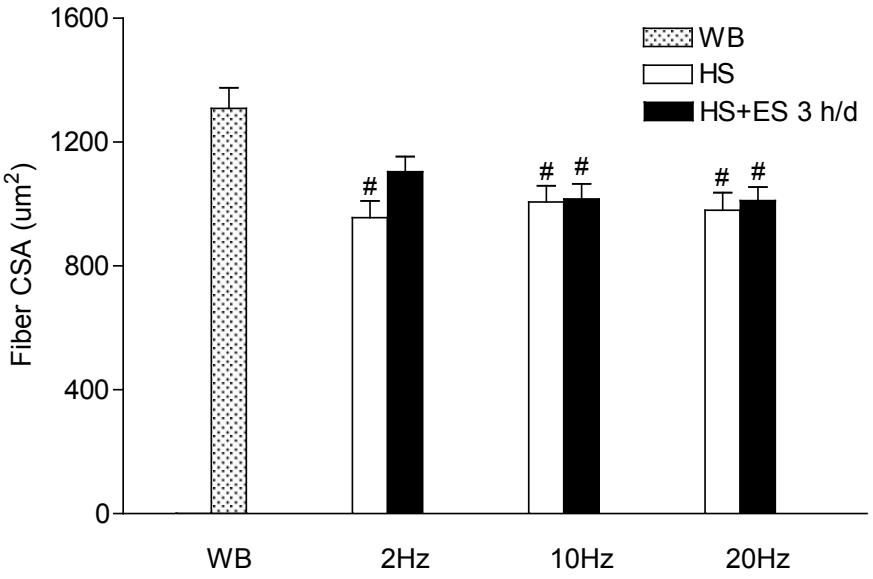

Figure 2.10 Fiber CSA in stimulated (HS+ES), HS and WB groups. Data are means ± SEM; # Statistical significance ($P < 0.05$) compared with WB group.

Muscle maximal tetanic force

After 14 d hindlimb suspension, the peak tetanic force (P_0/CSA) of the soleus muscle significantly decreased by 30 % compared with that of the WB group (HS: 509.53 ± 21.94 mN/mm^2; WB: 732.91 ± 19.69 mN/mm^2, $P < 0.05$).

None of these three electrical stimulation protocols had a significant effect on P_0/CSA (Fig. 2.11).

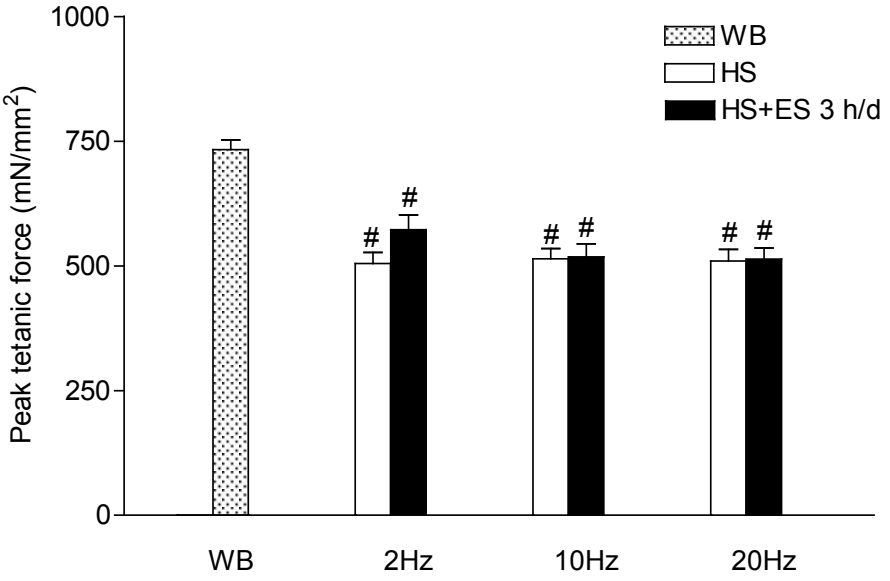

Figure 2.11 The peak tetanic force in stimulated (HS+ES), HS and WB groups. Data are means ± SEM; # Statistical significance ($P < 0.05$) compared with WB group.

Fiber type composition

The percentage of muscle fibers for type I and II on sections of soleus were measured using ATPase staining. There was a significant reduction in the percentage of type I fibers of the HS groups (35.30 ± 2.46 %) compared with the WB group (51.68 ± 1.39 %) after 14 d of hindlimb suspension ($P < 0.05$). However, there was no significant change in the percentage of type I fiber of the HS+ES groups at any of the frequencies tested compared with that of the HS groups (Fig. 2.12).

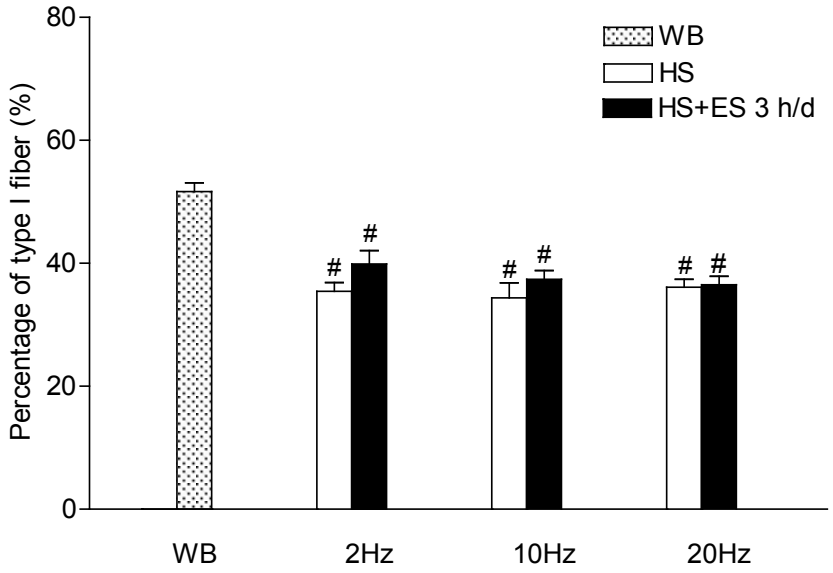

Figure 2.12 Type I fiber composition in stimulated (HS+ES), HS and WB groups using ATPase staining. Data are means ± SEM; # Statistical significance ($P < 0.05$) compared with WB group.

Satellite cell number and activity

Satellite cells in different status were identified by antibodies of specific markers. Immunofluorescence staining against Pax7 positive nuclei was performed to quantitatively evaluate total numbers of satellite cell in the soleus muscles. Double labeling of Pax7 and BrdU revealed proliferating satellite cells under different intervention conditions. To identify activated and differentiating satellite cells, MyoD and myogenin antibodies were used respectively and were double labeled with dystrophin to reveal the localization of the respective satellite cells.

The total number of satellite cells ($Pax7^{+}$) per 1000 fibers in the HS groups significantly decreased by 57 % after 14 d of hindlimb suspension. Electrical stimulation at 2 Hz for 3 h/d significantly increased the total number of satellite cells compared with that of the HS group (HS+ES: 6.42 ± 0.36; HS: 5.15 ± 0.27; $P < 0.05$), although it was still far below that of the WB group (WB: 15.05 ± 0.52). The other stimulation protocols had no significant effect in improving the number of satellite cells (Fig. 2.13).

The number of activated satellite cells ($MyoD^{+}$) in the HS groups significantly decreased after hindlimb suspension compared with that of the WB groups (HS: 3.23 ± 0.22; WB: 6.22 ± 0.46, $P < 0.05$) (Fig. 2.14). Electrical stimulation at 10 and 20 Hz for 3 h/d had no significant effect in improving the activated satellite cell number. Electrical stimulation at 2 Hz significantly attenuated the loss of activated satellite cells of the HS+ES group induced by hindlimb suspension compared with that of the HS group (HS+ES: 4.05 ± 0.31; HS: 3.22 ± 0.18; $P < 0.05$), however, this attenuation could not reach to the same level as in the WB group ($P < 0.05$).

The proliferating satellite cells ($Pax7^+/BrdU^+$) of the HS groups significantly decreased by 67 % (1.93 ± 0.13) compared with that of the WB group (5.81 ± 0.40) ($P < 0.05$). Electrical stimulation for 3 h/d at three frequencies had no significant effect in attenuating the decrease of proliferating satellite cells ($P > 0.05$) (Fig. 2.15).

The above results indicated that only electrical stimulation at 2 Hz for 3 h/d had some effect in attenuating the decrease of muscle mass, fiber CSA, the maximal tetanic force and improving satellite cell activity. One of the possibilities may be that the duration of stimulation (3 h/d) was too short to achieve the desired effect. As such, the next set of experiments performed was to ascertain the effect of electrical stimulation at a longer duration (2 × 3 h/d).

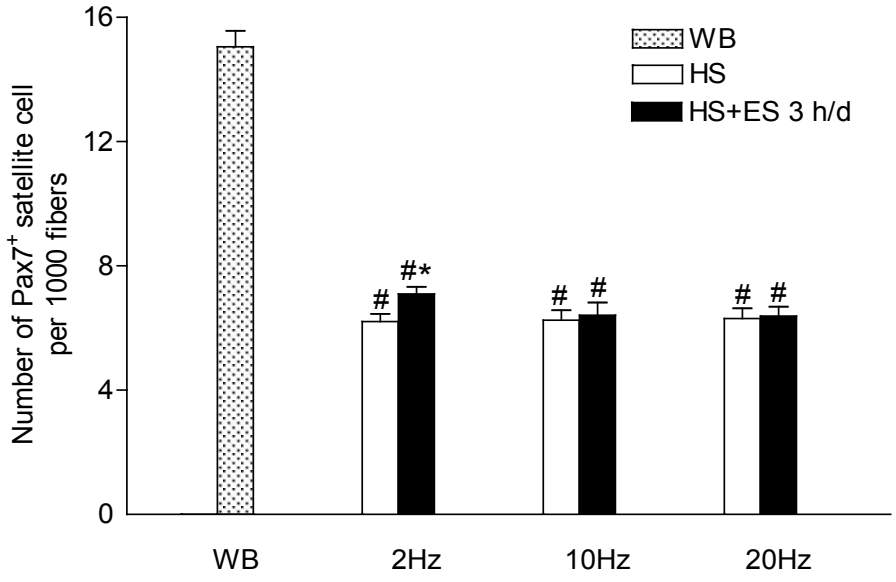

Figure 2.13 The total number ($Pax7^+$) of satellite cells per 1000 fibers in stimulated (HS+ES), HS and WB groups. Data are means ± SEM; # Statistical significance compared with WB group ($P < 0.05$); * Statistical significance between HS and HS+ES groups ($P < 0.05$).

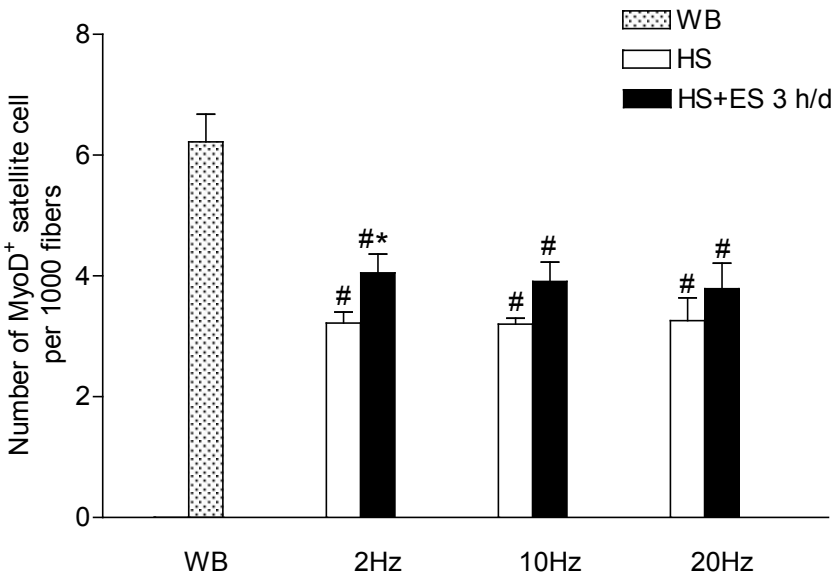

Figure 2.14 The number of activated ($MyoD^+$) satellite cells per 1000 fibers in stimulated (HS+ES), HS and WB groups. Data are means ± SEM; # Statistical significance compared with WB group ($P < 0.05$); * Statistical significance between HS and HS+ES groups ($P< 0.05$).

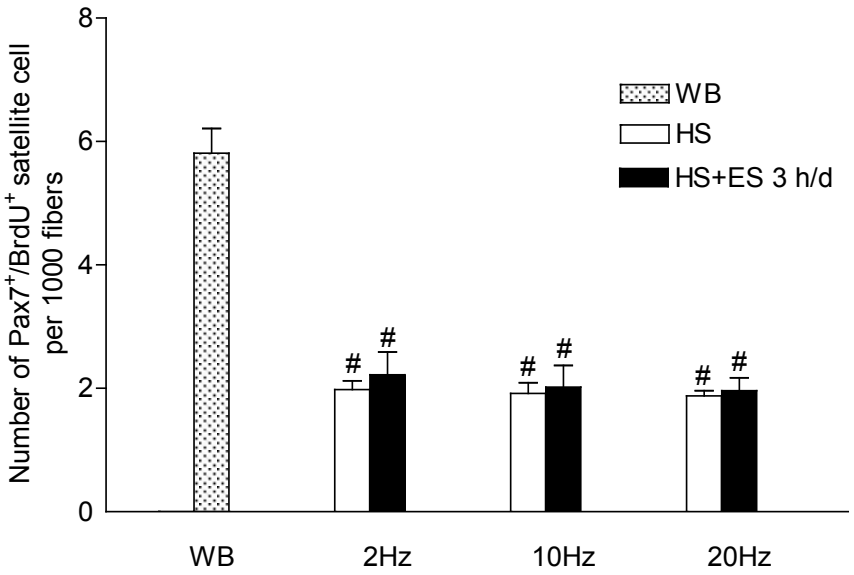

Figure 2.15 The number of proliferating ($Pax7^{+}/BrdU^{+}$) satellite cells per 1000 fibers in stimulated (HS+ES), HS and WB groups. Data are means ± SEM; # Statistical significance compared with WB group ($P < 0.05$).

2.3.4 Effect of different stimulation frequencies for 2 × 3 h/d on soleus disuse atrophy

The stimulation duration was prolonged to 2 × 3 h/d with 2 h interval to investigate its effect on muscle disuse atrophy during 14 d hindlimb suspension. To evaluate the fiber composition changed by hindlimb suspension accurately, real time polymerase chain reaction (PCR) was used for evaluation of MHC I, IIa and IIb mRNA expression. Apoptosis of myonuclei and satellite cells in disused soleus in response to electrical stimulation was also evaluated by TUNEL assay.

Body weight

The body weight between WB and HS+ES groups did not differ at the start of the experiment. Hindlimb suspension for 14 d induced a significant reduction of body weight in the HS+ES group (from 23.39 ± 0.20 g to 21.43 ± 0.19 g, $P < 0.001$). The body weight of the WB group increased by 2.6 % after 14 days.

Muscle mass and fiber CSA

The soleus muscle mass of the HS groups significantly reduced after hindlimb suspension compared with that of the WB group (HS: 8.25 ± 0.44 mg; WB: 14.13 ± 0.37 mg, $P < 0.001$). Electrical stimulation at 10 and 20 Hz for 2 × 3 h/d partially attenuated the decrease in muscle mass by 9.1 % and 7.5 % respectively, compared with that of the HS groups ($P < 0.05$). The 2 Hz stimulation protocol showed the greatest improvement of muscle mass by 32.4 % (10.75 ± 0.68 mg) when compared to that of the HS group (8.12 ± 0.61 mg) ($F_{(2.21)} = 4.57$, $P = 0.022$) (Fig. 2.16).

Similar to the previous experiments, hindlimb suspension induced significant reduction in fiber CSA of soleus. After 14 d, fiber CSA in the HS groups decreased by 23 % compared with that of the WB group (1309.31 ± 65.88 μm^2) ($P < 0.05$). Electrical stimulation using 2, 10 and 20 Hz for 2 × 3 h/d increased fiber CSA by 17 %, 8 % and 5 % compared with the HS groups, respectively (2 Hz: 1220.89 ± 16.15 μm^2, 10 Hz: 1110.58 ± 30.80 μm^2; 20 Hz: 1089.49 ± 30.52 μm^2). Significant difference in terms of fiber CSA was also observed between stimulation using 2 Hz and the higher frequencies (i.e. 10 Hz and 20 Hz; $F_{(2.20)} = 12.45$, $P < 0.001$) (Fig. 2.17). The representative pictures of H&E staining for fiber CSA in WB, HS and HS+ES group after stimulation at 2 Hz were illustrated in Fig. 2.18.

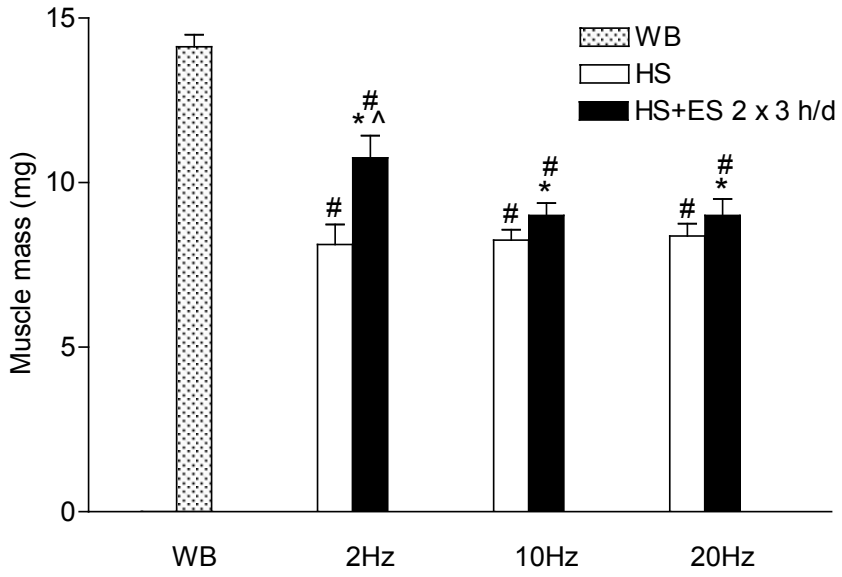

Figure 2.16 Muscle mass in stimulated (HS+ES for 2 × 3 h/d), HS and WB groups. Data are means ± SEM; * Statistical significance ($P < 0.05$) between HS+ES and HS groups using the same frequency. # Statistical significance ($P < 0.05$) compared with WB group. ^ Statistical significance ($P < 0.05$) compared with HS+ES at 10 and 20 Hz groups.

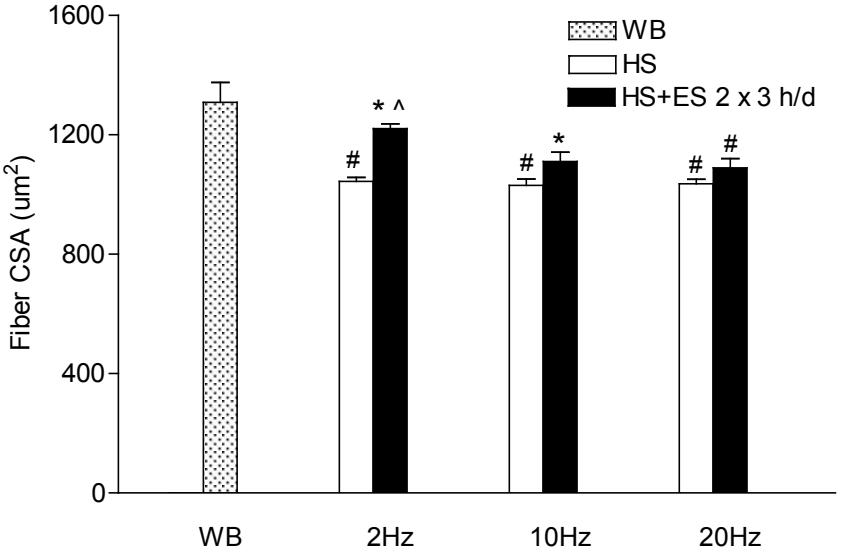

Figure 2.17 Fiber cross-sectional area in stimulated (HS+ES for 2 × 3 h/d), HS and WB groups. Data are means ± SEM; * Statistical significance ($P < 0.05$) between HS+ES and HS groups using the frequency. # Statistical significance ($P < 0.05$) compared with WB group. ^ Statistical significance ($P < 0.05$) between HS+ES at different frequencies.

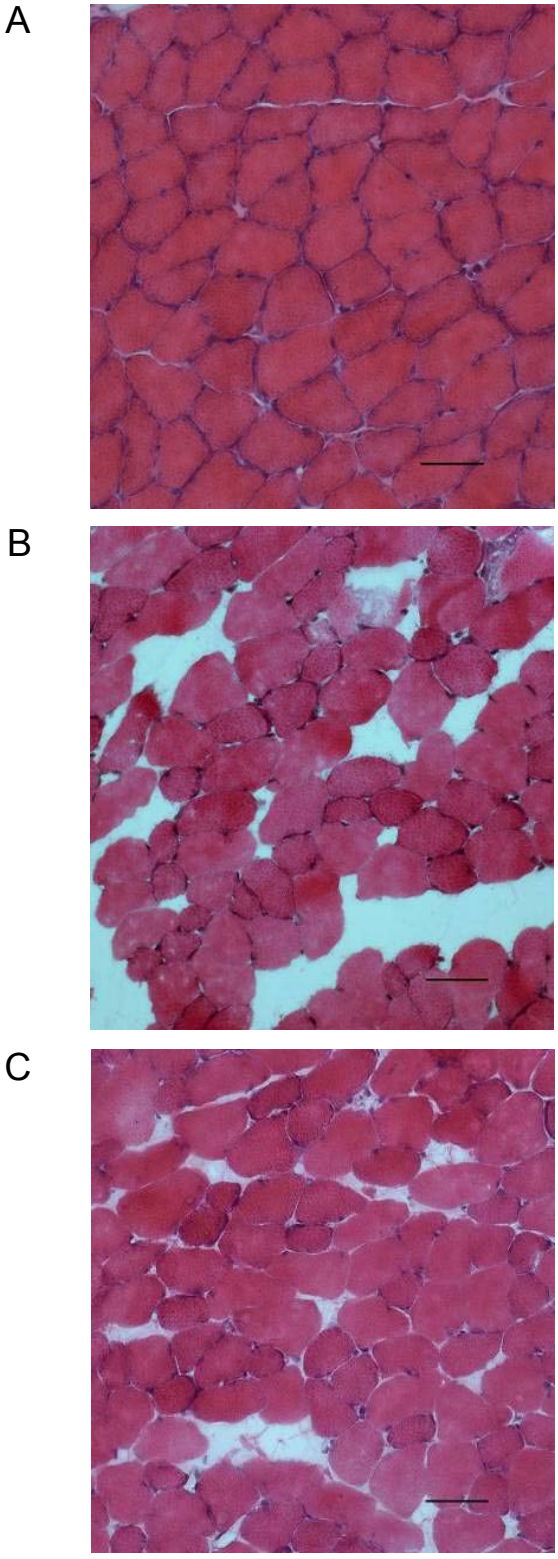

Figure 2.18 The H&E staining of soleus cross sections in WB (A), HS (B) and HS+ES at 2 Hz for 2 × 3 h/d (C) groups. Scale bar = 50 μm.

Muscle maximal tetanic force

After 14 d of hindlimb suspension, the P_0/CSA of soleus reduced by 40-45 % in the HS groups. Electrical stimulation using 2, 10 and 20 Hz for 2 × 3 h/d improved P_0/CSA by 33 %, 12 %, and 14 % respectively compared with that of the HS groups ($P < 0.05$). As shown in Fig. 2.19, stimulation frequency at 2 Hz for 2 × 3 h/d (P_0/CSA: 684.41 ± 24.63 mN/mm^2) attenuated force reduction upon hindlimb suspension more significantly than that at 10 Hz (P_0/CSA: 588.56 ± 16.05 mN/mm^2) and 20 Hz (P_0/CSA: 575.21 ± 16.0 mN/mm^2) ($F_{(2.20)} = 11.87$, $P < 0.001$).

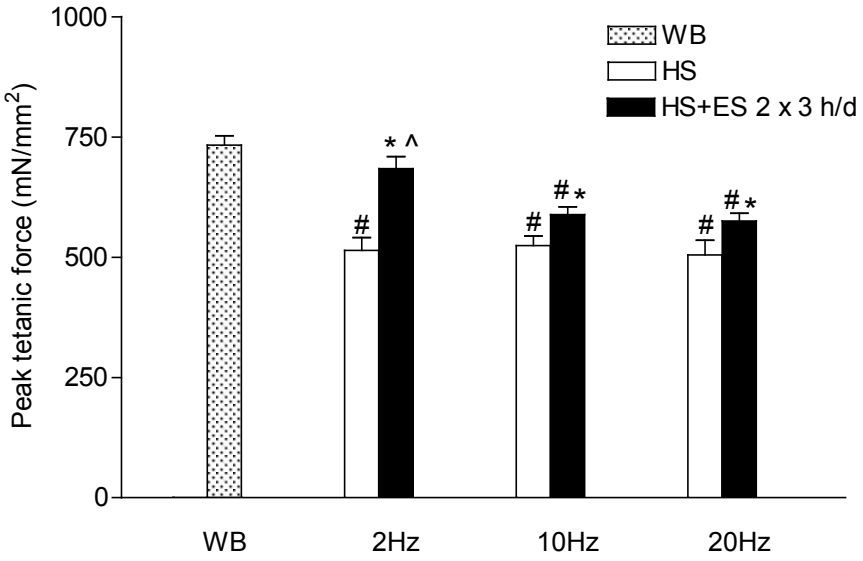

Figure 2.19 The peak tetanic force in stimulated (HS+ES for 2 × 3 h/d), HS and WB groups. Data are means ± SEM; * Statistical significance ($P < 0.05$) between HS+ES and HS groups using the frequency. # Statistical significance ($P < 0.05$) compared with WB group. ^ Statistical significance ($P < 0.05$) between HS+ES at different frequencies.

Fiber type transition

There was a significant reduction of percentage of type I fiber in soleus after hindlimb suspension (HS: 36 ± 2.12 %; WB: 51.68 ± 1.39 %, $P < 0.05$). Electrical stimulation at 2 Hz for 2 × 3 h/d significantly increased type I fiber composition compared with that of the HS group (HS+ES at 2 Hz: 47.52 ± 2.78 %; HS: 36.76 ± 3.01 %; $P < 0.05$). The HS+ES groups at 10 or 20 Hz had no significant effect in attenuating fiber transition following hindlimb suspension (Fig. 2.20). The representative pictures of ATPase staining in WB, HS, and HE+ES at 2 Hz are showed in Fig. 2.21.

The change of gene expression for MHC I, IIa and IIb in response to HS+ES at 2 Hz for 2 × 3 h/d was also evaluated using real time PCR. The results showed that hindlimb suspension significantly reduced MHC I expression by 50 % and increased the expression of MHC IIb by 12-fold compared with WB group ($P < 0.05$), and there was no significant change in MHC IIa expression. Electrical stimulation at 2 Hz for 2 × 3 h/d significantly prevented the transition of fiber type I to type IIb compared with HS group, indicated by a significant increase in MHC I expression as well as a reduction in MHC IIb expression ($P < 0.05$) (Fig. 2.22).

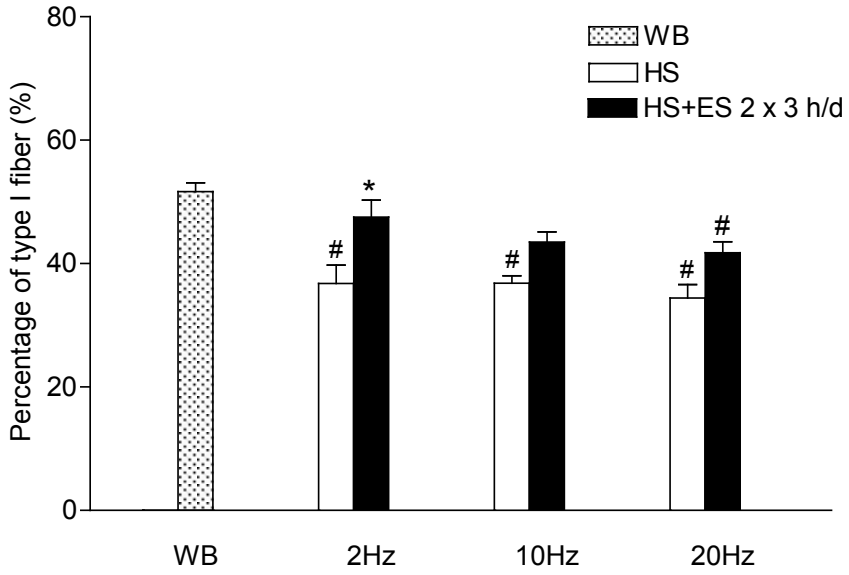

Figure 2.20 Type I fiber composition in stimulated (HS+ES for 2 × 3 h/d), HS and WB groups. Data are means ± SEM; * Statistical significance ($P < 0.05$) between HS+ES and HS groups using the same frequency. # Statistical significance ($P < 0.05$) compared with WB group.

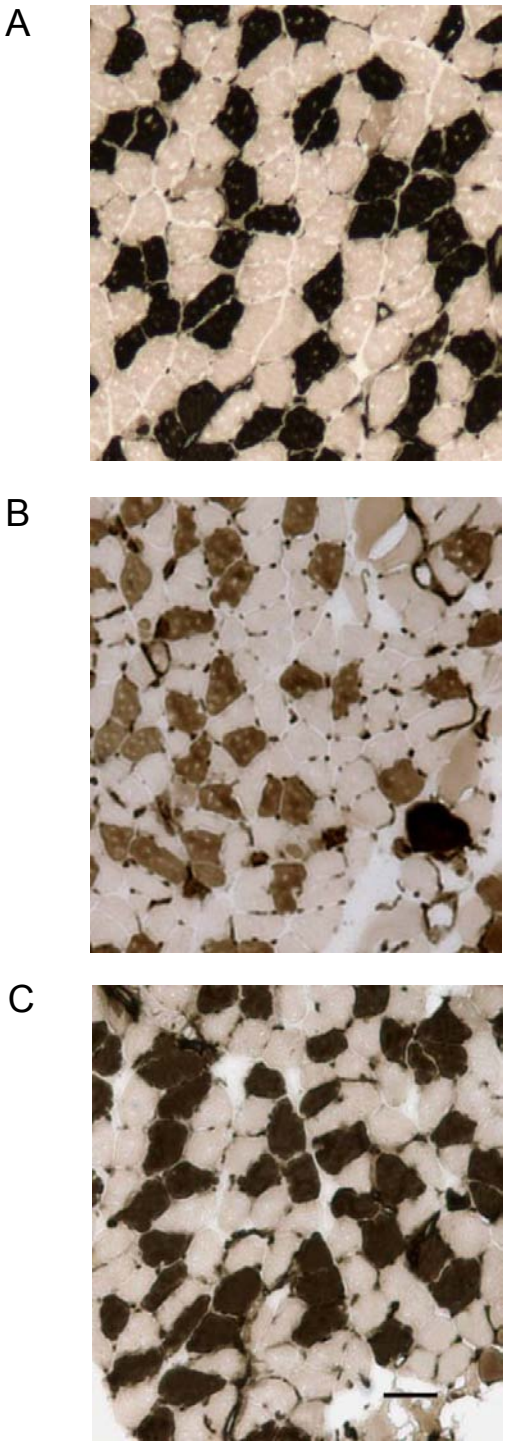

Figure 2.21 Images of ATPase staining for fiber-type compositions (Dark: type I fibers, Light: type II fibers) of soleus in WB (A), HS (B) and HS+ES at 2 Hz for 2 ×3 h/d (C) groups. Scale bar = 50 μm.

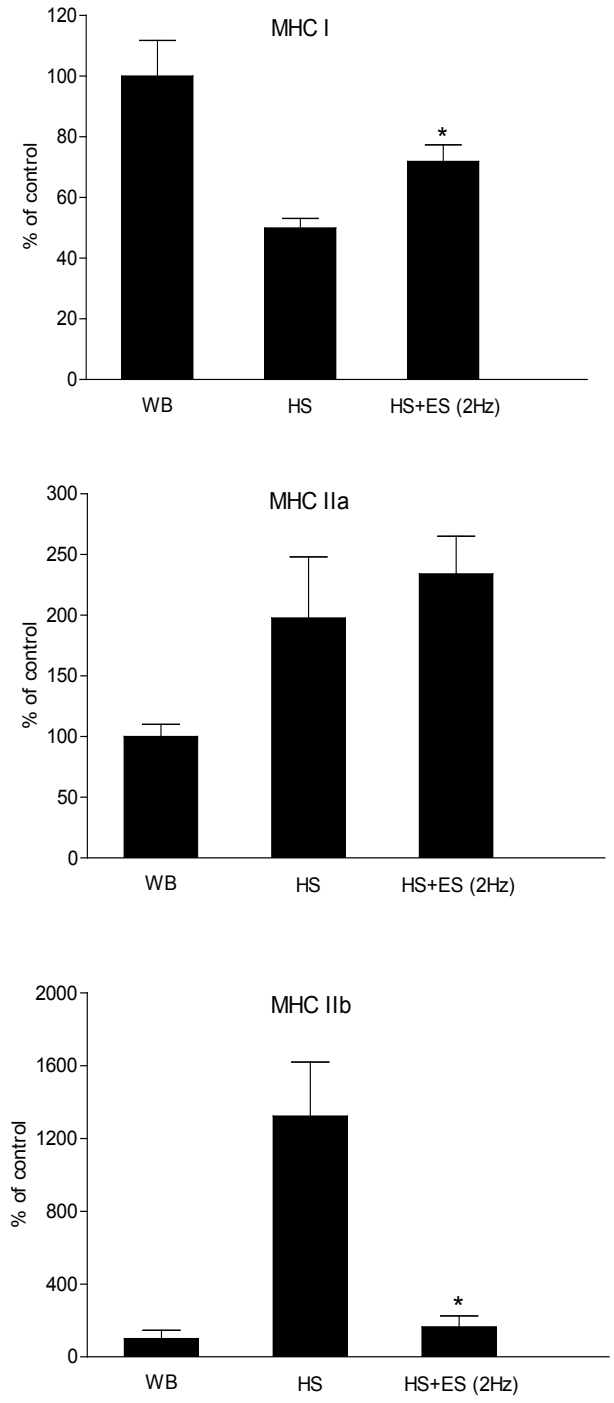

Figure 2.22 The mRNA expression for MHC I, IIa and IIb in WB, HS and HS+ES at 2 Hz for 2 × 3 h/d groups. Data are means ± SEM; n = 4 for each group. *Statistical significance between HS and HS+ES groups ($P < 0.05$).

Satellite cell number and activity

Hindlimb suspension significantly reduced the total number of satellite cells in the HS groups. Electrical stimulation at 10 Hz and 20 Hz for 2 × 3 h/d had a significant effect on preservation of satellite cell pool (Pax 7^{+}) by 32 and 10 %, respectively (10 Hz: HS 6.52 ± 0.47, HS+ES 8.08 ± 0.43; 20 Hz: HS 6.34 ± 0.22, HS+ES: 7.69 ± 0.53, $P < 0.05$); Low frequency electrical stimulation at 2 Hz significantly attenuated the decrease of total satellite cell number by 76 % compared with HS group (HS: 6.46 ± 0.29, HS+ES: 11.36 ± 0.59). The most significant effect using these three protocols was observed in HS+ES at 2 Hz group ($F_{(2.19)} = 14.93$, $P < 0.001$) (Fig. 2.23).

The number of active satellite cells identified by MyoD antibody was significantly increased with 3 different frequencies of electrical stimulation. However, 2 Hz group had a better improvement by 92 % in HS+ES for 2 × 3 h/d compared with HS group (HS: 3.08 ± 0.42, HS+ES: 5.90 ± 0.61, $P < 0.05$) (Fig. 2.24). Moreover, HS+ES at 2 Hz had a 1.2 fold increase in proliferating satellite cell number by using Pax7 and BrdU co-labeling compared with HS group (HS: 1.92 ± 0.10, HS+ES: 4.36 ± 0.33), HS+ES at 2 Hz group had more proliferating satellite cells than HS+ES at 10 and 20 Hz groups ($F_{(2.19)} = 10.88$, $P = 0.001$)(Fig. 2.25).

For differentiating satellite cells, hindlimb suspension reduced the population of myogenin^{+} satellite cells compared to WB group (HS: 1.39 ± 0.05, WB: 2.41 ± 0.20). Electrical stimulation at all frequencies for 2 × 3 h/d showed increased numbers of myogenin^{+} satellite cells compared with HS groups, but only HS+ES at 2 Hz exhibited a significant difference (HS: 1.38 ± 0.06, HS+ES: 1.91 ± 0.15; $P < 0.05$) (Fig. 2.26). The

representative images of detecting satellite cells at different status using specific markers were illustrated in Fig. 2.27.

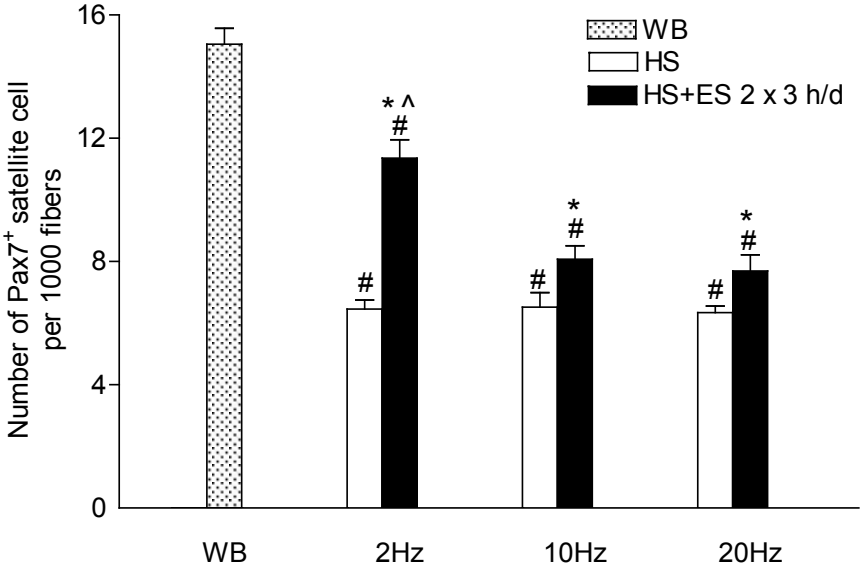

Figure 2.23 The number of total ($Pax7^{+}$) satellite cell per 1000 fibers in stimulated (HS+ES for 2 × 3 h/d), HS and WB groups. Data are means ± SEM; # Statistical significance compared with WB group ($P < 0.05$); * Statistical significance between HS and HS+ES groups ($P < 0.05$). ^ Statistical significance ($P < 0.05$) between HS+ES at different frequencies.

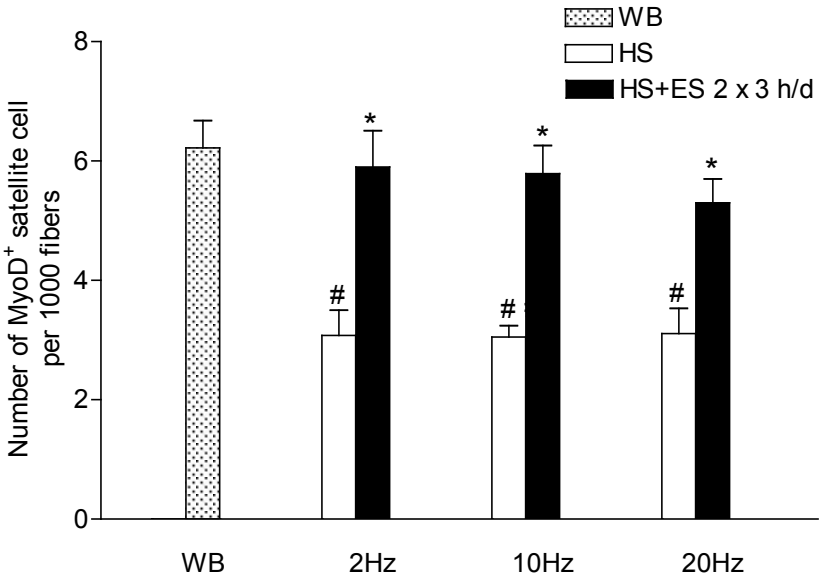

Figure 2.24 The number of activated ($MyoD^+$) satellite cell per 1000 fibers in stimulated (HS+ES for 2 × 3 h/d), HS and WB groups. Data are means ± SEM; # Statistical significance compared with WB group ($P < 0.05$); * Statistical significance between HS and HS+ES groups ($P < 0.05$).

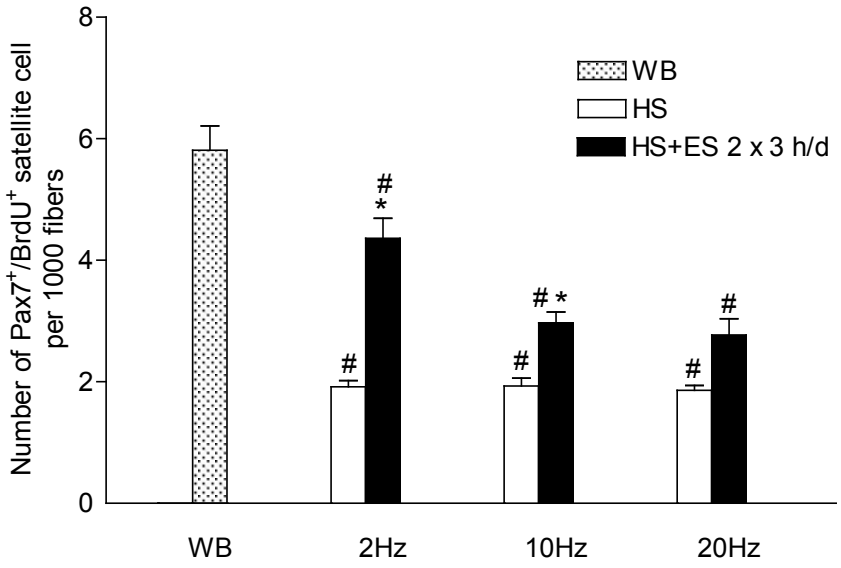

Figure 2.25 The number of proliferating ($Pax7^{+}/BrdU^{+}$) satellite cell per 1000 fibers in stimulated (HS+ES for 2 × 3 h/d), HS and WB groups. Data are means ± SEM; # Statistical significance compared with WB group; * Statistical significance between HS and HS+ES groups ($P < 0.05$).

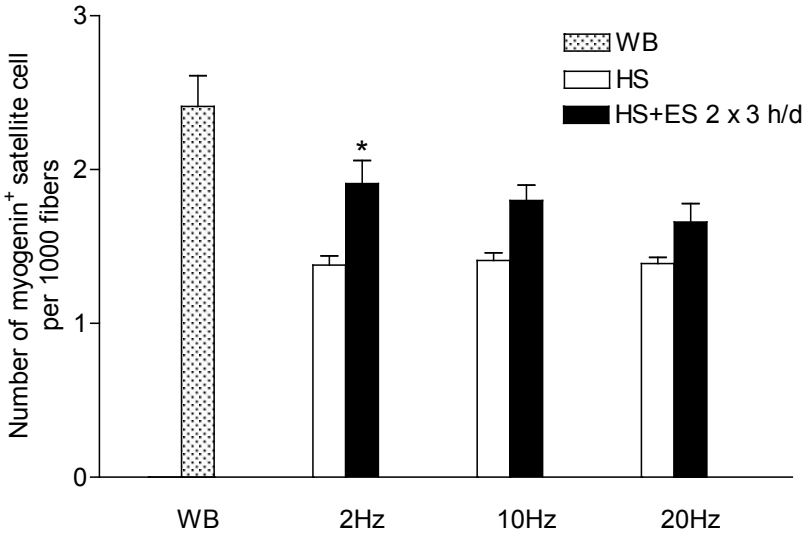

Figure 2.26 The number of differentiating (myogenin$^+$) satellite cell per 1000 fibers in stimulated (HS+ES for 2 × 3 h/d), HS and WB groups. Data are means ± SEM;

* Statistical significance between HS and HS+ES groups ($P < 0.05$).

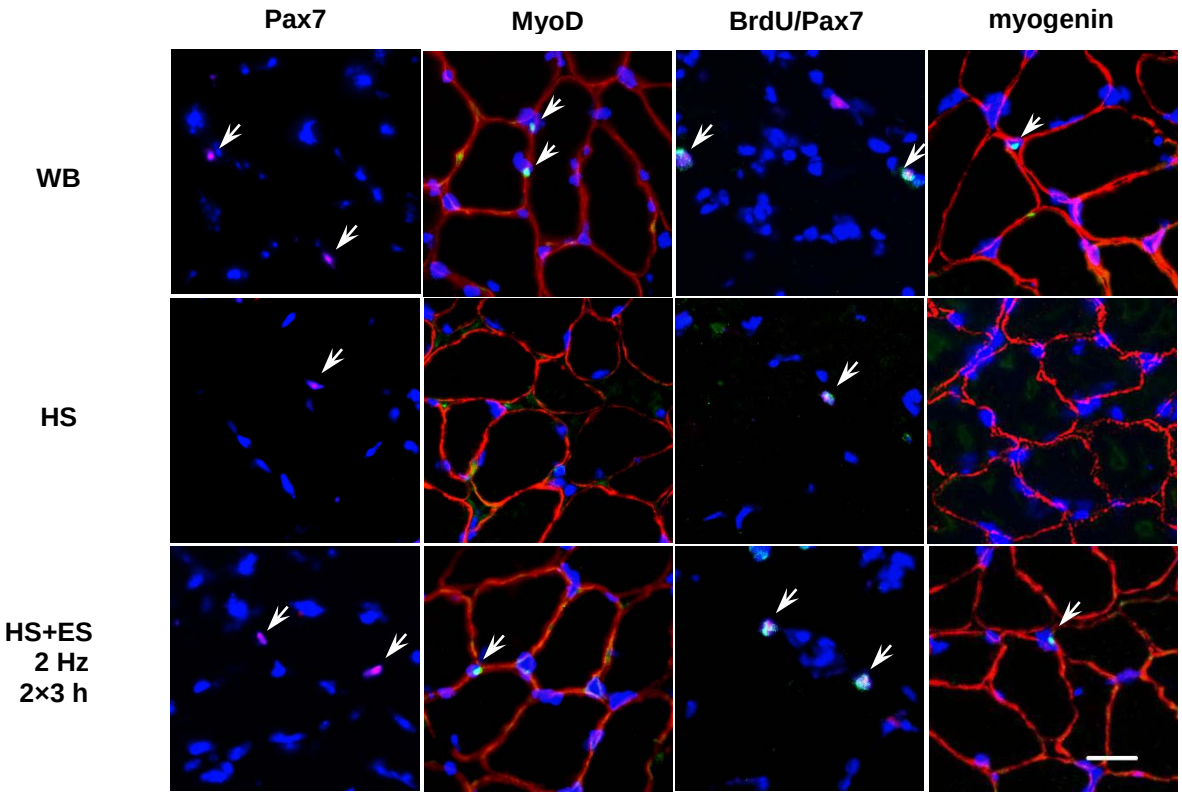

Figure 2.27 Representative images of immunohistochemical staining of total ($Pax7^+$), activated ($MyoD^+$), proliferating ($BrdU^+/Pax7^+$) and differentiating ($myogenin^+$) satellite cells (arrows) of soleus in WB, HS and HS+ES at 2 Hz for 2 × 3 h/d groups. Red: dystrophin, Blue: nuclei; Scale bar = 10 μm.

Apoptosis

TUNEL staining was performed on muscle cross sections to detect apoptotic cells (including myonuclei and satellite cells) in WB, HS and HS+ES at 2, 10 and 20 Hz for 2 × 3 h/d groups. Representative images reacted with TUNEL are shown in Fig. 2.28. The soleus in the WB group showed very few TUNEL-positive nuclei, but the incidence of total TUNEL-positive nuclei increased around 5-fold after hindlimb suspension (WB: 1.25 ± 0.33, HS: 7.07 ± 0.50; $P < 0.05$). Electrical stimulation at 2, 10 and 20 Hz had significantly decreased TUNEL-positive nuclei by 63 %, 40 % and 52 %, respectively ($P < 0.05$) (Fig. 2.29).

The above results demonstrated that electrical stimulation at 2, 10 and 20 Hz for 2 × 3 h/d had better improvement in attenuating muscle disuse atrophy, and with 2 Hz 2× 3 h/d being the best optimal parameter in improving muscle mass, fiber CSA, the maximal tetanic force and the number of satellite cells.

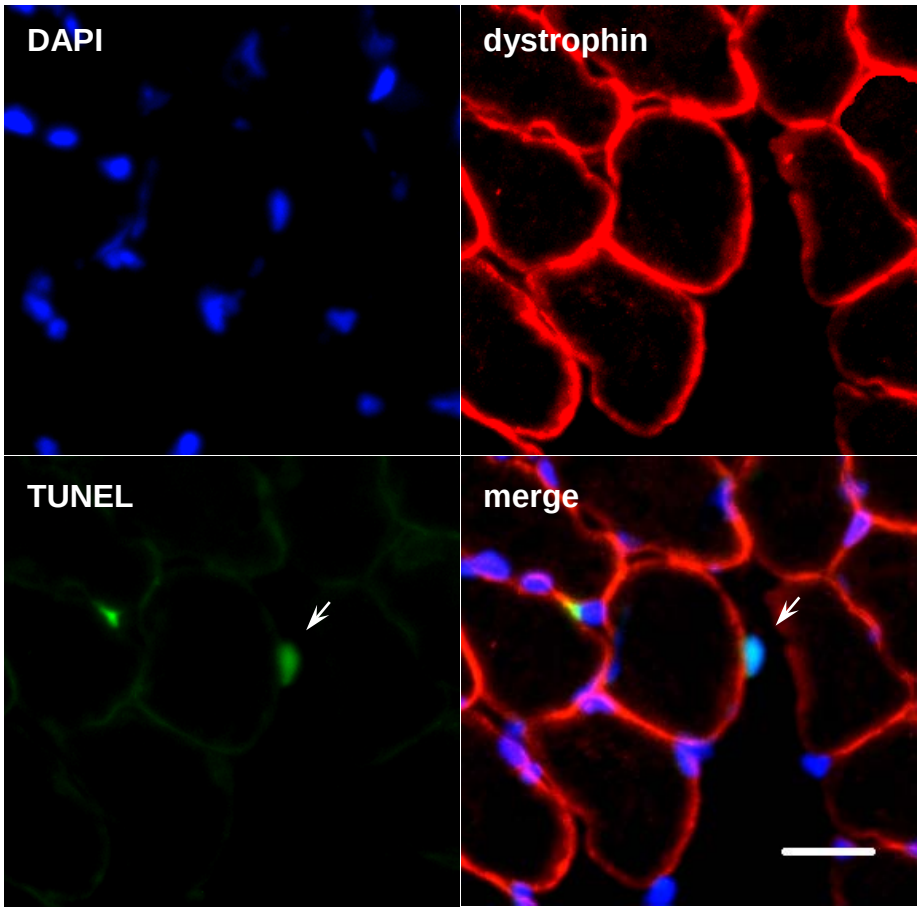

Figure 2.28 Images of the immunohistochemical staining for TUNEL^{+} cell, dystrophin and DAPI in transverse cryosection of the soleus muscle in HS+ES at 2 Hz for 2 × 3 h/d group. Arrow shows the TUNEL-positive nuclei located outside dystrophin. Scale bar = 10 μm.

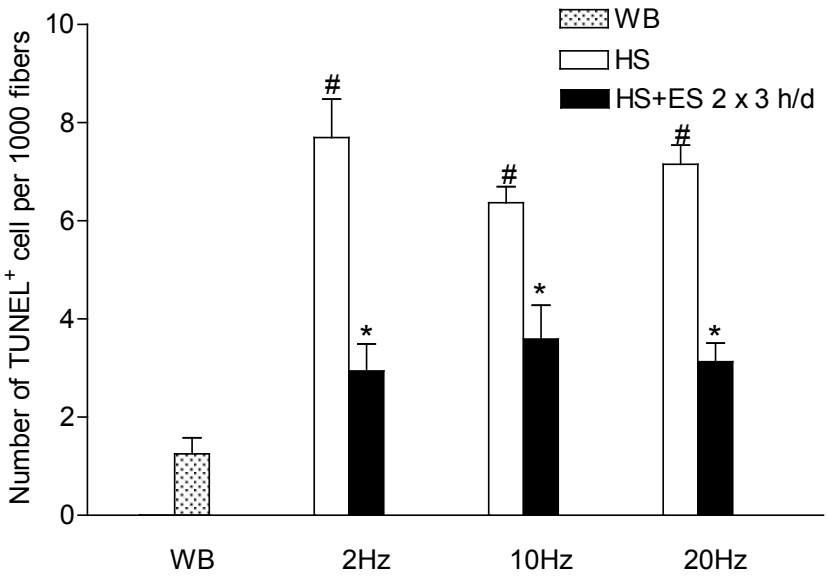

Figure 2.29 Number of TUNEL^{+} cell per 1000 fibers in stimulated (HS+ES for 2 × 3 h/d), HS and WB groups. Data are means ± SEM; * Statistical significance between HS and HS+ES groups ($P < 0.05$); $^{\#}$ Statistical significance between HS and WB groups ($P < 0.05$).

2.4 DISCUSSION

In this study, we used morphological and immunohistochemical analyses to determine the effects of low frequency electrical stimulation on anti-gravity soleus muscle undergoing disuse-induced atrophy. Our main findings were that (i) the reduction of muscle CSA and force of soleus muscle were attenuated by the application of electrical stimulation. Stimulation frequency at 2 Hz and the duration for 2 × 3 h/d produced the most beneficial effect; (ii) electrical stimulation increased the total number ($Pax7^+$), and the activated and proliferating satellite cell population ($MyoD^+$ and $Pax7^+/BrdU^+$) in the HS+ES group compared with HS group; and (iii) electrical stimulation for 2 × 3 h/d promoted satellite cell differentiation ($myogenin^+$) and protected cells from apoptosis.

We chose soleus as our target muscle because slow-twitch muscle showed greater atrophy than fast-twitch muscle in disuse experiments and satellite cells were reported to be more plentiful in slow twitch muscles than in fast twitch muscles regardless of species (Dusterhoft *et al.*, 1990). Non-invasive surface electrodes were used in this study to avoid injury to the muscle, since injury can be a trigger for satellite cell proliferation. In agreement with previous studies (Mitchell & Pavlath, 2004; Wang *et al.*, 2006; Kawano *et al.*, 2008; Matsuba *et al.*, 2009; Zhang *et al.*, 2010), the total number and mitotic activity of satellite cell decreased following hindlimb suspension. Our hindlimb suspension model was 14 d, and it was long enough to show a significant decrease by 57 % in total number of satellite cells. The loss of satellite cells was possibly related to a decrease in mechanical stress and an increase of satellite cells undergoing apoptosis. Technically, satellite cells were counted on transverse cryosections, the quantification result might be different from that of cell culture and single muscle fiber. We used Pax7

as the marker for satellite cell detection and co-labeled proliferating satellite cells with BrdU. Pax7 was reported to be expressed by both quiescent and proliferating satellite cells *in vitro* and *in vivo* (Zammit *et al.*, 2004), it would be more precise for quantification of satellite cells at specific status during cell cycle. BrdU was injected 24 h before the mice were sacrificed, therefore our results only reflected the proliferation activity of satellite cells at this given time point. Pulsing the satellite cells with BrdU for 24 h rather than for days has an advantage of demonstrating the exact numbers of proliferating cells in the past 24 h. Increasing the duration of BrdU incorporation may result in mistaking those $BrdU^+$ cells that divided days ago but no longer a dividing cell at this particular time point.

Skeletal muscle disuse atrophy following hindlimb suspension, immobilization, and denervation is associated with an increase of nuclei elimination from the existing fibers by apoptosis (Allen *et al.*, 1997; Leeuwenburgh *et al.*, 2005). In previous animal studies, skeletal muscle atrophy caused by disuse was related to myonuclei apoptosis (Allen *et al.*, 1997; Leeuwenburgh *et al.*, 2005; Dupont-Versteegden *et al.*, 2006b) and satellite cell nuclear apoptosis (Alway & Siu, 2008). In contrast to previous studies, a recent study used *in vivo* time-lapse microscopy to observe single fibers and found no loss of myonuclei in fast or slow twitch muscle fibers following denervation and unloading induced muscle atrophy (Bruusgaard & Gundersen, 2008). The result suggested that disuse induces apoptotic activity mainly in muscle stromal and satellite cells. In the present study, the total TUNEL-positive nuclei including myonuclei and satellite cells increased around 5-fold after 14 d of hindlimb suspension. In order to discriminate the apoptotic satellite cells from the apoptotic myonuclei, double labeling

with Pax7 and early apopotic marker such as cleaved form of caspase 3 should be performed in further studies.

Electrical stimulation is generally considered a countermeasure for disuse atrophy. According to the characteristics of slow-twitch soleus muscle, it contains more satellite cells than fast-twitch muscle and the rate of satellite cell loss after hindlimb suspension is greater in soleus than in fast muscles. The loss of satellite cells were related to a decrease in mechanical load (Zhang *et al.*, 2010). In the present study, the total satellite cell number, the proliferation and differentiation activities were improved in response to electrical stimulation, possibly through the mechanotransduction to satellite cells. The magnitude of improvement varied between different stimulation protocols.

The effect of electrical stimulation depends on the stimulation frequency. A previous study in our laboratory has shown that electrical stimulation at 20 Hz for 2 ×3 h/d produced some beneficial effect in rat skeletal muscle atrophy following 28 d of hindlimb suspension (Zhang *et al.*, 2010). Another study demonstrated that electrical stimulation at 10 Hz was less effective than 2 Hz at preventing disuse atrophy; rat soleus decreased in muscle mass by only 10 % when stimulated at 2 Hz for 10 h/d, compared to a reduction by 26 % when stimulated at 10 Hz for either 2 or 10 h/d for 7 days (Dupont Salter *et al.*, 2003). The result observed in the present study demonstrated that stimulation at 2 Hz was more efficient at preserving muscle mass, fiber CSA and muscle force than stimulation at 10 and 20 Hz. This low frequency pattern of stimulation matches slow-twitch muscle properties and the motor unit firing pattern could contribute to the beneficial effect. Low frequency electrical stimulation may generate a mechanical signal

that partially counteracts the degenerating effects on soleus muscles caused by disuse atrophy.

In consistent with previous studies (Putman *et al.*, 1999; Putman *et al.*, 2001), electrical stimulation induced fast-to-slow fiber type transformation. In the present study, electrical stimulation using 2 Hz for 2 × 3 h/d significantly increased type I fiber composition and increased MHC I mRNA expression compared with unloaded soleus muscle; however, there was no significant change observed for 3 h/d groups in any of the electrically stimulated frequencies tested. Moreover, longer duration of electrical simulation for 2 × 3 h/d achieved better effects on preservation of satellite cell pool and promotion of satellite cell proliferation and differentiation. There may be a threshold of mechanical signals needed by satellite cells. The signal provided by electrical stimulation for the duration of 3 h/d could well be below the threshold, whereas increasing the duration to 2 × 3 h/d reached a threshold to accumulate or attain sufficient signal required to elicit responses that counteracted muscle atrophy. That could possibly account for the detection of more proliferating satellite cells committed into myogenic differentiation (myogenin^{+} satellite cell) and significantly less cells undergoing apoptosis with the stimulation protocol of 2 × 3 h/d. The findings here suggest that the overall effect of electrical stimulation was duration dependent rather than frequency dependent.

The proliferation of satellite cells may be balanced by cell apoptosis, which may serve as a regulatory feedback response in hindlimb suspension induced skeletal muscle atrophy. In the present study, electrical stimulation at 2 Hz for 2 × 3 h/d had significantly decreased TUNEL-positive nuclei by 63 % after 14 d of hindlimb suspension. The effect

of electrical stimulation may contribute to maintenance of the balance of cell proliferation and apoptosis.

Unpublished data generated in our laboratory have shown that electrical stimulation significantly upregulated an anti-apoptotic regulatory factor, Bcl-2, in unloaded soleus muscles. Baewer *et al.* (2004) suggested that unloading-induced lesions might be related to Ca^{2+}-dependent protease calpain induced proteolysis. The authors further suggested that stretching might prevent Ca^{2+} accumulation by reducing the overlap of thick and thin filaments, and consequently promote diffusion and removal of Ca^{2+}. In fact, calpain has been shown to promote apoptosis by inducing cleavage of the Bcl-2 protein (Gil-Parrado *et al.*, 2002). Both stretching and electrical stimulation worked similarly by generating tension required by the slow-twitch muscle, thus it is possible that electrical stimulation improved muscle function by suppressing apoptosis of satellite cells through inhibition of Ca^{2+} accumulation and hence blocked the calpain-mediated Bcl-2 cleavage.

There are many other possible mechanisms of electrical stimulation in regulating satellite cell activity and preventing skeletal muscle disuse atrophy. A study provides evidence that the function of the nuclear factor of activated T cells (NFAT) as a transcriptional activator is regulated by neuromuscular stimulation, and the expression of transient receptor potential channel (TRPC3) is up-regulated by neuromuscular activity in a calcineurin-dependent manner (Rosenberg *et al.*, 2004). Cellular and molecular study has demonstrated that low frequency electrical stimulation induces angiogenesis in skeletal muscle by increasing vascular endotherial growth factor (VEGF) and HGF production (Nagasaka *et al.*, 2006). IGF-1 and MGF are closely related to satellite cell

proliferation (Machida & Booth, 2004; Goldspink, 2006), and MGF not only activates satellite cells but also upregulates protein synthesis in skeletal muscle, the expression pattern of IGF-1 and MGF and their function for regulation of muscle mass in response to electrical stimulation need to be further investigated.

2.5 CONCLUSION

This study has demonstrated that mechanical unloading induces disuse atrophy in slow-twitch soleus muscle leading to decreased muscle mass, fiber CSA, maximal tetanic force; slow-to-fast fiber transition, increased apoptosis and impaired satellite cell activities. Electrical stimulation can partially attenuate muscle disuse atrophy by improving muscle mass, fiber CSA, the maximal tetanic force, and the activation and proliferation of satellite cells. The results indicate that electrical stimulation at 2 Hz for 2 × 3 h/d is the optimal protocol in the attenuation of unloading-induced disuse atrophy.

CHAPTER 3

Expression of Mechano Growth Factor (MGF)

and Satellite Cell Activity

3.1 INTRODUCTION

The results in Chapter 2 demonstrated that decreased mechanical signals via hindlimb suspension lead to muscle disuse atrophy and impaired satellite cell activation and proliferation. Electrical stimulation attenuates muscle atrophy by increasing the muscle mass, fiber CSA and force production; moreover, the activation and proliferation of satellite cells have also improved in response to electrical stimulation.

The possible mechanism which may lead to the beneficial effects of electrical stimulation is not clear. There are many possible factors responsible for muscle regeneration and related to satellite cell proliferation, such as IGF-I (Velloso & Harridge, 2010), LIF (Broholm *et al.*, 2011) and HGF (Li *et al.*, 2009). Since some factors seem to be activated in response to muscle injury rather than mechanical signals, such as HGF (O'Reilly *et al.*, 2008), these candidates are not addressed in this investigation. IGF-1 is known to induce muscle hypertrophy. Yang *et al* (1996) demonstrated that murine IGF-1 was alternatively spliced into a systemic IGF-IEa (commonly known as IGF-I) and a muscle-specific IGF-IEb and is now termed mechano growth factor (MGF). However, several reports have indicated that MGF induced a more rapid and potent regenerative response as compared to IGF-I (Hameed *et al.*, 2003; see reviewed Philippou *et al*., 2007).

MGF serves as a tissue repair factor that responds to changes in local physiological conditions or environmental stimuli. In response to mechanical loading MGF expression has been shown to increase and it appears that this may be regulated transcriptionally (Yang *et al.*, 1996). Furthermore increased proliferation of satellite cells has also been shown to be regulated by MGF (Yang & Goldspink, 2002). Thus, taking these

observations into account, it is possible that MGF participates in the regulation of satellite cell activity in response to electrical stimulation.

The sensitivity of MGF to mechanical signals has been investigated using various models of mechanical stimulation in both animals and humans. MGF expression in the skeletal muscle of healthy humans has been demonstrated to be upregulated through resistance exercise (Hameed *et al.,* 2003; Hameed *et al.,* 2004), isometric (Greig *et al.,* 2006) and eccentric exercises (Hameed *et al.,* 2008). Studies have reported that this upregulation could occur as early as within 2.5 hours of the exercise bout followed by a prolonged increase of another splicing IGF-1Ea mRNA expression (Greig *et al*., 2006; (Philippou *et al.,* 2009). In rodent skeletal muscles, MGF mRNA expression is increased by electrical stimuli at 10 Hz (McKoy *et al.,* 1999) and mechanically induced local damage (Hill & Goldspink, 2003).

MGF was also demonstrated to activate satellite cell by *in vitro* experiments. When C2C12 cells were transfected with MGF cDNA, the cellular proliferation increased after 24 hours (Yang & Goldspink, 2002). This suggests that MGF may play a role in promoting cell proliferation *in vitro*. In a local muscle damage model of rat, MGF in the tibialis anterior muscle was produced as a pulse lasting for a few days in response to damage, and the mRNA level of MyoD as a marker for satellite cell activation significantly increased (Hill & Goldspink, 2003). Since there is no specific antibody against MGF, definitive evidence supporting the function of MGF is lacking. The time frame of MGF expression in relation to satellite cell proliferation in disuse muscle atrophy is not well understood.

3.1.1 Aim of the study

The purpose of this study is to observe MGF mRNA expression in soleus muscle in response to hindlimb suspension with and without electrical stimulation at day 2, 3 and 7 of unloading. Accordingly the satellite cell pool and proliferation activity at these time points were evaluated to investigate potential physiological function of MGF on satellite cell activity.

3.2 MATERIALS AND METHODS

3.2.1 Experimental design

Studies have reported that MGF upregulation could occur on a time scale of hours after the exercise bout (Greig *et al*., 2006; Philippou *et al*., 2009). As such changes of gene expression must be analyzed during the initial hours or days of unloading in order to define the molecular events underlying MGF. The expression of MGF was evaluated at day 2, 3 and 7 during hindlimb suspension. Male Balb/c mice (10 wk) were hindlimb suspended for 2, 3 and 7 d. The animals were subjected to hindlimb suspension as previously described in Chapter 2. At each time point, electrical stimulation at 2 Hz for 2 × 3 h/d was applied to both legs of the mice (HS+ES). Another group of animals were hindlimb unloaded without electrical stimulation (HS). Weight bearing mice served as control group (WB). The expression of MGF in the soleus muscle was evaluated using real time PCR. The satellite cell total number and proliferation were investigated using double-immunostaining with Pax 7 and BrdU. For animals subjected to satellite cell investigation, the mice were injected intraperitoneally with BrdU (30mg per kg body weight) daily during hindlimb suspension. The experimental design is illustrated in the following flowchart (Fig. 3.1). All the animal handling procedures and experimental protocols were approved by the Animal Subjects Ethics Committee of The Hong Kong Polytechnic University before conducting the experiments (ASESC No.09/12, Appendix V). A license to conduct animal experiments was also endorsed by the Department of Health of the Hong Kong Government (Appendix VI).

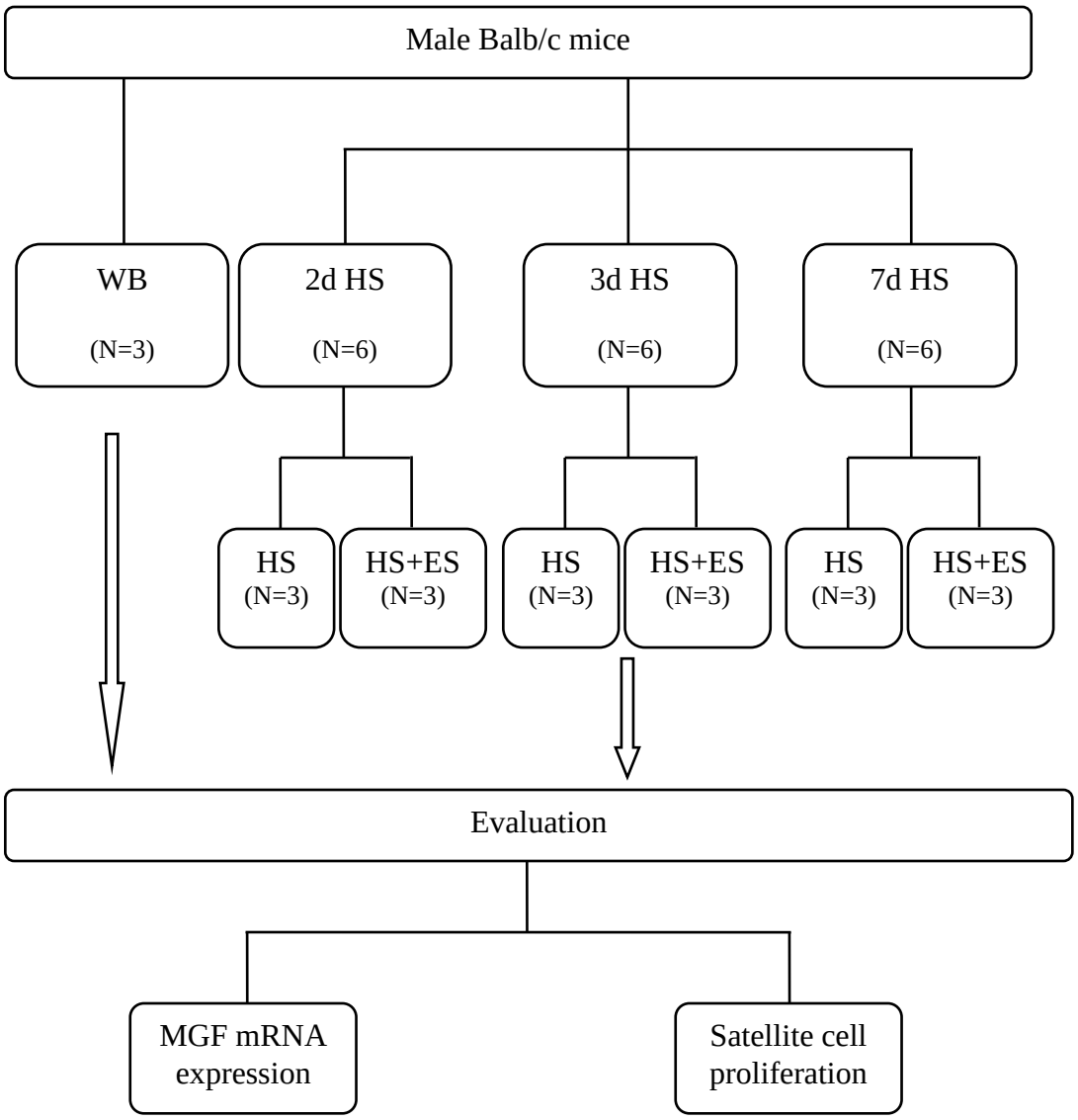

Figure 3.1 The experimental design.

3.2.2 Electrical stimulation protocol

The preparation and electrodes attachment processes are the same as previously described in Chapter 2. Electrical stimulation at 2 Hz for 2 × 3 h/d was used since this protocol has been demonstrated to be optimal in attenuating muscle atrophy.

3.2.3 MGF expression

The expression of MGF was examined using real-time PCR. The RNA of soleus was purified using the same protocol shown in Appendix III. Taqman-MGB probe of MGF (MGF-Ieb) (Applied Biosystems, Foster City, CA, USA) was used for PCR amplification. The sequences of the primers used were: forward primer is 5'-GACATGCCCAAGACTCAGAAGT-3'; reverse primer is 5'-CTTCTCCTTTGCAGCTTCGTTTT-3'. For each sample, 1.5 μl of cDNA was amplified in a 25 μl TaqMan Master Mix (Applied Biosystems, the component for each sample was 1.5 μl cDNA, 12.5 μl Master Mix, 1.25 μl probe and 9.75 μl H_20), using a 7500 real time PCR system (Applied Biosystems). GAPDH (Applied Biosystems) was used as the endogenous control. Relative changes in MGF gene expression were determined using the $2^{-\Delta\Delta Ct}$ method of analysis as described in Chapter 2.

3.2.4 Satellite cell activity

The mice were injected intraperitoneally with BrdU (30mg per kg body weight) daily during hindlimb suspension. To determine the total number of satellite cells and the proliferation activity, double immunostaining by Pax7 and BrdU were used. The protocol of immunostaining has been described in Chapter 2. The $Pax7^+$ nuclei and the

$Pax7^+/BrdU^+$ nuclei were counted respectively on two serial transverse sections of each sample. After immunostaining, the same sections were stained for H&E to count the total fiber number. The number of satellite cells and proliferating satellite cells were expressed per 1000 muscle fibers.

3.2.5 Statistics

The values were expressed as means ± SEM. Differences between group means were assessed by analyses of variance (one-way ANOVA) followed by post-hoc comparison t-tests with Bonferroni correction. Differences were considered significant using *P*-value with appropriate Bonferroni adjustment. The level of significance was set at $P < 0.05$.

3.3 RESULTS

3.3.1 MGF expression in soleus muscle

MGF mRNA expression in soleus of HS groups was compared with that in WB, and HS+ES groups at day 2, 3 and 7 of hindlimb suspension (Fig. 3.2). At days 2 and 3, MGF expression levels in the HS group were significantly decreased when compared with WB group (HS day 2: 0.93 ± 0.16, HS day 3: 1.21 ± 0.13, WB: 2.16 ± 0.21; $P < 0.05$). At all time points, the mRNA expression of MGF in HS+ES groups were higher than that in the HS groups. Electrical stimulation significantly upregulated MGF expression compared to that of the HS group at day 2 and 3 during hindlimb suspension (HS+ES day 2: 1.94 ± 0.21, HS+ES day 3: 2.18 ± 0.22, $F_{(6.32)} = 6.28$, $P < 0.001$). This increase is particularly evident in day 2 where MGF expression showed ~1-fold increase in the HS+ES group compared to that of the HS group. Although significant difference was not observed at day 7 between HS and HS+ES groups, MGF expression of HS+ES group still maintained at a higher level when compared with HS group. The results demonstrated that MGF mRNA expression were downregulated in response to mechanical unloading. On the contrary, electrical stimulation upregulated MGF expression at day 2 during hindlimb suspension and continued to maintain at a significantly higher level at day 3.

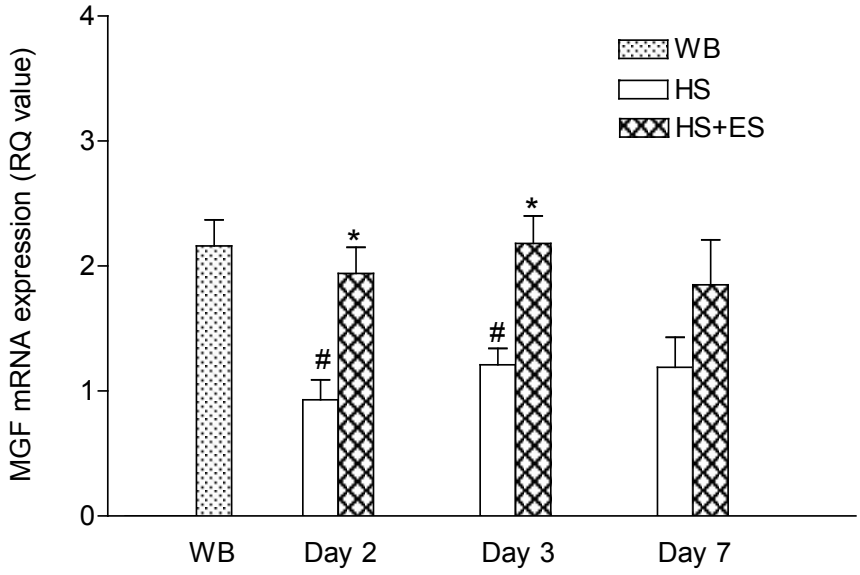

Figure 3.2 MGF mRNA expression in the soleus muscle of weight bearing (WB), hindlimb suspension (HS) groups and hindlimb suspension with electrical stimulation at 2 Hz for 2 × 3 h/d (HS+ES) at day 2, 3 and 7 using real time PCR experiment. Data are means ± SEM; # Statistical significance compared with WB group. * Statistical significance between HS and HS+ES groups.

3.3.2 Satellite cell proliferation

In order to relate the expression of MGF to the activity of satellite cells, immunostaining for the total number ($Pax7^+$) and proliferating satellite cells ($Pax7^+/BrdU^+$) in soleus muscle at day 2, 3 and 7 of hindlimb suspension with and without electrical stimulation were investigated (Fig. 3.3 & 3.4). At day 2 and 3 of hindlimb suspension, the expression level of MGF was upregulated in the HS+ES groups. Furthermore the total number of satellite cells (Pax 7^+) in HS+ES groups increased compared with that of HS groups (HS day 2: 9.44 ± 0.62, HS+ES day 2: 11.2 ± 0.73, HS day 3: 9.46 ± 0.43, HS+ES day 3 11.58 ± 0.43). At day 7 of hindlimb suspension, the total number of satellite cells significantly increased in the HS+ES group when compared with the HS group (HS: 8.58 ± 0.90; HS+ES: 12.00 ± 0.34, $F_{(5.20)} = 6.77$, $P = 0.001$).

Although the proliferating satellite cells detected by co-immunustaining of Pax7 and BrdU increased in HS+ES groups compared with HS groups during day 2 and day 3 of hindlimb suspension, the results were not significant (HS day 2: 2.93 ± 0.46, HS+ES day 2: 4.1 ± 0.57, HS day 3: 2.54 ± 0.07, HS+ES day 3: 3.64 ± 0.6). However, at day 7 of suspension, there was a significant increase in satellite cell proliferation activity ($Pax7^+/BrdU^+$) in the HS+ES group compared to the HS group (HS: 2.51 ± 0.47; HS+ES: 5.01 ± 0.50, $F_{(5.20)} = 5.29$, $P = 0.003$). The representative pictures of immunostaining for total number ($Pax7^+$) and proliferating satellite cells ($Pax7^+/BrdU^+$) in HS and HS+ES groups were illustrated in Fig. 3.5.

The peak of MGF expression at day 3 of hindlimb suspension occurred prior to the increase of satellite cell total number and proliferation at day 7 of hindlimb suspension.

This temporal relationship possibly suggests that the effect of electrical stimulation on MGF mRNA upregulation was prior to satellite cell proliferation improvement.

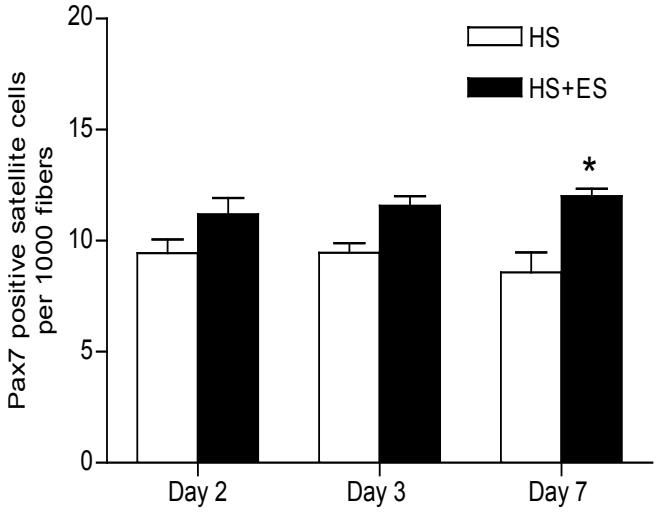

Figure 3.3 The total number ($Pax7^{+}$) of satellite cells in the soleus muscle of hindlimb suspension (HS) groups and hindlimb suspension with electrical stimulation at 2 Hz for 2 × 3 h/d (HS+ES) at day 2, 3 and 7. Data are means ± SEM; * Statistical significance between HS and HS+ES groups.

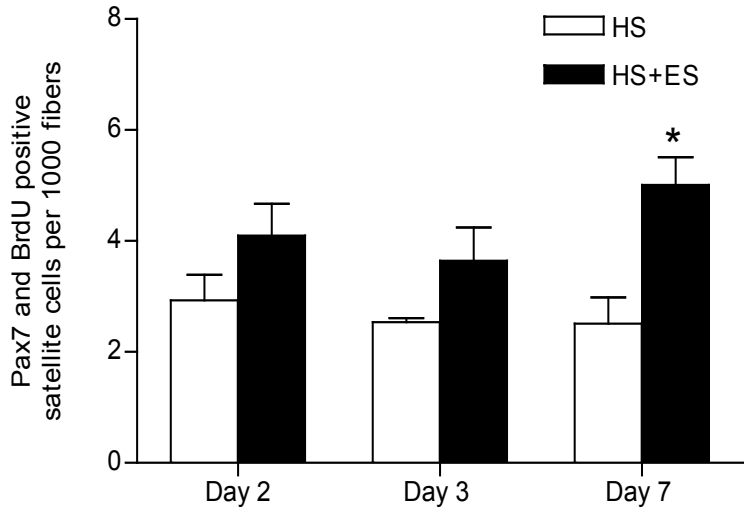

Figure 3.4 The proliferating ($Pax7^{+}/BrdU^{+}$) satellite cells in the soleus muscle of hindlimb suspension (HS) groups and hindlimb suspension with electrical stimulation at 2 Hz for 2 × 3 h/d (HS+ES) at day 2, 3 and 7. Data are means ± SEM; * Statistical significance between HS and HS+ES groups.

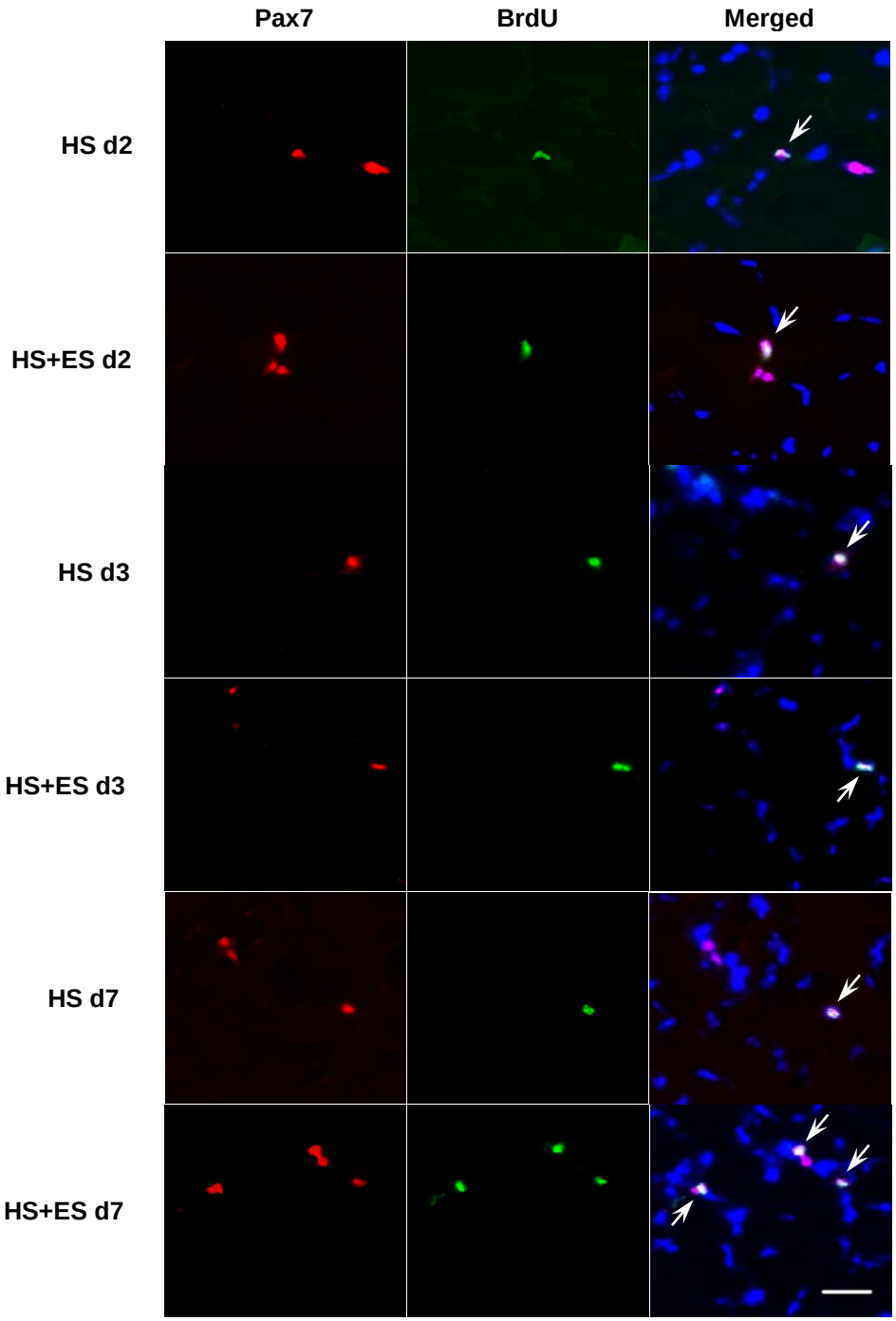

Figure 3.5 The representative images of immunostaining for total number ($Pax7^{+}$) and proliferating satellite cells ($Pax7^{+}/BrdU^{+}$, indicated by arrows) in HS and HS+ES groups at day 2, 3 and 7. Scale bar = 10 μm.

3.4 DISCUSSION

The purpose of this study is to understand the possible mechanism which may lead to the favorable changes induced from electrical stimulation through regulation of satellite cell proliferation. The results showed that the mRNA level of MGF in the soleus muscle significantly upregulated as early as day 2 and day 3 in response to electrical stimulation. This upregulation occurred prior to the increased satellite cell proliferation at day 7 of hindlimb suspension.

The result is in agreement with previous studies reporting that MGF expression responds quickly to mechanical stimuli. As early as 2.5 hours after eccentric cycling exercise, the MGF level in quadriceps muscle significantly increased in young subjects (Hameed *et al.*, 2008). In another animal study, MGF mRNA expression in rabbit skeletal muscle was observed to increase with electric stimuli at 10 Hz for 4 days (McKoy *et al.*, 1999). In the present study, we have shown that MGF expression was rapidly downregulated after 2 days of hindlimb unloading, further confirming that the regulation of MGF expression is mechanically sensitive. In addition, the mRNA level of MGF was significantly higher in the electrically stimulated HS+ES group as early as day 2. Although not statistically significant, the MGF expression in HS+ES group maintained at a higher level than that of HS group up to day 7 of hindlimb suspension. The expression of MGF provides a link between the mechanical signal and the upregulation of the gene expression involved in muscle adaptation and regeneration. This increased expression and maintenance of MGF possibly relates to the electric signal provided to the muscle or the mechanical signal induced by muscle contraction with electrical stimulation.

The growth and regeneration of postnatal skeletal muscle relies on satellite cell proliferation. The total number and the proliferation activity of satellite cells at different time points during hindlimb suspension were evaluated in parallel with MGF expression in the soleus muscle in the present study. The total number of satellite cell ($Pax7^{+}$) and the number of proliferating satellite cells ($Pax\ 7^{+}/BrdU^{+}$) were higher in HS+ES groups from day 2 compared with HS groups, and a significant difference was observed at day 7. The change of MGF level took precedence over that of the changes in satellite cell pool and proliferation activity. In a study by Hill and Goldspink (2003), the authors showed that MGF was upregulated at day 1 following local muscle damage and returned to normal levels within several days. The authors went on to show that the mRNA level of M-cadherin and transcript level of MyoD were significantly increased from day 1 to day 7 following the muscle damage. Based on this observation , it is possible that the mRNA level of the muscle regulatory factors are expressed even earlier in response to electrical stimulation during hindlimb suspension, and day 7 was the earliest time point that significant changes in satellite cell activity were observed. BrdU injection was performed daily during hindlimb suspension in this series of study. This method is different to that of Chapter 2 in which BrdU was injected once just before the mice were sacrificed. The purpose of daily injection BrdU was to increase the amount of labeling to reflect the population of newly proliferating satellite cells during the hindlimb suspension period.

In post-embryonic growth of skeletal muscle, there is no mitosis within myotubes and the extra nuclei required are derived from the satellite cells. It is possible that electrical stimulation protected the loss of satellite cells caused by mechanical unloading such that more satellite cells could be programmed to undergo proliferation and

differentiation process. However, there is not enough definitive evidence for a causal relationship between MGF and satellite cell activation and proliferation.

In a recent review, it has been hypothesized that MGF is responsible for activating quiescent satellite cells, promoting proliferation and depressing differentiation activity (Matheny *et al.*, 2010). As there is no commercial specific antibody against MGF, the protein level of this splice variant cannot be detected; maybe the protein products generated from MGF mRNA transcript is related to satellite cell activities. Addition of synthetic MGF peptide into skeletal muscle has been used to investigate the function of MGF *in vitro* (Yang and Goldspink, 2002) but at present, there is no definitive evidence to support that MGF exist *in vivo* in skeletal muscle.

In the present study, the mRNA of MGF was observed to be upregulated and the proliferation activity of satellite cells were increased in response to electrical stimulation in disused muscle. The local expression of MGF in skeletal muscle might be associated with activation and proliferation of satellite cells but further studies are needed to investigate the MGF expression *in vivo* and its direct role involved in skeletal muscle.

3.5 CONCLUSION

The experiments in this Chapter demonstrated that the mRNA expression of MGF in the disuse soleus muscle during hindlimb suspension was upregulated in response to electrical stimulation. Furthermore the total number and proliferation of satellite cells were increased with the intervention of electrical stimulation. The peak of MGF mRNA expression occurred prior to that of satellite cell activity. The results suggest that MGF may be, at least in part, related to the beneficial effects of electrical stimulation on satellite cell proliferation.

CHAPTER 4

Characterization of the Function of MGF *in vitro* and the Feasibility of Delivering MGF *in vivo*

4.1 INTRODUCTION

The growth of skeletal muscle is regulated by plenty of local and systemic factors. The growth hormone/insulin-like growth factor I (GH/IGF-I) axis is the main regulator of muscle mass through the activation of satellite cells (Machida & Booth, 2004; Goldspink, 2005). It has been demonstrated that IGF-I stimulates the proliferation of satellite cells isolated from transgenic mice which overexpressed IGF-I, and the role of IGF-I is associated with the activation of the PI3K/Akt signalling pathway (Chakravarthy *et al.*, 2000).

IGF-I can undergo alternative splicing to generate different gene products in response to exercise, muscle damage and hormones (Goldspink, 2005b). Alternative splicing of IGF-I pre-mRNA generates two isoforms in murine: IGF-IEa and Eb; In human, there are three isoforms including IGF-IEa, Eb, and Ec. Murine IGF-IEb isoform and human IGF-IEc isoform are the same molecule. The IGF-I gene contains six exons. Several transcripts can be derived by alternative splicing with the exon 4 spliced to exon 6 (Ea) or exon 4 spliced to exon 5 spliced to exon 6 (Eb in murine and Ec in human). The mRNA containing exon 5 spliced to exon 4 have been identified as Eb in human (Matheny *et al*., 2010). These mRNA splice variants encode C-terminal extensions are E-domains and translation of these alternatively spliced mRNA produced protein E-peptides. The murine IGF-IEb mRNA upregulates in response to mechanical loading or muscle damage (Goldspink, 2005a), it is also named as mechno-growth factor (MGF).

Previous studies on animal and human muscles have provided evidence that the splice variants of IGF-I are differentially regulated since the responses of IGF-IEa and MGF to exercise and muscle damage are different (Hameed *et al.*, 2003; Hill &

Goldspink, 2003) . The expression of MGF and IGF-IEa were both upregulated in muscles in response to muscle injury and high resistance exercise; however, MGF upregulated rapidly and the high level maintained for a short period of time as a pulse. IGF-IEa was more slowly upregulated as the level of MGF started to decrease. These results suggest that MGF and IGF-IEa have distinct functions.

In order to clarify the specific function of MGF, it is considered to use the synthetic E peptide to investigate the role of MGF because the peptide can be administered in a controlled manner. Yang and Goldspink (2002) have demonstrated that inhibition of IGF-I activity by blocking IGF-I receptors did not interfere with the function of synthetic MGF peptide, which induces C2C12 myoblast proliferation. The results indicate that MGF peptide stimulation of the proliferation of C2C12 myoblasts is not via the IGF-I receptor. The lack of specific antibodies of MGF and its undetermined receptor are the obstacles for us to understand the physiological function of MGF.

At present, there is little evidence for a direct relationship between MGF and the activation and proliferation of skeletal muscle satellite cells from *in vivo* experiments (Matheny *et al*., 2010). Furthermore, direct injection of naked DNA of MGF into skeletal muscle has been demonstrated to have poor efficiency (Magee *et al.*, 2006). Thus, electroporation technique is considered to increase the plasmid DNA uptake. By means of the application of electric pulses, the membranes of cells can be transiently permeabilized, which allows the plasmid DNA to enter into muscle tissues; this technique is frequently used for gene transfer and delivery of therapeutic proteins into muscles of both animals and humans (Gollins *et al.*, 2003; Magee *et al.*, 2006; Hojman, 2010) and is accepted as a safe, efficient and effective method at present. With administration of MGF

plasmid DNA into skeletal muscle, the function of MGF related to satellite cell activities at the transcriptional and protein level can be further investigated.

4.1.1 Aim of the study

The aim of this study is to use murine C2C12 skeletal muscle cell line to confirm the potential function of MGF in promoting skeletal muscle satellite cell proliferation; and to further evaluate the feasibility of delivering MGF plasmid DNA into skeletal muscle *in vivo* using electroporation.

4.2 MATERIALS AND METHODS

4.2.1 Experimental design

In vitro experiments

To examine the dynamic changes of the endogenous MGF in proliferating myoblast and differentiating myocytes, the mRNA level of MGF was evaluated in C2C12 cell culture at different time points (actively proliferation and 24 h, 48 h, 72 h post-differentiation).

To further characterize the function of MGF on promoting cell proliferation, the synthetic MGF peptides at different concentrations were added into C2C12 myoblasts. The proliferation of C2C12 cells was observed at 24 h and 48 h after MGF peptide treatment.

In vivo experiments

To evaluate the feasibility of delivering and overexpressing MGF gene in animal muscles using electroporation, a DNA vector containing the gene that coded for MGF was injected into the tibialis anterior (TA) muscle followed by electroporation. Male Balb/c mice (8-10 wk) were used in this study and the animal husbandry was described previously. For each mouse, one TA muscle was injected with a DNA vector containing MGF gene while the contralateral TA muscle was injected with vector only as control, followed by electroporation. The animals were sacrificed at 5 d post-electroporation and the MGF expression was evaluated using real time PCR experiment.

4.2.2 Cell culture

Mouse C2C12 myoblasts from the American Type Culture Collection (ATCC) were cultured at 37 ºC and 5 % CO_2 in growth medium (GM) consisting of Dulbecco's Modified Eagle's Medium (DMEM) (Gibco) supplemented with 10 % fetal bovine serum (Gibco) and antibiotics (100 units of penicillin and 100 μg of streptomycin/ml, Gibco). Myogenic differentiation was induced by replacing the GM with DMEM that contained 2% normal horse serum (Gibco) and antibiotics (differentiation medium, DM). To investigate if the expression level of endogenous MGF was changed during the course of myogenic differentiation, RNA for proliferating cultures was collected when the culture reached 80 % confluency, while those for differentiated cultures were collected from 1 day to 3 days post-differentiation (or post-transfection).

4.2.3 Synthetic Mechano Growth Factor (MGF) peptide

Mouse MGF peptide (NH2-YQPPSTNKNTKSQRRKGSTFEEHK-COOH) (Yang and Goldspink, 2002) of 24 amino acid residues was purchased from Bootech (Shanghai, China). The synthetic peptide had a molecular weight of 2849.12 with > 95 % purity. The MGF peptide was first dissolved in 0.9 % normal saline for storage at -20 °C. Subsequent dilution was made with serum-free DMEM.

4.2.4 Cell proliferation assay

To determine the effect of synthetic MGF peptide on C2C12 cell proliferation, MTT-based cell proliferation assay was performed. Briefly, 2×10^4 cells in 400 μl GM were seeded per well in 24-well plates. Twenty-four hours later, the GM was withdrawn

from the wells and was replaced with DM. Cells were allowed to culture for another 12 hours before addition of different concentrations (0, 2, 5, 10, 20 and 50 nM in DM) of synthetic MGF peptide. Cells were then cultured for an additional 24 h or 48 h in the presence of MGF peptide. After these time points, old medium in culture wells was withdrawn and was replaced with fresh DM containing MTT solution (with a final concentration at 0.5 mg/ml in culture medium, Roche). Cells were allowed to incubate with the diluted MTT solution at 37 °C in a 5 % CO_2 incubator for two hours. After discarding the MTT-containing medium, 200 μl of dimethyl sulfoxide (DMSO) was added to each well and the culture plate was subject to gentle shaking for 15 min at room temperature. Cell viability was then assessed by measuring the absorbance at 570 nm using a microplate reader (BioRad). Each experimental condition was performed in triplicate for the assay.

4.2.5 Preparation of plasmid DNA

The plasmid pEGFP-N1 (Clonetech), carrying a DNA insert corresponding to the exons 1, 3, 4, 5, 6 and parts of the introns 4 and 5 of MGF gene, was used (obtained from YH Li, State Key Laboratory of Space Medicine Fundamentals and Application, China Astronaut Research and Training Center). Under this construct, the full-length MGF gene was cloned into the multiple cloning site (MCS) using restriction enzymes NheI and BamHI. The MGF gene was cloned into the MCS immediately upstream of the start codon of an enhanced green fluorescent protein (EGFP) gene. The stop codon of the MGF gene was removed before cloning into the pEGFP-N1such that the MGF gene and the EGFP gene are in the same reading frame. In other words, the MGF gene will be expressed as fusion protein to the N-terminus of EGFP. Fusions to the N-terminus of

EGFP retain the fluorescent properties of the native protein, allowing the localization of the fusion protein *in vivo*. The DNA construct, now called pMGF-EGFP-N1, was transformed into E coli for amplification in the kanamycin-containing LB broth and purified using EndoFree Plasmid Maxi Kit (Qiagen) according to manufacturer's instruction.

4.2.6 Intramuscular injection of plasmid DNA and electroporation

Two hours before electroporation, each mouse was anaesthetized using a combination of ketamine (100 mg/kg) and xylazine (5 mg/kg) and the hindlimbs of each mouse were carefully shaved without any damage to the skin. The two TA muscles were injected transcutaneously with 0.4 U/μl of bovine hyaluronidase (Sigma) in 25 μl of normal saline to minimize damages due to injection and electroporation. After 2 h, one TA was injected with 25 μl plasmid DNA (pMGF-EGFP-N1, 1 μg/μl) in normal saline using a 29-gauge needle; the other TA was injected with vector only (pEGFP-N1) for control. All injections were carried out at a single site through the skin in a proximal to distal direction into the underlying TA muscles (Fig. 4.1). A voltage of 175 V/cm was applied in ten 20 ms square wave pulses at 1 Hz using a BTX ECM830 eletroporator (Fig. 4.2). Electroporation was conducted immediately after each injection by two stainless steel electrodes with interelectrode distance of 0.5 cm (Fig. 4.3).

The mice were sacrificed 5 days post-electroporation via cervical dislocation and the intact TA muscles were isolated. For real-time PCR, the TA muscles were collected and stored at -80°C until RNA extraction. For calculation of transfection efficiency, the muscles were snap frozen in liquid nitrogen-chilled isopentane and cryoembedded with

OCT for cryosectioning. The procedure of total RNA extraction and Real-time PCR procedures were performed as previously described in Chapter 3.

All the animal handling procedures and experimental protocols were approved by the Animal Subjects Ethics Committee of The Hong Kong Polytechnic University before conducting the experiments (ASESC No.09/12, Appendix V). A license to conduct animal experiments was also endorsed by the Department of Health of the Hong Kong Government (Appendix VI).

Figure 4.1 MGF plasmid DNA was injected through the skin in a proximal to distal direction into the underlying TA muscle.

Figure 4.2 The eletroporator (BTX ECM830) used in this study.

Figure 4.3 Electroporation was conducted by a two-needle array.

4.2.7 Calculation of transfection efficiency

Two cryostat serial sections (5 μm thick) were obtained from each muscle and the sections were immediately examined under the fluorescent microscope for EGFP expression. The images were captured with a Spots RT digital camera (Zeiss, Germany). Then H&E staining was performed to evaluate the total number of muscle fibers using an image morphometry program (ImageJ 1.32j, NIH, Bethesda, USA). The transfection efficiency was determined by the percentage of EGFP positive fibers over the total muscle fibers of a muscle.

4.3 RESULTS

4.3.1 MGF expression in proliferation and terminal differentiation of C2C12 cells

In order to determine the expression pattern of endogenous MGF during cell proliferation and differentiation, the mRNA level of MGF in proliferating and differentiating C2C12 cells was examined. Onset of C2C12 myogenic differentiation began upon serum starvation when the proliferating myoblasts experienced a shift from high serum condition to low serum condition. Total mRNA from proliferating C2C12, as well as from cells subjected to 24, 48, and 72 h post-differentiation was evaluated using real time PCR. Results from the real time PCR have demonstrated that endogenous MGF level was high in proliferating C2C12 myoblasts but the expression was gradually declined as differentiation proceeded, there was a significant decrease of endogenous MGF mRNA expression at 72 h post-differentiation (Fig. 4.4).

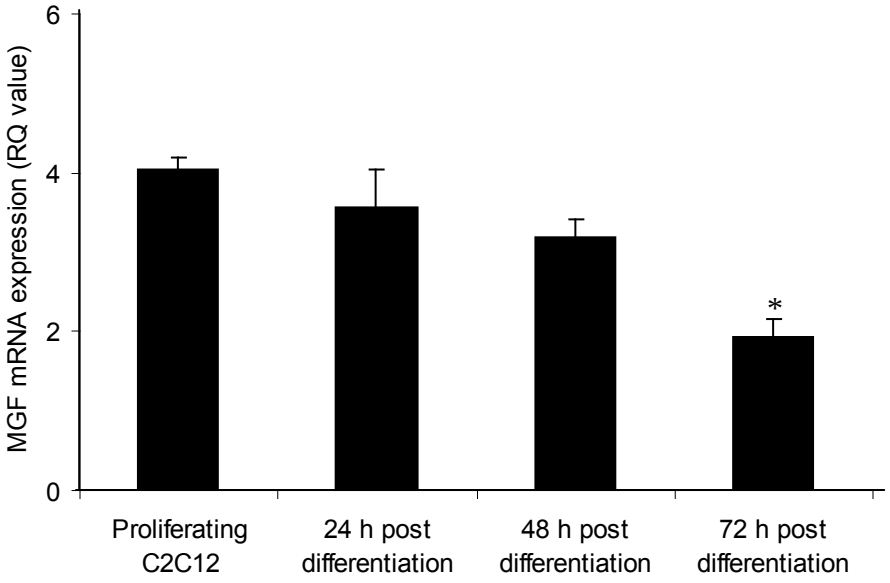

Figure 4.4 Endogenous MGF mRNA expression in proliferating C2C12 myoblasts and during C2C12 myogenic differentiation. * Statistical significance ($P < 0.05$) compared with proliferating C2C12 cells.

4.3.2 MGF promotes C2C12 cell proliferation

The proliferation of C2C12 cells with administration of exogenous MGF peptide was analyzed using standard MTT assay. The higher the absorbance measured in MTT assay, the more the cell density in the culture. The absorbance was measured at 24 h and 48 h after addition of different concentrations of MGF peptide. Twenty-four hours after MGF peptide addition, an increase in absorbance was not observed in 2 nM (Fig. 4.5A). There was a slight increase in absorbance when cells were treated with 5 nM MGF peptide but the difference was not significant. There was a significant increase in cell density with the concentrations of 10, 20 and 50 nM compared with control ($P < 0.001$). A dose-dependent increase in cell numbers was shown with the increase in MGF peptide concentration (Fig. 4.5A). The effect of MGF on cell proliferation was still detectable at 48 h after peptide treatment. Unlike at 24 h after MGF peptide treatment, in which significant difference in cell density was observed from 10 nM onward, the C2C12 myoblast proliferation was significantly promoted by MGF peptide with the concentration as low as 2 nM ($P < 0.05$) (Fig. 4.5B). When comparing the effects on the changes in cell density between 24 h and 48 h of MGF peptide treatment, the increment for 48 h treatment was 57 % (whereas 48 % for 24 h).

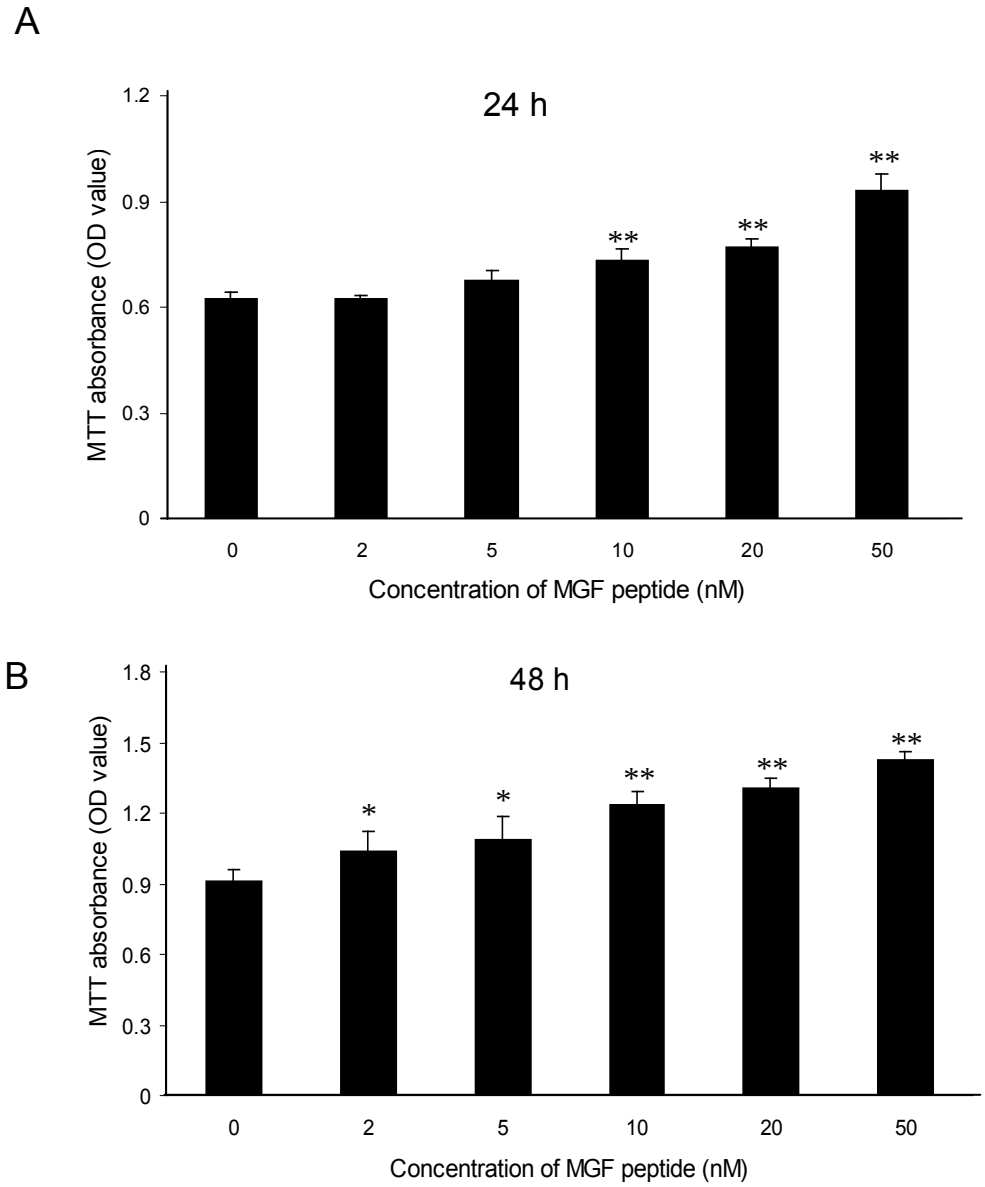

Figure 4.5 Cell proliferation assay (by MTT) to determine the effect of exogenous MGF peptide on C2C12 proliferation at 24 h (A) and 48 h (B) after MGF treatment. Data are means ± SEM (n = 4). * Statistical significance ($P < 0.05$) compared with control. ** Statistical significance ($P < 0.001$) compared with control.

4.3.3 The feasibility of using electroporation to constitutively express MGF *in vivo*

Electroporation was adopted as a strategy in an attempt to constitutively express our exogenous MGF gene into hindlimb muscle *in vivo*. In order to determine whether the pMGF plasmid was successfully delivered into TA muscle by electroporation and was properly expressed, TA muscles were isolated 5 days after electroporation. Total RNA from both vector-injected and pMGF-injected TA muscles was extracted and the expression of MGF transcripts was evaluated by real time PCR. Fig. 4.6 shows that the expression of MGF was significantly higher in pMGF-injected TA compared with that in vector-injected TA ($P < 0.05$). The expression level of MGF in the pMGF-injected TA muscles was approximately 2.9 fold of that in the vector-injected TA muscles. This result demonstrated that the pMGF plasmid was successfully delivered into muscle using the electroporation technique, and overexpression of MGF was retained at least 5 days post-electroporation. We then further investigated whether the gene delivered would be successfully expressed not only in transcriptional level but also in translational level. Due to a lack of reliable antibody against MGF, we were unable to detect the MGF protein expression. Instead, we examined the expression of EGFP, which theoretically, reflected the MGF protein expression due to the formation of fusion protein between MGF and EGFP in the pMGF plasmid. The EGFP signal in the vector-injected muscle indicated successful expression of EGFP protein. Fluorescent signal of EGFP was clearly detected in the muscle fibers of both vector- and pMGF-electroporated TA muscles (Fig. 4.7). We used EGFP protein expression as an indicator to estimate the transfection efficiency in order to ensure both vector and pMGF was similarly delivered and expressed in muscles of equal extent. The transfection efficiency of electroporation was nearly 40 % for both

vector and MGF injected muscles in this experiment without significant discrepancy (Fig. 4.8).

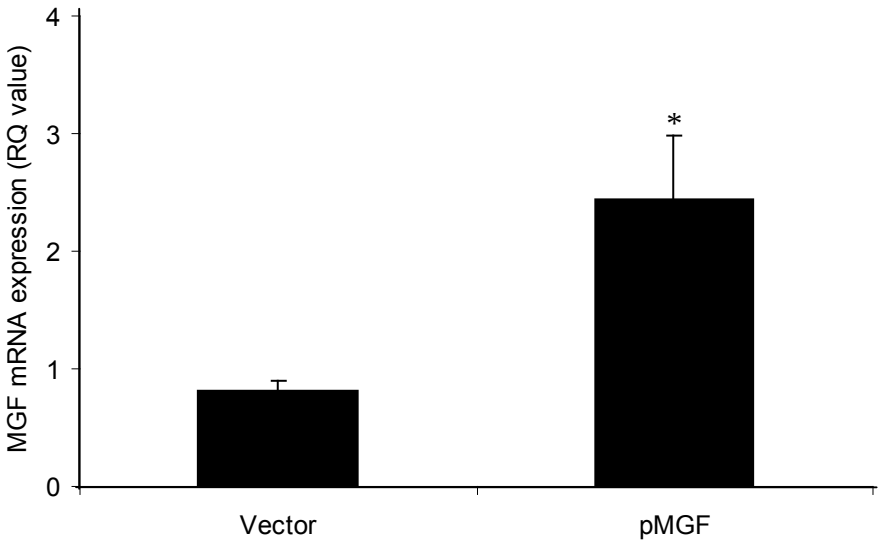

Figure 4.6 MGF mRNA expression in TA muscles harvested 5 days after electroporation of vector (p-EGFP-N1) only and pMGF. Data are means ± SEM (n = 6). * Statistical significance ($P < 0.05$) compared with vector-injected group.

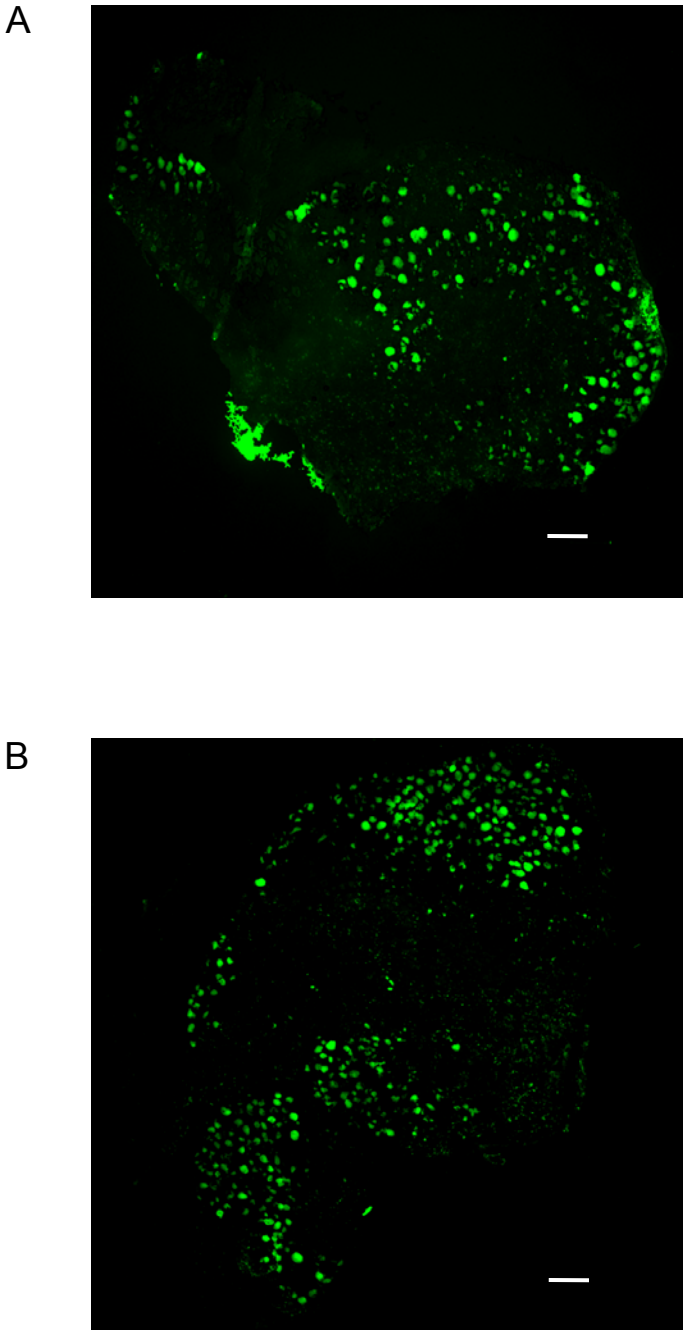

Figure 4.7 The expression of EGFP on fresh transverse frozen sections of TA muscles electroporated with vector (A) or pMGF (B). Scale bar = 100 μm.

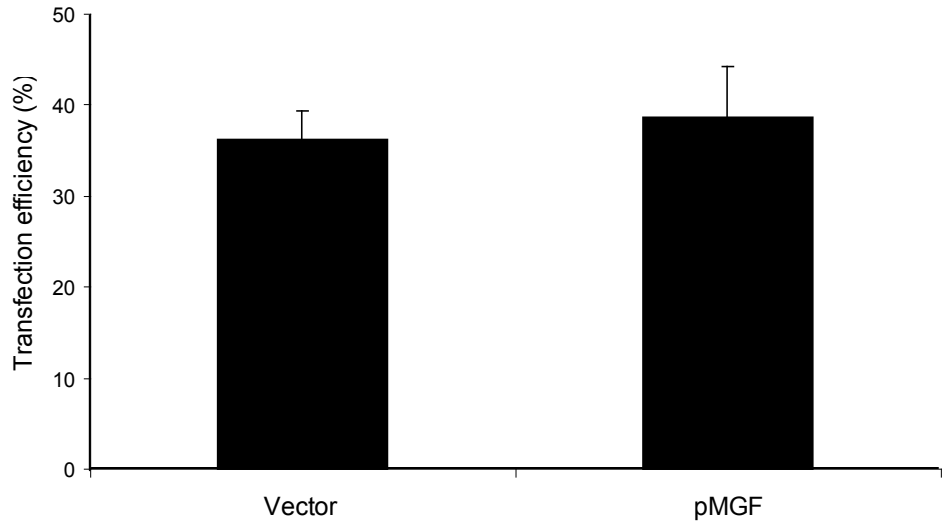

Figure 4.8 Transfection efficiency of TA muscles electroporated with vector and pMGF. The transfection efficiency was expressed as percentage of EGFP-possitive fibers of the total number of fibers counted in the same muscle sections. Data are means ± SEM (n = 4). There is no significant difference between two groups ($P > 0.05$).

4.4 DISCUSSION

There is only limited experimental evidence available to help define a potential direct involvement of MGF in satellite cell proliferation and differentiation. Therefore, the aim of this study was to investigate the effects of a synthetic MGF peptide during the process of C2C12 proliferation and to evaluate the feasibility of delivering MGF *in vivo* by electroporation technique. C2C12 is a mouse myoblast cell line originally derived from satellite cells from the thigh muscle of C3H mice after a crush injury (Yaffe & Saxel, 1977). These cells are capable of proliferation and differentiation, and the signals involved during C2C12 differentiation are similar to that of muscle satellite cells. Thus, this cell line is a frequently used model to study the signaling pathways involved in skeletal muscle differentiation and regeneration (Stuelsatz *et al.*, 2010; Tarabees *et al.*, 2011).

The results demonstrated that the endogenous MGF expression was high in proliferating C2C12 and gradually decreased with time during C2C12 terminal differentiation. The downregulation of MGF during myogenic differentiation of C2C12 myocytes might suggest that either (i) MGF is actively involved in myoblast proliferation and the extent of proliferation diminishes upon myogenic differentiation, or (ii) inhibition of MGF is required for myogenic differentiation to proceed. In addition, treatment with synthetic MGF peptide resulted in a dose-dependent increase in C2C12 cell proliferation. This indicated that MGF was possibly involved in C2C12 myoblast proliferation and MGF promoted cell proliferation. This observation confirms findings from previous studies describing myoblasts proliferation in myogenic precursor cells by administration of MGF peptide (Yang & Goldspink, 2002; Mills *et al.*, 2007).

Although addition of synthetic MGF peptide has proven its role in promoting myoblast proliferation, *in vivo* experiment to demonstrate the role of MGF on skeletal muscles is necessary to confirm that the results were not an *in vitro* artifact. However, injection of synthetic peptide into skeletal muscle has several limitations. First, it would be difficult to avoid degradation of peptides in an *in vivo* system. Second, it would also be difficult to estimate approximately the amount of peptides being delivered into muscles without leaking into microcirculation. Third, it seems impossible to extend the activity of the peptide if a long term monitoring is desired. In this study, the MGF plasmid DNA was delivered to mouse skeletal muscle by electroporation in order to investigate the effects of MGF *in vivo*. Gene delivery via electroporation allows direct entry of DNA plasmid into cells through pores generated in the cell membrane by means of electrical pulses. Expression of EGFP protein within muscle fibers indicated successful electroporation. Quantification of the EGFP-immunopositive fibers allowed comparison in transfection efficiency between groups and between experiments. In addition, *in vivo* electroporation allows constitutive expression of gene of interest so that long term monitoring on the effects of gene expression is feasible. Electroporation is frequently used for gene transfer and therapeutic proteins delivery into muscles of both animals and human (Gollins *et al.*, 2003; Magee *et al.*, 2006; Hojman, 2010).

The TA muscle was chosen as our target muscle which was different from our previous muscles of interest (soleus) because TA was anatomically superficial and easier for manipulation when compared to soleus. Our results indicated that we have successfully introduced the MGF gene into muscles through electroporation and overexpression of gene was achieved in both transcriptional and translational level. This

technique is feasible for further investigation of the role of MGF in muscle disuse atrophy *in vivo*.

A lot of preparation and technical issues can influence the transfection efficiency. The pretreatment of the muscle with hyaluronidase in this study aimed to improve the transfection efficiency and decrease muscle damage. Experimental evidence demonstrated that pretreatment with bovine hyaluronidase followed by electroporation resulted in significantly more transfected fibers being distributed across larger proportion of the muscle compared with electroporation alone (McMahon *et al.*, 2001). The transfer voltage used in this study was 175 V/cm, which could induce optimal electroporation efficiency with less muscle damage. Previous studies demonstrated that there was a proportional increase in the transfected fibers with increasing transfer voltage above 100 V/cm to 200 V/cm, and the number of transfected fibers was not significantly different at 175 V/cm compared with 200 V/cm. Because the high voltage at 200 V/cm caused unacceptable muscle damage, 175 V/cm was accepted as the optimal transfer voltage (McMahon *et al.*, 2001; Molnar *et al.*, 2004). The plasmid DNA was injected into TA at one injection site in this study. It was reported that the presence of a central tendon in TA influenced efficient plasmid DNA transfer and more than one injection were considered (McMahon *et al.*, 2001). On the other hand, several injection sites might lead to muscle damage and a strong inflammatory response in the muscle. Two injections at the proximal and distal part of TA into different depth could be tried in further experiments.

In the present study, the expression of MGF was evaluated at 5 d post-electroporation allowing the muscle recover from inflammation due to injection and

electroporation. A previous study evaluated the longevity of transgene expression by electroporation and found that the percentage of transfected fibers was about 80 % during 3 d to 7 d post electroporations and the high transfection efficiency was maintained to 21 d and 30 d post electroporation with the percentage of transfected fibers of 70 % and 50 %, respectively (Dona *et al.*, 2003). Since the EGFP was a fusion protein, the detectable expression of EGFP in the present study implied that the MGF transcript had translated into protein by day 5. By successfully electroporated pMGF into muscles, we can perform experiments to test the hypothesis that whether administration of MGF into skeletal muscles promoted cell proliferation *in vivo*. Satellite cell proliferation can be detected using BrdU incorporation and other markers such as PCNA or Ki67 by immunostaining at 5 d-post electroporation.

There are many other possible candidates responsible for muscle regeneration and related to satellite cell proliferation, such as LIF and HGF. LIF is expressed by skeletal muscle and it has been demonstrated that LIF can induce C2C12 myoblasts proliferation (Spangenburg & Booth, 2002) and stimulate the proliferation of isolated satellite cells from human biopsy (Broholm *et al.*, 2011). The resistance exercise significantly upregulated the mRNA expression of LIF 6 h post-exercise, but the mRNA level returned to pre-exercise level by 24 h after the exercise. Furthermore, the protein expression of LIF was not significantly increased by exercise (Broholm *et al.*, 2011). It indicated that the effect of LIF lasted for a very short period of time and it might be difficult to evaluate the effect of LIF on satellite cell proliferation *in vivo*. HGF is also regarded as one of those autocrin/paracrine growth factors like MGF; it has been shown to activate quiescent satellite cells by binding to its specific receptor, c-met (Tatsumi *et al.*, 1998). A few

recent studies have demonstrated that the expression of a HGF family member protein is associated with satellite cell activation, proliferation and differentiation activities. *In vitro* experiments showed that HGF stimulated proliferation of myoblasts and high concentrations of HGF inhibited satellite cell proliferation (Li *et al.*, 2009). A human *in vivo* study found that there was a significant increase in serum HGF at 4 h after eccentric exercise induced muscle damage followed by expanded satellite cell pool (O'Reilly *et al.*, 2008). Since HGF seems to be activated in response to muscle injury rather than mechanical signals (O'Reilly *et al.*, 2008), this growth factor was not chosen for the investigation of effects of electrical stimulation. There are multiple signaling pathways regulating muscle regeneration, we have only focused on the possible mediator related to mechanical signals.

4.5 CONCLUSION

This study has provided evidence that the proliferation of myoblasts may be, at least in part, regulated by the presence of MGF. The MGF plasmid DNA can be successfully transferred into skeletal muscle fibers using electroporation and overexpression of MGF gene can be achieved in both transcriptional and translational level. With further technical optimization, *in vivo* electroporation would be an extremely good tool not only to help understand the physiological function of MGF but also help explore novel therapeutic approaches towards various types of muscle atrophy.

CHAPTER 5

General Discussion

Skeletal muscle disuse atrophy is commonly seen after immobilization, bed rest or spaceflight resulting in decreased muscle CSA and force production. Since skeletal muscles are highly adaptive for functional changes in response to external stimuli such as exercise and mechanical signals, the atrophy of muscle can be attenuated by mechanical interventions. Electrical stimulation has been frequently used as a countermeasure for attenuating skeletal muscle atrophy, but the underlying mechanisms responsible for its beneficial effects are far from clear.

The effects of electrical stimulation depend on the parameters, particularly the stimulation frequency and duration. It has been previously demonstrated in our laboratory that low-frequency electrical stimulation at 20 Hz for 2 × 3 h/d produced some beneficial effects on mouse soleus muscle during hindlimb suspension. This electrical stimulation protocol improved fiber CSA and partially attenuated the decreased satellite cell proliferation (Zhang *et al*., 2010). In the present study, the efficacy of different electrical stimulation protocols with 2 different durations and 3 frequencies were evaluated with the aim of determining the optimal stimulation parameters in attenuating muscle atrophy.

The results demonstrated that electrical stimulation with the frequency at 2 Hz and the duration for 2 × 3 h/d had the most significant effect in attenuating the decrease of muscle mass, fiber CSA, peak tetanic force and the slow-to-fast fiber transitions. On the other hand, hindlimb suspension induced an impaired satellite cell proliferation and increased cell apoptosis after 14 days. The optimal stimulation protocol that we have exhibited also increased satellite cell number, enhanced satellite cell activation, proliferation and subsequent myogenic differentiation; and rescued cells from undergoing apoptosis. The low frequency pattern in our optimal stimulation protocol matches slow

twitch muscle properties and the motor unit firing pattern, thus likely to generate a mechanical signal that partially counteracts the degenerating effects on soleus muscles caused by disuse atrophy. Nevertheless, we also believe that the duration of this low frequency pattern is crucial in attaining such a significant effect. The experiments in the present study provided evidence that electrical stimulation may individually contribute to the maintenance of satellite cell pool and regulation of its activities, as well as protection of satellite cells and myonuclei from undergoing apoptosis. The balance of satellite cell proliferation and apoptosis not only maintains mature skeletal muscle mass but also secures a healthy and sufficient pool of reserve (i.e. satellite cells) for regeneration upon appropriate stimuli (e.g. reloading).

Unpublished data generated in our laboratory have shown that electrical stimulation significantly upregulated Bcl-2 in unloaded soleus muscles that accounted for the anti-apoptotic effects observed upon electrical stimulation. We suggested that electrical stimulation attenuated cell apoptosis in a way similar to inducing muscle stretching because both approaches generated muscle movement. It was possible that the electrical stimulation increased Bcl-2 protein expression by preventing Ca2+ accumulation, which could otherwise result in the calpain-mediated Bcl-2 cleavage.

The underlying mechanisms which may lead to the beneficial induced-changes from electrical stimulation, particularly on inducing satellite cell proliferation, are not known. One of the possible regulatory factors involved may be mechano growth factor (MGF). MGF is a splice variant of the IGF-I gene, which has been demonstrated to be an important regulating factor of muscle mass (Goldspink, 2005a). Moreover, MGF is upregulated in response to mechanical stimulus and muscle damage; it is therefore

possible that MGF participates in the regulation of satellite cell activity in response to electrical stimulation. To investigate the possible involvement of MGF and the time frame of MGF expression in relation to satellite cell proliferation following hindlimb suspension, the transcriptional level of MGF was evaluated at day 2, 3 and 7 during hindlimb suspension with electrical stimulation and satellite cell proliferation was evaluated at the corresponding time points. It was interesting to observe that significant upregulation of MGF was detected as early as day 2 of hindlimb unloading. We then followed the changes in satellite cell proliferation and we found that a significant increase in satellite cell proliferation in unloaded soleus with electrical stimulation was observed only at day 7. The upregulation of MGF at day 2 which preceded that of satellite cell proliferation demonstrated at day 7 suggests a possible relationship between MGF and satellite cell proliferation.

To examine if MGF was dynamically changed during myogenic differentiation, we investigated the expression pattern of endogenous MGF during C2C12 differentiation. Endogenous MGF expression was high in proliferating myoblasts but the expression gradually declined when the myoblasts were committed into myogenic differentiation and differentiated into myocytes. To further characterize the function of MGF, C2C12 myoblasts were treated with synthetic MGF E peptides. *In vitro* results showed that the synthetic MGF E peptides promoted C2C12 myoblasts proliferation in a dose-dependent manner. This result might explain the increase of proliferating satellite cells detected by Pax7 and BrdU at day 7 in response to electrical stimulation; the effect of MGF may be transient at the earlier time and electrical stimulation improved satellite cell proliferation via upregulation of MGF.

After gaining insight on the potential role of MGF on myoblast proliferation *in vitro*, we attempted to explore if MGF has the same role *in vivo*. Currently, the lack of known receptors for MGF and the unavailability of specific antibody against MGF have hampered progress in understanding the functional role of MGF *in vivo*. Therefore, we made use of *in vivo* electroporation technology to deliver MGF gene into mouse muscles. The formation of fusion protein between MGF and EGFP in the pMGF plasmid makes it possible to track MGF protein in muscle sections through examining the expression of EGFP under fluorescent microscope. The fluorescent signal of EGFP on the transverse section of muscle was clearly detected in both vector- and pMGF-electroporated TA muscles. The overexpression of MGF retained for at least 5 days when the animals were sacrificed. The results indicated that the MGF plasmid DNA could be successfully delivered into the tibialis anterior muscle and overexpression of MGF could be attained using electroporation technique. As such, this technique may be a feasible method to further study the function of MGF on skeletal muscles.

The present study has provided experimental evidence of optimal electrical stimulation protocol for counteracting muscle disuse atrophy and formed basis for further investigation into the mechanism for the improvements seen in electrical stimulation for disuse atrophy as well as the functional role of MGF.

CHAPTER 6

Conclusion

The main findings from this investigation of the effect of electrical stimulation on muscle disuse atrophy were:

1. Hindlimb suspension for 14 days induced significant muscle atrophy in the soleus muscle leading to reduction in muscle mass, fiber cross-sectional area, maximal tetanic force, and a slow-to-fast fiber transformation. Furthermore there was an associated decrease in the satellite cell number, impaired satellite cell activation and proliferation, and increased cell apoptosis.
2. Electrical stimulation could partially attenuate muscle disuse atrophy by improving muscle mass, fiber CSA and maximal tetanic force, attenuating the fiber type transition, promoting the activation, proliferation and differentiation of satellite cells as well as protecting cells from apoptosis. Combination of different frequencies and durations of stimulation exhibited different extents of protective effects against hindlimb unloading-induced muscle atrophy. Compared with other protocols tested, electrical stimulation at 2 Hz for 2 × 3 h/d provided the best optimal paradigm for attenuation of muscle disuse atrophy.
3. To understand the possible mechanism which may lead to the favorable induced-changes from electrical stimulation, mechano growth factor (MGF), a splice variant of the insulin-like growth factor-I gene was investigated. This is because MGF is upregulated in response to mechanical stimulus and muscle damage, it is therefore possible that MGF participates in the regulation of satellite cell activity in response to electrical stimulation. Hindlimb suspension induced downregulation of MGF. The mRNA expression of MGF in the soleus muscle was upregulated in response to electrical stimulation as early as at day 2 during

hindlimb suspension. Furthermore the total number and proliferation of satellite cells were increased at day 7 with the intervention of electrical stimulation. The peak of MGF mRNA expression occurred prior to that of satellite cell activity. The results suggested that expression of MGF was mechanically sensitive and might be, at least in part, related to the beneficial effects of electrical stimulation on satellite cell proliferation.

4. To characterize the function of MGF, an *in vitro* model using C2C12 myogenic cell culture was adopted which showed that endogenous MGF expression was high in proliferating myoblasts but gradually downregulated as differentiation proceeded. Treatment of the C2C12 myoblasts with the synthetic MGF E peptides promoted myoblast proliferation in a dose-dependent manner. The induction of proliferation of C2C12 myoblasts by MGF was obvious within 24 hours after peptide treatment and the effect was still detectable at 48 hours after peptide treatment. The results not only demonstrated that MGF promotes satellite cell proliferation *in vitro*, but also suggested that MGF may be involved in electrical stimulation-induced satellite cell proliferation.
5. The *in vitro* results raise the possible therapeutic potential of MGF in disuse muscle atrophy. Using electroporation in an *in vivo* model, the feasibility of delivering MGF was evaluated. The DNA plasmid containing MGF gene was injected into the tibialis anterior (TA) muscle followed by an electroporation. The DNA plasmid was designed in a way that MGF will form fusion protein with enhanced green fluorescent protein (EGFP). DNA plasmid without MGF gene was used as control that also expressed EGFP upon successful delivery and

expression. The fluorescent signal of EGFP on the transverse section of muscle was comparable in both vector- and pMGF-electroporated TA muscles. The overexpression of MGF retained for at least 5 days. The results indicated that the MGF plasmid DNA could be successfully delivered into muscle and overexpression of MGF *in vivo* could be attained using electroporation technique.

6. Findings from this study will form basis for further investigation into the mechanism for the improvements seen in electrical stimulation for disuse atrophy as well as the functional role of MGF.

THE HONG KONG
POLYTECHNIC UNIVERSITY
香港理工大學

Appendix I

[redacted]

MEMO

To : Dr Ella Yeung, Department of Rehabilitation Sciences

From : Dr Maureen Boost, Chairman, Animal Subjects Ethics Sub-committee

Ref. : _____ Your Ref. : _____

Tel. No. : Ext. 6391 Date : 21 DEC 2007

Application for Ethical Review for the Use of Animals in Teaching or Research
[In Search of a Novel Electrical Stimulation Paradigm for Satellite Cell Activation in Preventing Skeletal Muscle Atrophy]
(ASESC No. 07/23)
[The role of TRPC channels in skeletal muscle atrophy and regrowth]
(ASESC No. 07/24)

Your application for ethics review for the use of animals in the above project has been approved for a period of two years from the date of this memo subject to the investigator ensuring that regular inspection of tails for damage is performed as described in the protocol.

You are required to inform the Animal Subjects Ethics Sub-committee if at any time the conditions under which the animals are kept and cared for no longer fully meet the requirements of the Procedures for the Care of Laboratory Animals. If you are keeping animals in the University's animal holding room, you should state the full title of the approved project and the ASESC no. on the cage cards of the cages holding the animals. The members of the Sub-committee may visit the animal holding room unannounced at any reasonable time.

I would like to draw your attention to the University requirement that holders of licences under Cap. 340 must provide the Animal Subjects Ethics Sub-committee with a copy of their licences and a copy of their annual returns to the Licensing Authority. These must be kept up to date for the duration of the above work.

Dr Maureen Boost
Chairman
Animal Subjects Ethics Sub-committee

c.c. Chairman, DRC (RS)

Form 2

Appendix II

Licence to Conduct Experiments

Name : WAN Qing [Ref No.: (08-49) in DH/HA&P/8/2/4 Pt.1]

Address : Department of Rehabilitation Sciences, The Hong Kong Polytechnic University

By virtue of section 7 of the Animals (Control of Experiments) Ordinance, Chapter 340, the above-named is hereby licensed to conduct the type of experiment(s), at the place(s) and upon the conditions, hereinafter mentioned.

Type of experiment(s)

Rats and mice will be used in the experiment. The hind limbs of the animals will be unloaded for 7 to 21 days by means of tail traction system. During the unloading period, low frequency transcutaneous electrical stimulation with intensity just at pain threshold will be applied to one of the unloaded hind limbs. Tails of the animals will be inspected daily to check for any discoloration and lesion. Body weight and general well being of the animals will be monitored regularly. After the unloading period, the animals will be sacrificed by cervical dislocation. The hind limb muscles will then be harvested for muscle weight measurement, frozen sections with different staining techniques and morphometry.
During the unloading period, animals showing signs of distress or intolerance will be removed from the experiment. They will become weight bearing control if their conditions improve or otherwise be sacrificed by cervical dislocation.

Place(s) where experiment(s) may be conducted

Muscle Physiology Laboratory (ST402a) 4/F, S Core and Centralized Animal Facilities, The Hong Kong Polytechnic University, Hung Hom, Kowloon

---

Conditions

1. Such experiment(s) may only be conducted for the following purposes-
To examine the muscle physiology in unloading animal models and the response of unloaded muscle towards low frequency electrical stimulation.

2. This licence is valid from 6 January 2009 to 5 January 2011

Dated 6 January 2009

DEPARTMENT OF HEALTH 衞生署 HONG KONG

Licensing Authority

Appendix III

RNA Isolation Protocol

1. RNA lysis buffer (175 µl) was transferred to a sterile microcentrifuge tube and one soleus sample was added by RNase-free pipettes.

2. The sample was homogenized by a pellet pestle motor.

3. RNA dilution buffer (350 µl) was added to the lysate and mixed by inverting 3-4 times.

4. The tube was placed in a heating block at 70 °C for 3 min.

5. The lysate was centrifuged for 10 min at 13,000 × g.

6. The cleared lysate solution was transferred to a fresh microcentrifuge tube by pipetting.

7. Ethanol (95 % 200 µl) was added to the cleared lysate and mixed by pipetting 3-4 times. This mixture was transferred to the spin column assembly.

8. The mixture was centrifuged for 1 min at 13,000 × g.

9. The liquid in the collection tube was discarded and the spin basket was put back into the collection tube. RNA wash solution (600 µl) was added to the spin column assembly and the tube was centrifuged for 1 min at 13,000 × g.

10. The collection tube was emptied as before and placed in a rack. The DNase incubation mix was prepared by combining 40 µl yellow core buffer, 5 µl 0.99M $MnCl_2$ and 5 µl of DAase I enzyme per sample in a sterile tube in this order and mixed. 50 µl of DNase incubation mix was added to the membrane inside the spin basket.

11. Incubation was kept at 20-25° C for 15 min.

12. DNase stop solution (200 µl) was added to the spin basket, and then centrifuged for 1 min at 13,000 × g.

13. RNA wash solution (600 µl) was added and the spin column assembly was centrifuged for 1 min at 13,000 × g.

14. The collection tube was emptied and 250 µl of RNA wash solution was added, and then centrifuged for 2 min at 13,000 × g.

15. The cap of the spin basket was removed and the spin basket was transferred from the collection tube to the elution tube. Nuclease-free water (50 µl) was added to the membrane.

16. The spin basket assemblies were centrifuged for 1 min at 13,000 × g, the spin basket was removed and the elution tube containing the purified RNA of each sample was stored at -70 °C.

Appendix IV

cDNA Synthesis Procedure

1. Each sample was diluted according to the lowest concentration of one sample. 8 µl of RNA of each sample was used.

2. Random Hexamers (1 µl) and dNTPs (1 µl) were added to 8 µl of RNA, the mixture was kept at 65 °C for 5 min.

3. The samples were placed on ice for at least 1 min.

4. cDNA synthesis mix (a total of 10 µl for each sample) was freshly prepared, the component for each sample was showed below.

10× RT Buffer	2 µl
25 mM $MgCl_2$	4 µl
0.1 M DTT	2 µl
RNaseOUT	1 µl
SuperScript III	1 µl

5. The cDNA synthesis mix was added to RNA mixture and stored at 25 °C for 10 min.

6. The cDNA synthesis was kept at 50 °C for 50 min, and then the terminate reaction was kept at 85 °C for 5 min.

7. In order to remove RNA, 1 µl of RNase H was added to the cDNA and kept at 37 °C for 20 min.

8. The cDNA of each sample was stored at - 20 °C before PCR amplification.

Appendix V

THE HONG KONG
POLYTECHNIC UNIVERSITY
香港理工大學

- 5 JUN 2009
Research Office

MEMO

To : Dr Ella Yeung (RS)

From : Dr Mason Leung, Chairman, Animal Subjects Ethics Sub-committee

Ref. : _____ Your Ref. : _____

Tel. No. : Ext. 4831 Date : 10 JUN 2009

Application for Ethical Review for the Use of Animals in Teaching or Research

Project Title: The Role of Mechanogrowth Factor (MGF) During Skeletal Muscle Atrophy and Remodeling
Application No.: ASESC No. 09/12

Your application for ethics review for the use of animals in the above project has been approved for a period of two years from the date of this memo.

You are required to inform the Animal Subjects Ethics Sub-committee if at any time the conditions under which the animals are kept and cared for no longer fully meet the requirements of the Procedures for the Care of Laboratory Animals. If you are keeping animals in the University's animal holding room, you should state the full title of the approved project and the ASESC no. on the cage cards of the cages holding the animals. The members of the Sub-committee may visit the animal holding room unannounced at any reasonable time.

I would like to draw your attention to the University requirement that holders of licences under Cap. 340 must provide the Animal Subjects Ethics Sub-committee with a copy of their licences and a copy of their annual returns to the Licensing Authority. These must be kept up to date for the duration of the above work.

Mason Leung (Dr)
Chairman
Animal Subjects Ethics Sub-committee

c.c. Chairman, DRC(RS)

Form 2

Appendix VI

Licence to Conduct Experiments

Name : WAN Qing [Ref No.: (10-97) in DH/HA&P/8/2/4 Pt.4]

Address : Department of Rehabilitation Sciences, The Hong Kong Polytechnic University

By virtue of section 7 of the Animals (Control of Experiments) Ordinance, Chapter 340, the above-named is hereby licensed to conduct the type of experiment(s), at the place(s) and upon the conditions, hereinafter mentioned.

Type of experiment(s)

Mice and rats will be used in the experiment. The hindlimbs of the animals will be unloaded using a tail traction system for about 7 to 21 days. During the unloading period, the animals will be subjected to low frequency transcutaneous electrical stimulation with the intensity just at the threshold where no pain will be caused to the animals. At the end of the experiment, the animals will be sacrificed by cervical dislocation. Hindlimb muscles will be harvested for analyses. During the experiment, the conditions of the animals will be monitored. The tail of the animals will be inspected closely to check for any discolouration and lesion. Body mass will be evaluated as an indication of tolerance to suspension condition. Animals showing signs of distress or intolerance to suspension will be immediately removed from the experiment. They will become weight bearing control if their conditions improve or otherwise be sacrificed by cervical dislocation.

Place(s) where experiment(s) may be conducted

Muscle Physiology Laboratory (ST402a) and Centralised Animal Facilities (Y1422), The Hong Kong Polytechnic University

---

Conditions

1. Such experiment(s) may only be conducted for the following purposes-

   Using hindlimb unloading as a model to investigate the detrimental effects of immobilisation on the structure and function of skeletal muscles and to investigate the effects of low frequency electrical stimulation on unloaded muscle.

2. This licence is valid from 6 January 2011 to 5 January 2013

Dated 6 January 2011

DEPARTMENT OF HEALTH 衞生署 HONG KONG

Licensing Authority

References

Adams CM, Suneja M, Dudley-Javoroski S & Shields RK. (2011). Altered mRNA expression after long-term soleus electrical stimulation training in humans with paralysis. *Muscle Nerve* **43,** 65-75.

Adams GR, Caiozzo VJ & Baldwin KM. (2003). Skeletal muscle unweighting: spaceflight and ground-based models. *J Appl Physiol* **95,** 2185-2201.

Adams GR, Haddad F, Bodell PW, Tran PD & Baldwin KM. (2007). Combined isometric, concentric, and eccentric resistance exercise prevents unloading-induced muscle atrophy in rats. *J Appl Physiol* **103,** 1644-1654.

Allen DL, Linderman JK, Roy RR, Bigbee AJ, Grindeland RE, Mukku V & Edgerton VR. (1997). Apoptosis: a mechanism contributing to remodeling of skeletal muscle in response to hindlimb unweighting. *Am J Physiol* **273,** C579-587.

Allen DL, Yasui W, Tanaka T, Ohira Y, Nagaoka S, Sekiguchi C, Hinds WE, Roy RR & Edgerton VR. (1996). Myonuclear number and myosin heavy chain expression in rat soleus single muscle fibers after spaceflight. *J Appl Physiol* **81,** 145-151.

Alway SE & Siu PM. (2008). Nuclear apoptosis contributes to sarcopenia. *Exerc Sport Sci Rev* **36,** 51-57.

Anderson JE. (2000). A role for nitric oxide in muscle repair: nitric oxide-mediated activation of muscle satellite cells. *Mol Biol Cell* **11,** 1859-1874.

Arakawa T, Katada A, Shigyo H, Kishibe K, Adachi M, Nonaka S & Harabuchi Y. (2010). Electrical stimulation prevents apoptosis in denervated skeletal muscle. *NeuroRehabilitation* **27,** 147-154.

Arbogast S, Smith J, Matuszczak Y, Hardin BJ, Moylan JS, Smith JD, Ware J, Kennedy AR & Reid MB. (2007). Bowman-Birk inhibitor concentrate prevents atrophy, weakness, and oxidative stress in soleus muscle of hindlimb-unloaded mice. *J Appl Physiol* **102,** 956-964.

Ates K, Yang SY, Orrell RW, Sinanan AC, Simons P, Solomon A, Beech S, Goldspink G & Lewis MP. (2007). The IGF-I splice variant MGF increases progenitor cells in ALS, dystrophic, and normal muscle. *FEBS Lett* **581,** 2727-2732.

Babault N, Cometti G, Bernardin M, Pousson M & Chatard JC. (2007). Effects of electromyostimulation training on muscle strength and power of elite rugby players. *J Strength Cond Res* **21,** 431-437.

Baewer DV, Hoffman M, Romatowski JG, Bain JL, Fitts RH & Riley DA. (2004). Passive stretch inhibits central corelike lesion formation in the soleus muscles of hindlimb-suspended unloaded rats. *J Appl Physiol* **97,** 930-934.

Bajotto G & Shimomura Y. (2006). Determinants of disuse-induced skeletal muscle atrophy: exercise and nutrition countermeasures to prevent protein loss. *J Nutr Sci Vitaminol (Tokyo)* **52,** 233-247.

Banerjee P, Caulfield B, Crowe L & Clark A. (2005). Prolonged electrical muscle stimulation exercise improves strength and aerobic capacity in healthy sedentary adults. *J Appl Physiol* **99,** 2307-2311.

Bax L, Staes F & Verhagen A. (2005). Does neuromuscular electrical stimulation strengthen the quadriceps femoris? A systematic review of randomised controlled trials. *Sports Med* **35,** 191-212.

Beauchamp JR, Heslop L, Yu DS, Tajbakhsh S, Kelly RG, Wernig A, Buckingham ME, Partridge TA & Zammit PS. (2000). Expression of CD34 and Myf5 defines the majority of quiescent adult skeletal muscle satellite cells. *J Cell Biol* **151,** 1221-1234.

Belka C & Budach W. (2002). Anti-apoptotic Bcl-2 proteins: structure, function and relevance for radiation biology. *Int J Radiat Biol* **78,** 643-658.

Berg HE, Dudley GA, Haggmark T, Ohlsen H & Tesch PA. (1991). Effects of lower limb unloading on skeletal muscle mass and function in humans. *J Appl Physiol* **70,** 1882-1885.

Berg HE, Larsson L & Tesch PA. (1997). Lower limb skeletal muscle function after 6 wk of bed rest. *J Appl Physiol* **82,** 182-188.

Blaauw B, Canato M, Agatea L, Toniolo L, Mammucari C, Masiero E, Abraham R, Sandri M, Schiaffino S & Reggiani C. (2009). Inducible activation of Akt increases skeletal muscle mass and force without satellite cell activation. *FASEB J* **23,** 3896-3905.

Bodine SC, Latres E, Baumhueter S, Lai VK, Nunez L, Clarke BA, Poueymirou WT, Panaro FJ, Na E, Dharmarajan K, Pan ZQ, Valenzuela DM, DeChiara TM, Stitt TN, Yancopoulos GD & Glass DJ. (2001a). Identification of ubiquitin ligases required for skeletal muscle atrophy. *Science* **294,** 1704-1708.

Bodine SC, Stitt TN, Gonzalez M, Kline WO, Stover GL, Bauerlein R, Zlotchenko E, Scrimgeour A, Lawrence JC, Glass DJ & Yancopoulos GD. (2001b). Akt/mTOR pathway is a crucial regulator of skeletal muscle hypertrophy and can prevent muscle atrophy in vivo. *Nat Cell Biol* **3,** 1014-1019.

Boonyarom O & Inui K. (2006). Atrophy and hypertrophy of skeletal muscles: structural and functional aspects. *Acta Physiol (Oxf)* **188,** 77-89.

Boonyarom O, Kozuka N, Matsuyama K & Murakami S. (2009). Effect of electrical stimulation to prevent muscle atrophy on morphologic and histologic properties of hindlimb suspended rat hindlimb muscles. *Am J Phys Med Rehabil* **88,** 719-726.

Booth FW. (1982). Effect of limb immobilization on skeletal muscle. *J Appl Physiol* **52,** 1113-1118.

Broholm C, Laye MJ, Brandt C, Vadalasetty R, Pilegaard H, Pedersen BK & Scheele C. (2011). LIF is a contraction-induced myokine stimulating human myocyte proliferation. *J Appl Physiol* **111,** 251-259.

Brotchie D, Davies I, Ireland G & Mahon M. (1995). Dual-channel laser scanning microscopy for the identification and quantification of proliferating skeletal muscle satellite cells following synergist ablation. *J Anat* **186 (Pt 1),** 97-102.

Bruusgaard JC & Gundersen K. (2008). In vivo time-lapse microscopy reveals no loss of murine myonuclei during weeks of muscle atrophy. *J Clin Invest* **118,** 1450-1457.

Cai D, Frantz JD, Tawa NE, Jr., Melendez PA, Oh BC, Lidov HG, Hasselgren PO, Frontera WR, Lee J, Glass DJ & Shoelson SE. (2004). IKKbeta/NF-kappaB activation causes severe muscle wasting in mice. *Cell* **119,** 285-298.

Caiozzo VJ, Baker MJ, McCue SA & Baldwin KM. (1997). Single-fiber and whole muscle analyses of MHC isoform plasticity: interaction between T3 and unloading. *Am J Physiol* **273,** C944-952.

Caiozzo VJ, Haddad F, Baker MJ, Herrick RE, Prietto N & Baldwin KM. (1996). Microgravity-induced transformations of myosin isoforms and contractile properties of skeletal muscle. *J Appl Physiol* **81,** 123-132.

Canon F, Goubel F & Guezennec CY. (1998). Effects of chronic low frequency stimulation on contractile and elastic properties of hindlimb suspended rat soleus muscle. *Eur J Appl Physiol Occup Physiol* **77,** 118-124.

Chakravarthy MV, Davis BS & Booth FW. (2000). IGF-I restores satellite cell proliferative potential in immobilized old skeletal muscle. *J Appl Physiol* **89,** 1365-1379.

Chazaud B, Sonnet C, Lafuste P, Bassez G, Rimaniol AC, Poron F, Authier FJ, Dreyfus PA & Gherardi RK. (2003). Satellite cells attract monocytes and use macrophages as a support to escape apoptosis and enhance muscle growth. *J Cell Biol* **163,** 1133-1143.

Chung L & Ng YC. (2006). Age-related alterations in expression of apoptosis regulatory proteins and heat shock proteins in rat skeletal muscle. *Biochim Biophys Acta* **1762,** 103-109.

Coleman ME, DeMayo F, Yin KC, Lee HM, Geske R, Montgomery C & Schwartz RJ. (1995). Myogenic vector expression of insulin-like growth factor I stimulates muscle cell differentiation and myofiber hypertrophy in transgenic mice. *J Biol Chem* **270,** 12109-12116.

Conboy IM & Rando TA. (2002). The regulation of Notch signaling controls satellite cell activation and cell fate determination in postnatal myogenesis. *Dev Cell* **3,** 397-409.

Cornelison DD, Filla MS, Stanley HM, Rapraeger AC & Olwin BB. (2001). Syndecan-3 and syndecan-4 specifically mark skeletal muscle satellite cells and are implicated in satellite cell maintenance and muscle regeneration. *Dev Biol* **239,** 79-94.

Cornelison DD & Wold BJ. (1997). Single-cell analysis of regulatory gene expression in quiescent and activated mouse skeletal muscle satellite cells. *Dev Biol* **191,** 270-283.

Cotter MA, Cameron NE, Barry JA & Pattullo MC. (1991). Chronic stimulation accelerates functional recovery of immobilized soleus muscles of the rabbit. *Exp Physiol* **76,** 201-212.

Crassous B, Richard-Bulteau H, Deldicque L, Serrurier B, Pasdeloup M, Francaux M, Bigard X & Koulmann N. (2009). Lack of effects of creatine on the regeneration of soleus muscle after injury in rats. *Med Sci Sports Exerc* **41,** 1761-1769.

Cregan SP, Dawson VL & Slack RS. (2004). Role of AIF in caspase-dependent and caspase-independent cell death. *Oncogene* **23,** 2785-2796.

Dapp C, Schmutz S, Hoppeler H & Fluck M. (2004). Transcriptional reprogramming and ultrastructure during atrophy and recovery of mouse soleus muscle. *Physiol Genomics* **20,** 97-107.

Dedkov EI, Kostrominova TY, Borisov AB & Carlson BM. (2003). MyoD and myogenin protein expression in skeletal muscles of senile rats. *Cell Tissue Res* **311,** 401-416.

Delitto A, Rose SJ, McKowen JM, Lehman RC, Thomas JA & Shively RA. (1988). Electrical stimulation versus voluntary exercise in strengthening thigh musculature after anterior cruciate ligament surgery. *Phys Ther* **68,** 660-663.

Dhawan J & Rando TA. (2005). Stem cells in postnatal myogenesis: molecular mechanisms of satellite cell quiescence, activation and replenishment. *Trends Cell Biol* **15,** 666-673.

Dona M, Sandri M, Rossini K, Dell'Aica I, Podhorska-Okolow M & Carraro U. (2003). Functional in vivo gene transfer into the myofibers of adult skeletal muscle. *Biochem Biophys Res Commun* **312,** 1132-1138.

Dupont-Versteegden EE, Fluckey JD, Knox M, Gaddy D & Peterson CA. (2006a). Effect of flywheel-based resistance exercise on processes contributing to muscle atrophy during unloading in adult rats. *J Appl Physiol* **101,** 202-212.

Dupont-Versteegden EE, Murphy RJ, Houle JD, Gurley CM & Peterson CA. (1999). Activated satellite cells fail to restore myonuclear number in spinal cord transected and exercised rats. *Am J Physiol* **277,** C589-597.

Dupont-Versteegden EE, Strotman BA, Gurley CM, Gaddy D, Knox M, Fluckey JD & Peterson CA. (2006b). Nuclear translocation of EndoG at the initiation of disuse muscle atrophy and apoptosis is specific to myonuclei. *Am J Physiol Regul Integr Comp Physiol* **291,** R1730-1740.

Dupont Salter AC, Richmond FJ & Loeb GE. (2003). Prevention of muscle disuse atrophy by low-frequency electrical stimulation in rats. *IEEE Trans Neural Syst Rehabil Eng* **11,** 218-226.

Durmus D, Alayli G & Canturk F. (2007). Effects of quadriceps electrical stimulation program on clinical parameters in the patients with knee osteoarthritis. *Clin Rheumatol* **26,** 674-678.

Dusterhoft S, Yablonka-Reuveni Z & Pette D. (1990). Characterization of myosin isoforms in satellite cell cultures from adult rat diaphragm, soleus and tibialis anterior muscles. *Differentiation* **45,** 185-191.

Edgerton VR, Zhou MY, Ohira Y, Klitgaard H, Jiang B, Bell G, Harris B, Saltin B, Gollnick PD, Roy RR & et al. (1995). Human fiber size and enzymatic properties after 5 and 11 days of spaceflight. *J Appl Physiol* **78,** 1733-1739.

Elmore S. (2007). Apoptosis: a review of programmed cell death. *Toxicol Pathol* **35,** 495-516.

Engert JC, Berglund EB & Rosenthal N. (1996). Proliferation precedes differentiation in IGF-I-stimulated myogenesis. *J Cell Biol* **135,** 431-440.

Falempin M & Mounier Y. (1998). Muscle atrophy associated with microgravity in rat: basic data for countermeasures. *Acta Astronaut* **42,** 489-502.

Ferrando AA, Stuart CA, Brunder DG & Hillman GR. (1995). Magnetic resonance imaging quantitation of changes in muscle volume during 7 days of strict bed rest. *Aviat Space Environ Med* **66,** 976-981.

Ferreira R, Neuparth MJ, Ascensao A, Magalhaes J, Vitorino R, Duarte JA & Amado F. (2006). Skeletal muscle atrophy increases cell proliferation in mice gastrocnemius during the first week of hindlimb suspension. *Eur J Appl Physiol* **97,** 340-346.

Ferreira R, Neuparth MJ, Vitorino R, Appell HJ, Amado F & Duarte JA. (2008). Evidences of apoptosis during the early phases of soleus muscle atrophy in hindlimb suspended mice. *Physiol Res* **57,** 601-611.

Fitts RH, Riley DR & Widrick JJ. (2000). Physiology of a microgravity environment invited review: microgravity and skeletal muscle. *J Appl Physiol* **89,** 823-839.

Fitzgerald GK, Piva SR & Irrgang JJ. (2003). A modified neuromuscular electrical stimulation protocol for quadriceps strength training following anterior cruciate ligament reconstruction. *J Orthop Sports Phys Ther* **33,** 492-501.

Florini JR, Ewton DZ & Coolican SA. (1996). Growth hormone and the insulin-like growth factor system in myogenesis. *Endocr Rev* **17,** 481-517.

Fluck M. (2006). Functional, structural and molecular plasticity of mammalian skeletal muscle in response to exercise stimuli. *J Exp Biol* **209,** 2239-2248.

Fluck M & Hoppeler H. (2003). Molecular basis of skeletal muscle plasticity--from gene to form and function. *Rev Physiol Biochem Pharmacol* **146,** 159-216.

Fujita N, Murakami S, Arakawa T, Miki A & Fujino H. (2011). The combined effect of electrical stimulation and resistance isometric contraction on muscle atrophy in rat tibialis anterior muscle. *Bosn J Basic Med Sci* **11,** 74-79.

Gil-Parrado S, Fernandez-Montalvan A, Assfalg-Machleidt I, Popp O, Bestvater F, Holloschi A, Knoch TA, Auerswald EA, Welsh K, Reed JC, Fritz H, Fuentes-Prior P, Spiess E, Salvesen GS & Machleidt W. (2002). Ionomycin-activated calpain triggers apoptosis. A probable role for Bcl-2 family members. *J Biol Chem* **277,** 27217-27226.

Goldspink G. (2005a). Impairment of IGF-I gene splicing and MGF expression associated with muscle wasting. *Int J Biochem Cell Biol* **37,** 2012-2022.

Goldspink G. (2005b). Mechanical signals, IGF-I gene splicing, and muscle adaptation. *Physiology (Bethesda)* **20,** 232-238.

Goldspink G. (2006). Impairment of IGF-I gene splicing and MGF expression associated with muscle wasting. *Int J Biochem Cell Biol* **38,** 481-489.

Gollins H, McMahon J, Wells KE & Wells DJ. (2003). High-efficiency plasmid gene transfer into dystrophic muscle. *Gene Ther* **10,** 504-512.

Gomes MD, Lecker SH, Jagoe RT, Navon A & Goldberg AL. (2001). Atrogin-1, a muscle-specific F-box protein highly expressed during muscle atrophy. *Proc Natl Acad Sci U S A* **98,** 14440-14445.

Greig CA, Hameed M, Young A, Goldspink G & Noble B. (2006). Skeletal muscle IGF-I isoform expression in healthy women after isometric exercise. *Growth Horm IGF Res* **16,** 373-376.

Haddad F, Roy RR, Zhong H, Edgerton VR & Baldwin KM. (2003). Atrophy responses to muscle inactivity. I. Cellular markers of protein deficits. *J Appl Physiol* **95,** 781-790.

Halloran BP, Bikle DD, Cone CM & Morey-Holton E. (1988). Glucocorticoids and inhibition of bone formation induced by skeletal unloading. *Am J Physiol* **255,** E875-879.

Hameed M, Lange KH, Andersen JL, Schjerling P, Kjaer M, Harridge SD & Goldspink G. (2004). The effect of recombinant human growth hormone and resistance training on IGF-I mRNA expression in the muscles of elderly men. *J Physiol* **555,** 231-240.

Hameed M, Orrell RW, Cobbold M, Goldspink G & Harridge SD. (2003). Expression of IGF-I splice variants in young and old human skeletal muscle after high resistance exercise. *J Physiol* **547,** 247-254.

Hameed M, Toft AD, Pedersen BK, Harridge SD & Goldspink G. (2008). Effects of eccentric cycling exercise on IGF-I splice variant expression in the muscles of young and elderly people. *Scand J Med Sci Sports* **18,** 447-452.

Harridge SD. (2007). Plasticity of human skeletal muscle: gene expression to in vivo function. *Exp Physiol* **92,** 783-797.

Hasegawa S, Kobayashi M, Arai R, Tamaki A, Nakamura T & Moritani T. (2011). Effect of early implementation of electrical muscle stimulation to prevent muscle atrophy and weakness in patients after anterior cruciate ligament reconstruction. *J Electromyogr Kinesiol* **21,** 622-630.

Herbison GJ, Jaweed MM & Ditunno JF. (1979). Muscle atrophy in rats following denervation, casting, inflammation, and tenotomy. *Arch Phys Med Rehabil* **60,** 401-404.

Hershko A & Ciechanover A. (1998). The ubiquitin system. *Annu Rev Biochem* **67,** 425-479.

Hespel P, Op't Eijnde B, Van Leemputte M, Urso B, Greenhaff PL, Labarque V, Dymarkowski S, Van Hecke P & Richter EA. (2001). Oral creatine supplementation facilitates the rehabilitation of disuse atrophy and alters the expression of muscle myogenic factors in humans. *J Physiol* **536,** 625-633.

Hill M & Goldspink G. (2003). Expression and splicing of the insulin-like growth factor gene in rodent muscle is associated with muscle satellite (stem) cell activation following local tissue damage. *J Physiol* **549,** 409-418.

Hojman P. (2010). Basic principles and clinical advancements of muscle electrotransfer. *Curr Gene Ther* **10,** 128-138.

Holterman CE & Rudnicki MA. (2005). Molecular regulation of satellite cell function. *Semin Cell Dev Biol* **16,** 575-584.

Ingalls CP, Warren GL & Armstrong RB. (1999). Intracellular Ca2+ transients in mouse soleus muscle after hindlimb unloading and reloading. *J Appl Physiol* **87,** 386-390.

Irintchev A, Zeschnigk M, Starzinski-Powitz A & Wernig A. (1994). Expression pattern of M-cadherin in normal, denervated, and regenerating mouse muscles. *Dev Dyn* **199,** 326-337.

Jackman RW & Kandarian SC. (2004). The molecular basis of skeletal muscle atrophy. *Am J Physiol Cell Physiol* **287,** C834-843.

Kamei Y, Miura S, Suzuki M, Kai Y, Mizukami J, Taniguchi T, Mochida K, Hata T, Matsuda J, Aburatani H, Nishino I & Ezaki O. (2004). Skeletal muscle FOXO1 (FKHR) transgenic mice have less skeletal muscle mass, down-regulated Type I (slow twitch/red muscle) fiber genes, and impaired glycemic control. *J Biol Chem* **279,** 41114-41123.

Kandarian SC & Jackman RW. (2006). Intracellular signaling during skeletal muscle atrophy. *Muscle Nerve* **33,** 155-165.

Kasper CE, Talbot LA & Gaines JM. (2002). Skeletal muscle damage and recovery. *AACN Clin Issues* **13,** 237-247.

Kaufmann U, Martin B, Link D, Witt K, Zeitler R, Reinhard S & Starzinski-Powitz A. (1999). M-cadherin and its sisters in development of striated muscle. *Cell Tissue Res* **296,** 191-198.

Kawano F, Takeno Y, Nakai N, Higo Y, Terada M, Ohira T, Nonaka I & Ohira Y. (2008). Essential role of satellite cells in the growth of rat soleus muscle fibers. *Am J Physiol Cell Physiol* **295,** C458-467.

Kawashima S, Akima H, Kuno SY, Gunji A & Fukunaga T. (2004). Human adductor muscles atrophy after short duration of unweighting. *Eur J Appl Physiol* **92,** 602-605.

Koishi K, Zhang M, McLennan IS & Harris AJ. (1995). MyoD protein accumulates in satellite cells and is neurally regulated in regenerating myotubes and skeletal muscle fibers. *Dev Dyn* **202,** 244-254.

Koryak Y. (1999). The effects of long-term simulated microgravity on neuromuscular performance in men and women. *Eur J Appl Physiol Occup Physiol* **79,** 168-175.

Kosek DJ, Kim JS, Petrella JK, Cross JM & Bamman MM. (2006). Efficacy of 3 days/wk resistance training on myofiber hypertrophy and myogenic mechanisms in young vs. older adults. *J Appl Physiol* **101,** 531-544.

Krajnak K, Waugh S, Miller R, Baker B, Geronilla K, Alway SE & Cutlip RG. (2006). Proapoptotic factor Bax is increased in satellite cells in the tibialis anterior muscles of old rats. *Muscle Nerve* **34,** 720-730.

Lake DA. (1992). Neuromuscular electrical stimulation. An overview and its application in the treatment of sports injuries. *Sports Med* **13,** 320-336.

Leeuwenburgh C, Gurley CM, Strotman BA & Dupont-Versteegden EE. (2005). Age-related differences in apoptosis with disuse atrophy in soleus muscle. *Am J Physiol Regul Integr Comp Physiol* **288,** R1288-1296.

Li J, Reed SA & Johnson SE. (2009). Hepatocyte growth factor (HGF) signals through SHP2 to regulate primary mouse myoblast proliferation. *Exp Cell Res* **315,** 2284-2292.

Lim JY & Han TR. (2010). Effect of electromyostimulation on apoptosis-related factors in denervation and reinnervation of rat skeletal muscles. *Muscle Nerve* **42,** 422-430.

Livak KJ & Schmittgen TD. (2001). Analysis of relative gene expression data using real-time quantitative PCR and the 2(-Delta Delta C(T)) Method. *Methods* **25**, 402-408.

Machida S & Booth FW. (2004). Insulin-like growth factor 1 and muscle growth: implication for satellite cell proliferation. *Proc Nutr Soc* **63,** 337-340.

Magee TR, Artaza JN, Ferrini MG, Vernet D, Zuniga FI, Cantini L, Reisz-Porszasz S, Rajfer J & Gonzalez-Cadavid NF. (2006). Myostatin short interfering hairpin RNA gene transfer increases skeletal muscle mass. *J Gene Med* **8,** 1171-1181.

Martel GF, Roth SM, Ivey FM, Lemmer JT, Tracy BL, Hurlbut DE, Metter EJ, Hurley BF & Rogers MA. (2006). Age and sex affect human muscle fibre adaptations to heavy-resistance strength training. *Exp Physiol* **91,** 457-464.

Martins KJ, Gordon T, Pette D, Dixon WT, Foxcroft GR, Maclean IM & Putman CT. (2006). Effect of satellite cell ablation on low-frequency-stimulated fast-to-slow fibre-type transitions in rat skeletal muscle. *J Physiol* **572,** 281-294.

Matheny RW, Jr., Nindl BC & Adamo ML. (2010). Minireview: Mechano-growth factor: a putative product of IGF-I gene expression involved in tissue repair and regeneration. *Endocrinology* **151,** 865-875.

Matsuba Y, Goto K, Morioka S, Naito T, Akema T, Hashimoto N, Sugiura T, Ohira Y, Beppu M & Yoshioka T. (2009). Gravitational unloading inhibits the regenerative potential of atrophied soleus muscle in mice. *Acta Physiol (Oxf)* **196,** 329-339.

McCroskery S, Thomas M, Maxwell L, Sharma M & Kambadur R. (2003). Myostatin negatively regulates satellite cell activation and self-renewal. *J Cell Biol* **162,** 1135-1147.

McKinnell IW, Ishibashi J, Le Grand F, Punch VG, Addicks GC, Greenblatt JF, Dilworth FJ & Rudnicki MA. (2008). Pax7 activates myogenic genes by recruitment of a histone methyltransferase complex. *Nat Cell Biol* **10,** 77-84.

McKoy G, Ashley W, Mander J, Yang SY, Williams N, Russell B & Goldspink G. (1999). Expression of insulin growth factor-1 splice variants and structural genes in rabbit skeletal muscle induced by stretch and stimulation. *J Physiol* **516 (Pt 2),** 583-592.

McMahon JM, Signori E, Wells KE, Fazio VM & Wells DJ. (2001). Optimisation of electrotransfer of plasmid into skeletal muscle by pretreatment with hyaluronidase -- increased expression with reduced muscle damage. *Gene Ther* **8,** 1264-1270.

Megeney LA, Kablar B, Garrett K, Anderson JE & Rudnicki MA. (1996). MyoD is required for myogenic stem cell function in adult skeletal muscle. *Genes Dev* **10,** 1173-1183.

Mills P, Dominique JC, Lafreniere JF, Bouchentouf M & Tremblay JP. (2007). A synthetic mechano growth factor E Peptide enhances myogenic precursor cell transplantation success. *Am J Transplant* **7,** 2247-2259.

Mitchell PO & Pavlath GK. (2004). Skeletal muscle atrophy leads to loss and dysfunction of muscle precursor cells. *Am J Physiol Cell Physiol* **287,** C1753-1762.

Miyazaki M & Esser KA. (2009). Cellular mechanisms regulating protein synthesis and skeletal muscle hypertrophy in animals. *J Appl Physiol* **106,** 1367-1373.

Molnar MJ, Gilbert R, Lu Y, Liu AB, Guo A, Larochelle N, Orlopp K, Lochmuller H, Petrof BJ, Nalbantoglu J & Karpati G. (2004). Factors influencing the efficacy, longevity, and safety of electroporation-assisted plasmid-based gene transfer into mouse muscles. *Mol Ther* **10,** 447-455.

Morey-Holton ER & Globus RK. (2002). Hindlimb unloading rodent model: technical aspects. *J Appl Physiol* **92,** 1367-1377.

Morgan JE & Partridge TA. (2003). Muscle satellite cells. *Int J Biochem Cell Biol* **35,** 1151-1156.

Mozdziak PE, Pulvermacher PM & Schultz E. (2001). Muscle regeneration during hindlimb unloading results in a reduction in muscle size after reloading. *J Appl Physiol* **91,** 183-190.

Musacchia XJ, Deavers DR, Meininger GA & Davis TP. (1980). A model for hypokinesia: effects on muscle atrophy in the rat. *J Appl Physiol* **48,** 479-486.

Nagasaka M, Kohzuki M, Fujii T, Kanno S, Kawamura T, Onodera H, Itoyama Y, Ichie M & Sato Y. (2006). Effect of low-voltage electrical stimulation on angiogenic growth factors in ischaemic rat skeletal muscle. *Clin Exp Pharmacol Physiol* **33,** 623-627.

O'Reilly C, McKay B, Phillips S, Tarnopolsky M & Parise G. (2008). Hepatocyte growth factor (HGF) and the satellite cell response following muscle lengthening contractions in humans. *Muscle Nerve* **38,** 1434-1442.

Olguin HC & Olwin BB. (2004). Pax-7 up-regulation inhibits myogenesis and cell cycle progression in satellite cells: a potential mechanism for self-renewal. *Dev Biol* **275,** 375-388.

Olguin HC, Yang Z, Tapscott SJ & Olwin BB. (2007). Reciprocal inhibition between Pax7 and muscle regulatory factors modulates myogenic cell fate determination. *J Cell Biol* **177,** 769-779.

Owino V, Yang SY & Goldspink G. (2001). Age-related loss of skeletal muscle function and the inability to express the autocrine form of insulin-like growth factor-1 (MGF) in response to mechanical overload. *FEBS Lett* **505,** 259-263.

Peter JB, Barnard RJ, Edgerton VR, Gillespie CA & Stempel KE. (1972). Metabolic profiles of three fiber types of skeletal muscle in guinea pigs and rabbits. *Biochemistry* **11,** 2627-2633.

Philippou A, Papageorgiou E, Bogdanis G, Halapas A, Sourla A, Maridaki M, Pissimissis N & Koutsilieris M. (2009). Expression of IGF-1 isoforms after exercise-induced

muscle damage in humans: characterization of the MGF E peptide actions in vitro. *In Vivo* **23,** 567-575.

Poggi P, Marchetti C & Scelsi R. (1987). Automatic morphometric analysis of skeletal muscle fibers in the aging man. *Anat Rec* **217,** 30-34.

Putman CT, Dusterhoft S & Pette D. (1999). Changes in satellite cell content and myosin isoforms in low-frequency-stimulated fast muscle of hypothyroid rat. *J Appl Physiol* **86,** 40-51.

Putman CT, Dusterhoft S & Pette D. (2000). Satellite cell proliferation in low frequency-stimulated fast muscle of hypothyroid rat. *Am J Physiol Cell Physiol* **279,** C682-690.

Putman CT, Sultan KR, Wassmer T, Bamford JA, Skorjanc D & Pette D. (2001). Fiber-type transitions and satellite cell activation in low-frequency-stimulated muscles of young and aging rats. *J Gerontol A Biol Sci Med Sci* **56,** B510-519.

Requena Sanchez B, Padial Puche P & Gonzalez-Badillo JJ. (2005). Percutaneous electrical stimulation in strength training: an update. *J Strength Cond Res* **19,** 438-448.

Riley DA, Bain JL, Romatowski JG & Fitts RH. (2005). Skeletal muscle fiber atrophy: altered thin filament density changes slow fiber force and shortening velocity. *Am J Physiol Cell Physiol* **288,** C360-365.

Rittweger J, Felsenberg D, Maganaris C & Ferretti JL. (2007). Vertical jump performance after 90 days bed rest with and without flywheel resistive exercise, including a 180 days follow-up. *Eur J Appl Physiol* **100,** 427-436.

Rittweger J, Frost HM, Schiessl H, Ohshima H, Alkner B, Tesch P & Felsenberg D. (2005). Muscle atrophy and bone loss after 90 days' bed rest and the effects of flywheel resistive exercise and pamidronate: results from the LTBR study. *Bone* **36,** 1019-1029.

Rivalta M, Sighinolfi MC, De Stefani S, Micali S, Mofferdin A, Grande M & Bianchi G. (2009). Biofeedback, electrical stimulation, pelvic floor muscle exercises, and vaginal cones: a combined rehabilitative approach for sexual dysfunction associated with urinary incontinence. *J Sex Med* **6,** 1674-1677.

Rosenberg P, Hawkins A, Stiber J, Shelton JM, Hutcheson K, Bassel-Duby R, Shin DM, Yan Z & Williams RS. (2004). TRPC3 channels confer cellular memory of recent neuromuscular activity. *Proc Natl Acad Sci U S A* **101,** 9387-9392.

Sacheck JM, Ohtsuka A, McLary SC & Goldberg AL. (2004). IGF-I stimulates muscle growth by suppressing protein breakdown and expression of atrophy-related

ubiquitin ligases, atrogin-1 and MuRF1. *Am J Physiol Endocrinol Metab* **287,** E591-601.

Sandri M, Sandri C, Gilbert A, Skurk C, Calabria E, Picard A, Walsh K, Schiaffino S, Lecker SH & Goldberg AL. (2004). Foxo transcription factors induce the atrophy-related ubiquitin ligase atrogin-1 and cause skeletal muscle atrophy. *Cell* **117,** 399-412.

Schuler M & Pette D. (1996). Fiber transformation and replacement in low-frequency stimulated rabbit fast-twitch muscles. *Cell Tissue Res* **285,** 297-303.

Schultz E & McCormick KM. (1994). Skeletal muscle satellite cells. *Rev Physiol Biochem Pharmacol* **123,** 213-257.

Seale P, Sabourin LA, Girgis-Gabardo A, Mansouri A, Gruss P & Rudnicki MA. (2000). Pax7 is required for the specification of myogenic satellite cells. *Cell* **102,** 777-786.

Shefer G, Van de Mark DP, Richardson JB & Yablonka-Reuveni Z. (2006). Satellite-cell pool size does matter: defining the myogenic potency of aging skeletal muscle. *Dev Biol* **294,** 50-66.

Sheffler LR & Chae J. (2007). Neuromuscular electrical stimulation in neurorehabilitation. *Muscle Nerve* **35,** 562-590.

Siu PM. (2009). Muscle apoptotic response to denervation, disuse, and aging. *Med Sci Sports Exerc* **41,** 1876-1886.

Siu PM, Pistilli EE, Butler DC & Alway SE. (2005). Aging influences cellular and molecular responses of apoptosis to skeletal muscle unloading. *Am J Physiol Cell Physiol* **288,** C338-349.

Spangenburg EE & Booth FW. (2002). Multiple signaling pathways mediate LIF-induced skeletal muscle satellite cell proliferation. *Am J Physiol Cell Physiol* **283,** C204-211.

Stelzer JE & Widrick JJ. (2003). Effect of hindlimb suspension on the functional properties of slow and fast soleus fibers from three strains of mice. *J Appl Physiol* **95,** 2425-2433.

Stevens L, Firinga C, Gohlsch B, Bastide B, Mounier Y & Pette D. (2000). Effects of unweighting and clenbuterol on myosin light and heavy chains in fast and slow muscles of rat. *Am J Physiol Cell Physiol* **279,** C1558-1563.

Stitt TN, Drujan D, Clarke BA, Panaro F, Timofeyva Y, Kline WO, Gonzalez M, Yancopoulos GD & Glass DJ. (2004). The IGF-1/PI3K/Akt pathway prevents

expression of muscle atrophy-induced ubiquitin ligases by inhibiting FOXO transcription factors. *Mol Cell* **14,** 395-403.

Stuelsatz P, Pouzoulet F, Lamarre Y, Dargelos E, Poussard S, Leibovitch S, Cottin P & Veschambre P. (2010). Down-regulation of MyoD by calpain 3 promotes generation of reserve cells in C2C12 myoblasts. *J Biol Chem* **285,** 12670-12683.

Tarabees R, Hill D, Rauch C, Barrow PA & Loughna PT. (2011). Endotoxin transiently inhibits protein synthesis through Akt and MAPK mediating pathways in C2C12 myotubes. *Am J Physiol Cell Physiol* **301,** C895-902.

Tatsumi R, Anderson JE, Nevoret CJ, Halevy O & Allen RE. (1998). HGF/SF is present in normal adult skeletal muscle and is capable of activating satellite cells. *Dev Biol* **194,** 114-128.

Tesch PA, Trieschmann JT & Ekberg A. (2004). Hypertrophy of chronically unloaded muscle subjected to resistance exercise. *J Appl Physiol* **96,** 1451-1458.

Thomason DB & Booth FW. (1990). Atrophy of the soleus muscle by hindlimb unweighting. *J Appl Physiol* **68,** 1-12.

van Dijk-Ottens M, Vos IH, Cornelissen PW, de Bruin A & Everts ME. (2010). Thyroid hormone-induced cardiac mechano growth factor expression depends on beating activity. *Endocrinology* **151,** 830-838.

Veldhuizen JW, Verstappen FT, Vroemen JP, Kuipers H & Greep JM. (1993). Functional and morphological adaptations following four weeks of knee immobilization. *Int J Sports Med* **14,** 283-287.

Verdijk LB, Koopman R, Schaart G, Meijer K, Savelberg HH & van Loon LJ. (2007). Satellite cell content is specifically reduced in type II skeletal muscle fibers in the elderly. *Am J Physiol Endocrinol Metab* **292,** E151-157.

Wang XD, Kawano F, Matsuoka Y, Fukunaga K, Terada M, Sudoh M, Ishihara A & Ohira Y. (2006). Mechanical load-dependent regulation of satellite cell and fiber size in rat soleus muscle. *Am J Physiol Cell Physiol* **290,** C981-989.

Widrick JJ, Stelzer JE, Shoepe TC & Garner DP. (2002). Functional properties of human muscle fibers after short-term resistance exercise training. *Am J Physiol Regul Integr Comp Physiol* **283,** R408-416.

Wittwer M, Fluck M, Hoppeler H, Muller S, Desplanches D & Billeter R. (2002). Prolonged unloading of rat soleus muscle causes distinct adaptations of the gene profile. *FASEB J* **16,** 884-886.

Yablonka-Reuveni Z & Rivera AJ. (1994). Temporal expression of regulatory and structural muscle proteins during myogenesis of satellite cells on isolated adult rat fibers. *Dev Biol* **164,** 588-603.

Yaffe D & Saxel O. (1977). Serial passaging and differentiation of myogenic cells isolated from dystrophic mouse muscle. *Nature* **270,** 725-727.

Yang S, Alnaqeeb M, Simpson H & Goldspink G. (1996). Cloning and characterization of an IGF-1 isoform expressed in skeletal muscle subjected to stretch. *J Muscle Res Cell Motil* **17,** 487-495.

Yang SY & Goldspink G. (2002). Different roles of the IGF-I Ec peptide (MGF) and mature IGF-I in myoblast proliferation and differentiation. *FEBS Lett* **522,** 156-160.

Zammit PS, Golding JP, Nagata Y, Hudon V, Partridge TA & Beauchamp JR. (2004). Muscle satellite cells adopt divergent fates: a mechanism for self-renewal? *J Cell Biol* **166,** 347-357.

Zammit PS, Partridge TA & Yablonka-Reuveni Z. (2006a). The skeletal muscle satellite cell: the stem cell that came in from the cold. *J Histochem Cytochem* **54,** 1177-1191.

Zammit PS, Relaix F, Nagata Y, Ruiz AP, Collins CA, Partridge TA & Beauchamp JR. (2006b). Pax7 and myogenic progression in skeletal muscle satellite cells. *J Cell Sci* **119,** 1824-1832.

Zhang BT, Yeung SS, Liu Y, Wang HH, Wan YM, Ling SK, Zhang HY, Li YH & Yeung EW. (2010). The effects of low frequency electrical stimulation on satellite cell activity in rat skeletal muscle during hindlimb suspension. *BMC Cell Biol* **11,** 87.

Zhang LF, Sun B, Cao XS, Liu C, Yu ZB, Zhang LN, Cheng JH, Wu YH & Wu XY. (2003). Effectiveness of intermittent -Gx gravitation in preventing deconditioning due to simulated microgravity. *J Appl Physiol* **95,** 207-218.

Zhang P, Chen X & Fan M. (2007). Signaling mechanisms involved in disuse muscle atrophy. *Med Hypotheses* **69,** 310-321.